The Pennsylvania State University

The Graduate School

Department of Geosciences

DEFORMATION, LAVA DOME EVOLUTION, AND ERUPTION CYCLICITY AT MERAPI VOLCANO, INDONESIA

A Thesis in

Geosciences

by

Kirby D. Young

Submitted in Partial Fulfillment
of the Requirements
for the Degree of

Doctor of Philosophy

August 2007

The thesis of Kirby D. Young was reviewed and approved* by the following:

Barry Voight
Professor of Geology and Geological Engineering
Thesis Advisor
Co-chair of Committee

Terry Engelder
Professor of Geosciences
Co-chair of Committee

Derek Elsworth
Professor of Energy and Geo-Environmental Engineering

Donald M. Fisher
Professor of Geosciences

Katherine H. Freeman
Professor of Geosciences
Associate Head of the Graduate Program

*Signatures are on file in the Graduate School

ABSTRACT

Deformation monitoring results are reported here for the period 1988-1998 at Merapi volcano, one of the most active and dangerous volcanoes in Indonesia. Comprehensive databases of various geophysical parameters were concurrently studied and analyzed to 2000, and similar data were subsequently considered during periods of eruption crisis in 2001 and 2006. Of particular emphasis was the study of lava eruption rates based on dome volume estimates and seismic proxies for dome collapse volumes. The detailed study period of deformation includes a major resumption in lava effusion in January 1992 and major dome collapses in November 1994, January 1997, and July 1998. Monitoring techniques employed in the field are of two types. Translational movements were recorded via electronic distance measurements (EDM) on a summit trilateration network, slope distance changes measured to the upper flanks, and other data collected from 1988 to 1995. Tilt changes were detected by a summit and flank network of tilt stations that operated at various times from 1993 to 1998. A major consequence of the deformation results is the documentation of a significant 4-year period of deformation precursory to the 1992 eruption. Cross-crater strain rates accelerated from less than 3 x 10^{-6} /day between 1988 and 1990 to more than 11 x 10^{-6} /day just prior to the January 1992 activity, representing a general, asymmetric extension of the summit during high-level conduit pressurization. After the vent opened and effusion of lava resumed, strain occurred at a much reduced rate of less than 2 x 10^{-6} /day. The Gendol breach, a pronounced depression formed by the juxtaposition of old lava coulées on the southeast flank, functioned as a major displacement discontinuity.

An elevated phase of magma production with respect to the long-term rate for the 20th Century characterized the activity at Merapi volcano, Central Java/Yogyakarta, Indonesia, for the period 1992-2006. Most large (0.2 - 3.4 x 106 m^3) dome collapses or dome collapse episodes in the 1990s were initiated during elevated short-term extrusion rates, at Merapi typically 0.2 m^3 s^{-1} or greater. Large collapses were often preceded by variable inflationary tilt of the crater rim, by increasing numbers of rockfalls and their associated seismicity, and by intensifying multiphase earthquake activity. Multiphase earthquakes, rockfall counts, and amplitude-duration data established from seismic records show varying positive correlations with extrusion rate. Pyroclastic flow and rockfall seismic amplitude-duration data were calibrated as proxies to enable estimates of collapsed lava volume. For the 20th Century as a whole, observed magma production rates suggest long-term cycles of ca. 30 years spacing that begin with heightened magma flux over 2 to 15 years with greater potential for explosive eruptive activity, followed by much-diminished mean magma flux in the concluding ~15-25 years of the cycle. The data examined through 2006 suggest that if similar cycles are to continue well into the 21st Century, activity at Merapi will now experience relatively lower magma production for the next ~15 years, compared to the most recent eruptive phase during 1992-2006.

TABLE OF CONTENTS

List of Figures

List of Tables

Acknowledgements

A difficult to fathom number of years and tens of thousands of travel miles have finally culminated in the completion of a dissertation that required the help of a disparate and international group of people. I first must thank my thesis advisor, Professor Barry Voight, who maintained nearly infinite patience with me as I so very slowly proceeded towards a conclusion to my graduate education. Barry provided the inspiration, a keen research insight, and funding that allowed me to see and experience many special and unusual places of this world. He also could be counted on to provide exhaustive and inciteful editorial comments that inevitably improved whatever manuscript or draft I happened to be working on. He will be not just a past thesis advisor, but a life-long colleague and friend.

I wish to thank the members of the thesis committee, Professors Terry Engelder, Derek Elsworth, and Don Fisher, who oversaw the dissertation in its final stages and remained patient with me as I struggled to complete it. Also notably patient with me in the Department of Geosciences were Professors Katherine Freeman and Peter Deines, who supported my efforts to complete my degree when their input was needed by the Graduate School. I also thank Angela Rothrock, Graduate Program Assistant in the Dept. of Geosciences, who was of great help in administrative matters towards the end.

Valuable professional collaboration and assistance came from numerous people at institutions scattered around the world. Many of these people are named in the acknowledgements specific to the individual Chapters of the dissertation. I nevertheless will repeat certain of their names here. A number of U.S. Geological Survey colleagues

provided help. Rick Lahusen was invaluable in tiltmeter station design and electronics assembly, while Jeff Marso provided needed logistical help and instruction in tiltmeter station construction. Tom Murray provided much helpful advice in the assembly of portable RSAM and SSAM packages. He also provided certain electronics components needed to complete the RSAM/SSAM assemblies. John Rogers was key in providing advice and graphics hardware for SSAM data display and analysis. Willie Lee gave very useful instruction and recommendations for the establishment of seismic data acquisition systems generally, and his help specifically led to deployment of SSAM systems at Merapi and Semeru volcanoes. Further inspiration at key moments came from VDAP Head C. Dan Miller and also from Dr. Chris Newhall of the USGS and University of Washington.

The many months spent in Indonesia at Merapi Volcano Observatory working collaboratively with Volcanological Survey of Indonesia personnel formed the heart of this project. Formost in making the collaboration possible were the successive heads of VSI at the time, Dr. Subroto Mojo, Dr. Wimpy S. Tjetjep, and Dr. R. (Jerry) Sukhyar. Pak Wimpy through much of my project tenure provided encouragement and approved financial assistance for some field logistics. Jerry Sukhyar, eventual head of VSI, provided great assistance with logistical problems, and acted frequently as our informal liaison to VSI. I thank Pak Surono, stationed at the time at VSI Bandung, for the gracious accommodations he made in allowing me to cooperate in a seismic monitoring campaign at Semeru volcano. I also thank Dr. Suparto Siswowidjoyo, at the time head of

the VSI East Java section, for facilitating my visits to volcanoes in that part of Java, in particular Bromo, Kawah Ijen, and Kelud.

At Merapi Volcano Observatory itself, special thanks are due to the succeeding heads of MVO during my visits there, namely Dr. Mas Olas, Dr. Sutikno Bronto, and Dr. Ir. Mas Atje Purbawinata. Also of great help was eventual MVO head Dr. A. Ratdomopurbo, particularly in regards to seismological monitoring and visual observations of the lava dome. His initiative in establishing daily photographic monitoring of the summit of Merapi helped immeasurably in the interpretation of our own data. Field work based out of MVO was at times extremely difficult, both with respect to tiltmeter maintenance and monitoring at the summit of Merapi, and also in the repeated EDM measurement campaigns that took place there and on the lower flanks of the volcano. Foremost in this effort was collaboration with the "Deforrmation" team at MVO, at the time headed by Subandrio. I thank him and his fellow MVO staff members Sajiman, Miswanto, and Paijo. Sajiman drafted many of the topographic base maps of the summit area that were used in the field. Miswanto could always be relied upon to be patient and hard working during the many field hours spent at the summit. Further field help with tiltmeter installation and maintenance came from MVO staff Suparban and Made. Special thanks go to Suharno, who has maintained the MVO database of geophysical parameters for many years. Also providing help and kindness were Agus and Ahreef, among others. Finally I thank Dr. Supriyati Andreastuti of MVO for informative discussions, encouragement, and friendship.

I thank the successive French Cooperants based at MVO during the time of my field work at Merapi, specifically Philippe Jousset, Jacques Tondeur, Francois Beauducel, and Michel Dejean. To Michel I give special thanks for being a very good friend.

At Penn State I would very much like to thank Dr. Dannie Hidayat for his friendship, technical assistance, and discussions about Merapi and other volcanoes. Special thanks to Nebil and Ulku Orkan, two of my closest friends, for their support and love over the years. I always felt welcomed in their like I was one of their family.

Finally, I must thank with great fondness my sweetheart and best friend Amy Clifton, who came late into my life, but gave me the courage and support I needed, particularly at some very low moments, so that I could finally complete this incredibly long project. Without her, I would never have finished it.

Chapter 1

Introduction

1.1 Overview

Merapi volcano, an andesitic stratocone located in Central Java, Indonesia (Fig. 1), has experienced episodic extrusion of lava and frequent volcanic explosions over the last two and a half centuries (Berthommier et al., 1992; Siswowidjoyo et al., 1995; Andreastuti et al., 2000; Camus et al., 2000; Newhall et al., 2000; Voight et al., 2000a), typically forming lava domes and tongues within or near a summit crater (Fig. 2). Frequent gravitational collapses of portions of these domes have produced dangerous pyroclastic flows, and pyroclastic flows from fountain collapse have also occurred (Voight et al., 2000a). The dome-collapse type, so-called "Merapi-type" nuées ardentes, have been dominant over the last two decades (Abdurachman et al., 2000; Voight et al., 2000a,b). Over the longer term, historical records for the past few centuries and the volcanic stratigraphy deposited since the mid-Holocene reveal Merapi to have experienced relatively violent explosive eruptions as well, including Plinian and sub-Plinian activity at intervals of a few centuries between events (Andreastuti et al., 2000; Newhall et al., 2000).

Merapi is one of numerous active volcanoes on the island of Java comprising a segment of the 3000-km long Sunda volcanic arc, a linear archipelago of volcanic summits, forearc deformation, and sedimentation stretching from northern Sumatra to the Banda Sea. Relative plate motion drives 7 cm/a subduction of the Australian plate

beneath an outlier of Eurasia lithosphere in the area of central Java (Hamilton, 1979; Lee and Lawver, 1995; Hall, 1996), based on the NUVEL-1A plate motion model (DeMets et al., 1994).

The Merapi volcanic edifice rises to some 2962 m elevation asl, with relief above surrounding agricultural lands of at least 1800 m. Major population centers within 30 km of Merapi are the cities of Yogyakarta and Surakarta, comprising a total population of at least one million people (Thouret et al., 2000). More significant is the high population density of the rural areas that include hundreds of villages. Estimates compiled by Thouret et al. (2000, their Table 1) suggest that at least one million people live within 20 km of Merapi, a distance attainable by the largest pyroclastic flows and debris avalanche deposits based on historical and stratigraphic records. Some 80,000 rural inhabitants likely live within a proximal zone defined somewhat arbitrarily 60 years ago as "forbidden" (Voight et al., 2000a).

Because of the proximity of a high population density and the frequent and potentially violent nature of its volcanic activity, Merapi volcano poses extraordinary hazards to people and culture. At the same time it affords an opportunity to test volcano monitoring techniques and to develop basic ideas on how volcanoes work. For these reasons, Merapi was designated a "Decade Volcano" as part of the International Decade for Natural Disaster Reduction, one of sixteen volcanoes worldwide identified by the International Association of Volcanology and Chemistry of the Earth's Interior (IAVCEI) as deserving of special attention by volcano researchers and hazard managers. Scientists from numerous countries have thus been drawn to Merapi, particularly since 1990, including multidisciplinary programs of France, Japan, Germany, and the United States.

A recent compilation of results from many of these projects appeared in a special issue of the Journal of Volcanology and Geothermal Research (JVGR, Vol. 100, Nos. 1-4) published in 2000.

The Volcanological Survey of Indonesia (VSI; formally the Center for Volcanology and Geological Hazard Mitigation) has the administrative responsibility as representative of the government of Indonesia for monitoring Merapi and assessing its volcanic hazards (Voight et al., 2000a). During volcanic activity, it collaborates with Civil Defense authorities should evacuation of nearby inhabitants be deemed necessary. Day-to-day efforts are conducted at the Merapi Volcano Observatory (MVO, formally known as the Office of Volcano Research and Technology Development) located in the nearby city of Yogyakarta. Cooperative efforts in the early 1980's between the U.S. Geological Survey (USGS) and VSI formed the basis for a seismic monitoring program that operates today at MVO (Ratdomopurbo and Poupinet, 2000; Voight et al., 2000a). Since then, MVO has continued to expand its breadth of capabilities via the systematic monitoring of ground deformation, gas geochemistry, and magnetic measurements, along with long-maintained programs of visual and geological observations. An important contribution to the visual, plume, and meteorological monitoring is an array of field observation posts situated about the base of the volcano (Plawangan, Ngepos, Babadan, Jrakah, Selo), staffed by local people trained to record systematic observations and measurements.

1.2 Organization and Objectives of the Dissertation

The work presented here comprises the results of a multiple-year campaign of field work at Merapi that initially emphasized measurements of ground deformation by distance measurements and telemetered tiltmeters. Focus of the work had the dual objectives of developing a better understanding of how Merapi worked, as revealed by deformation measurements, and establishing a system of monitoring that had the potential to evolve into a practical and reliable method for anticipating impending volcanic eruptions. As time progressed in the research, it proved advantageous to examine Merapi more comprehensively in terms of the geophysical parameters that were being routinely measured by MVO and to further study processes related to dome growth and collapse.

The content of the dissertation that follows this introductory chapter in great measure consists of two papers designed for publication in refereed journals. As such, they stand on their own in terms of containing their own introductions and their own specific conclusions. The first of these papers, presented here as Chapter 2 was published by me as Young et al. (2000) in the Merapi special issue of JVGR, and includes five co-authors. In spite of the co-authorship listed for the published version of this chapter, it should be emphasized that I wrote all drafts of this chapter and prepared all the figures. Described below are the specific contributions by the co-authors to the development of what is presented here as Chapter 2.

Second author listed is Dr. Barry Voight, who is serving as Ph.D. dissertation advisor on this project. Dr. Voight initiated an electronic distance measuring (EDM) campaign at the summit of Merapi as part of a project supported by the United States

Geological Survey (USGS), the United States Agency for International Development (US AID), and VSI (Voight, 1988; Voight et al., 1989). Subsequent work described here operated mainly with NSF support. Dr. Voight's efforts included working with Indonesian colleagues in establishing campaign survey benchmarks at the summit of Merapi and subsequently establishing the first (baseline) EDM measurements on this network in July and August of 1988. He also spearheaded the establishment of fixed prisms in 1988 and 1990 for flank EDM measurements. Dr. Voight participated with the author in EDM measurements at the summit of Merapi and from lower flank stations in 1990 and afterward. In preparation of the Young et al. (2000) paper, Dr. Voight served as the main internal editor of the manuscript drafts written by me.

Subandrio (aka Subandriyo), Sajiman, and Miswanto are Indonesian volcanologists of single name who appear as third, fourth, and fifth authors of Young et al. (2000), respectively. Their inclusion reflects the collaborative nature of volcano research, a necessity when working at an active volcano monitored closely by local officials in a foreign country. At the time of the principal field work described in Chapter 2, all served on the staff of the Merapi Volcano Observatory office of VSI in a capacity that focused on deformation measurements and occasional other monitoring field work. Subandrio was head of deformation studies at MVO in this regard. They were invaluable colleagues in coordinating logistics in the field for the deformation campaigns, assisted with all summit EDM measurements, and conducted some EDM measurements on their own as part of the MVO monitoring effort at Merapi. EDM measurements were coordinated entirely by them during the summit network campaign in 1991, and flank EDM measurements were conducted by them at various other times.

T. J. Casadevall is the final author listed on Young et al. (2000). Dr. Casadevall, a senior research volcanologist and former Deputy Director of the USGS, was instrumental in developing the collaboration of Indonesian and USGS volcanologists beginning in the 1980's, and in encouraging the participation of Dr. Voight in these endeavors. His listing as author is in recognition of this contribution, a legacy that continues to this day (2006) in the studies by Penn State Department of Geosciences researchers at Merapi.

Chapter 2 presents the data and analysis of the electronic distance measurement (EDM) program for the period 1988-1995. The discussion concentrates on deformation experienced by the upper edifice of the volcano. Specifically, results from Chapter 2 incorporate the summit network of benchmarks, which were surveyed at least once per year, and data for a series of fixed prisms on the lava dome and south flank that were surveyed frequently from lower-flank benchmarks.

The second major section of this dissertation, appearing organizationally as Chapter 3, has been written in a stand-alone format suitable, but not yet submitted, for publication in a refereed journal. It presents results from an analysis of a variety of geophysical parameters collected at Merapi volcano, mostly between 1992 and 1999. Of these data, field campaigns performed by me for this dissertation focused on the installation and maintenance of a telemetered tiltmeter network at or near the summit of Merapi, and design and installation of real-time seismic amplitude monitoring (RSAM) and Seismic Spectral Amplitude Monitoring (SSAM) equipment at MVO and other volcanoes of opportunity. Results from these instruments were compared with the data of other geophysical parameters compiled by MVO staff such as seismic events counts,

seismic amplitudes and durations, $S0_2$ concentrations in the plume, and visual observations such as pyroclastic flow events and runout distances. During the course of the field campaigns, geological observations were made on the evolution and collapse of the active lava dome complex at the summit of Merapi.

In Chapter 3, the broad range of geophysical parameters measured at Merapi during 1992-1999 are compared to the eruptive activity in order to assess the existence of eruption precursors (in hindsight), to gain a better understanding of the driving mechanisms of dome collapse, and to develop best estimates for magma extrusion rates (flux). The data of Chapter 3 come mainly from my dissertation field work focusing on tiltmeters, RSAM/SSAM monitoring, and geological evolution of the lava dome, and from the unpublished Merapi Volcano Observatory geophysical and observational database. It should be emphasized that as part of the original research conducted by me and described in Chapter 3, all summit tiltmeters referred to in the text were installed at sites selected by me and constructed by me with the assistance of MVO staff. Subsequent campaigns to maintain and upgrade the tilt stations were coordinated and carried out by me in cooperation with MVO through 1995. Later maintenance was conducted by MVO as they saw fit until the loss of the last summit tilt station in 1998. As regards the flank tilt stations, equipment and suggestions for site design were provided by Penn State University through me to MVO staff in 1994 and 1995. Installation of tiltmeters at the flank locations occurred during field campaigns by MVO in those years.

A concluding aspect of Chapter 3 is the examination of magma flux exiting the conduit at Merapi. Flux rates calculated here for 1992-1999 were the first attempt at Merapi to include an allowance for dome volume loss due to rockfalls, in addition to the

volume change measured for the lava dome. These calculations are thus likely more accurate as assessments of actual magma flux than previous measurements which had not considered rockfall volumes. The timing of elevated extrusion rates determined from these results is compared to the occurrences of major dome collapse events. Variations in magma flux suggest cyclicity in rates both within the period 1992-1999, and over the last 100 years.

A draft of Chapter 3 was provided to the hazards teams (VSI and USGS) responding to the 2006 volcano crisis at Merapi, and was used by them as a guide for calculating lava extrusion fluxes during the crisis (C. Newhall, written communication, 2006). The flux measurement was one of the few critical parameters used to assess the hazards and risks during this crisis.

Finally, Chapter 4 integrates the results of the stand-alone works presented as Chapters 2 and 3, and presents a set of comprehensive conclusions for the dissertation research.

1.3 References

Abdurachman, E.K., Bourdier, J.-L., Voight, B., 2000. Nuées ardentes of November 22 1994 at Merapi Volcano, Java, Indonesia. J. Volcanol. Geotherm. Res. 100, 345-361.

Andreastuti, S.D., Alloway, B.V., Smith, I.E.M., 2000. A detailed tephrostratigraphic framework at Merapi Volcano, Central Java, Indonesia: Implications for eruption predictions and hazard assessment. J. Volcanol. Geotherm. Res. 100, 51-67.

Beauducel, F., Agung Nandaka, M., Cornet, F.H., Diament, M., 2006. Mechanical discontinuities monitoring at Merapi volcano using kinematic GPS. J. Volcanol. Geotherm. Res. 150, 300-312.

Berthommier, P.-C., Bahar, I., Boudon, G., Camus, G., Gourgaud, A., Lajoie, J., Vincent, P.-M., 1992. Le Mérapi et ses éruptions: importance des mécanismes phréatomagmatiques. Bull. Soc. Géol. Fr. 5, 635-644 (in French).

Camus, G., Gourgaud, A., Mossand-Berthommier, P.C., Vincent, P.-M., 2000. Merapi (Central Java, Indonesia): An outline of the structural and magmatological evolution, with a special emphasis to the major pyroclastic events J. Volcanol. Geotherm. Res. 100, 139-163.

DeMets, C., Gordon, R. G., Argus, D.F., Stein, S., 1994. Effect of recent revisions to the geomagnetic reversal time scale on estimates of current plate motions, Geophys. Res. Lett. 21, 2191-2194.

Hall, R., 1996. Reconstructing Cenozoic SE Asia. In: Hall, R., Blundell, D. J. (eds), Tectonic Evolution of SE Asia. Geological Society of London Special Publication 106, 153-184.

Hamilton, W., 1979. Tectonics of the Indonesian region. U. S. Geol. Surv. Prof. Paper 1078, 345pp.

Lee, T.-Y., Lawver, L.A., 1995. Cenozoic plate reconstruction of Southeast Asia. Tectonophys. 251, 85-138.

Newhall, C.G., Bronto, S., Alloway, B., Banks, N.G., Bahar, I., del Marmol, M.A., Hadisantono, R.D., Holcomb, R.T., McGeehin, J., Miksic, J.N., Rubin, M., Sayudi, S.D., Sukhyar, R., Andreastuti, S., Tilling, R.I., Torley, R., Trimble, D., Wirakusumah, A.D., 2000. 10,000 Years of explosive eruptions at Merapi Volcano, Central Java: archaeological and modern implications. J. Volcanol. Geotherm. Res. 100, 9-50.

Ratdomopurbo, A., Poupinet, G., 2000. An overview of the seismicity of Merapi volcano (Java, Indonesia), 1983-1994. J. Volcanol. Geotherm. Res. 100, 193-214.

Siswowidjoyo, S., Suryo, I., Yokohama, I., 1995. Magma eruption rates of Merapi volcano, central Java, Indonesia during one century (1890-1992). Bull. Volcanol. 57, 111-116.

Thouret, J.-C., Lavigne, F., Kelfoun, K., Bronto, S., 2000. Toward a revised hazard assessment at Merapi volcano, Central Java. J. Vol. Geotherm. Res. 100, 497-502.

Voight, B., 1988. Development of geodetic monitoring program at Merapi volcano, Java: US AID/OFDA, unpub. report, 30pp.

Voight, B., Casadevall, T., and Cornelius, R.C., 1989. Development of geodetic monitoring program at Merapi volcano, Indonesia: General Assembly, International Association of Volcanology and Chemistry of the Earth's Interior, Santa Fe, NM, USA.

Voight, B., Constantine, E.K., Siswowidjoyo, S., Torley, R., 2000a. Historical eruptions of Merapi Volcano, Central Java, Indonesia, 1768-1998. J. Volcanol. Geotherm. Res. 100, 69-138.

Voight, B., Young, K.D., Hidayat, D., Subandrio, Purbawinata, M.A., Ratdomopurbo, A., Suharna, Panut, Sayudi, D.S., LaHusen, R., Marso, J., Murray, T.L., Dejean, M., Iguchi, M., Ishihara, K., 2000b. Deformation and seismic precursors to dome-collapse and fountain-collapse nuées ardentes at Merapi Volcano, java, Indonesia, 1994—1998, J. Volcanol. Geotherm. Res. 100, 261-287.

Young, K.D., Voight, B., Subandriyo, Sajiman, Miswanto, Casadevall, T.J., 2000. Ground deformation at Merapi Volcano, Java, Indonesia: distance changes, June 1988--October 1995. J. Volcanol. Geotherm. Res. 100, 233-259.

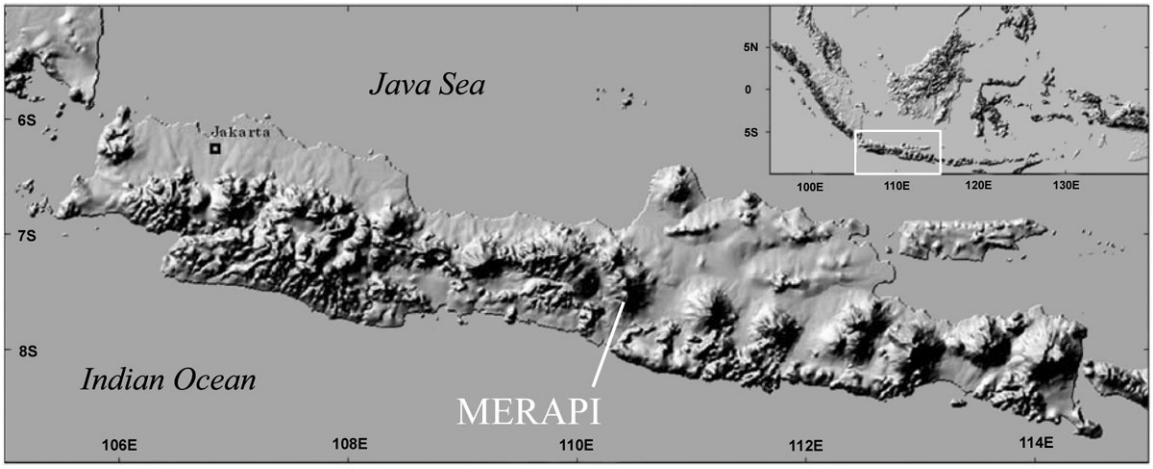

Figure 1-1. Location of Merapi volcano on the island of Java, Indonesia, as represented in a shaded relief digital elevation model modified slightly from Beauducel et al. (2006). Inset shows location of map within the Indonesian Archipelago.

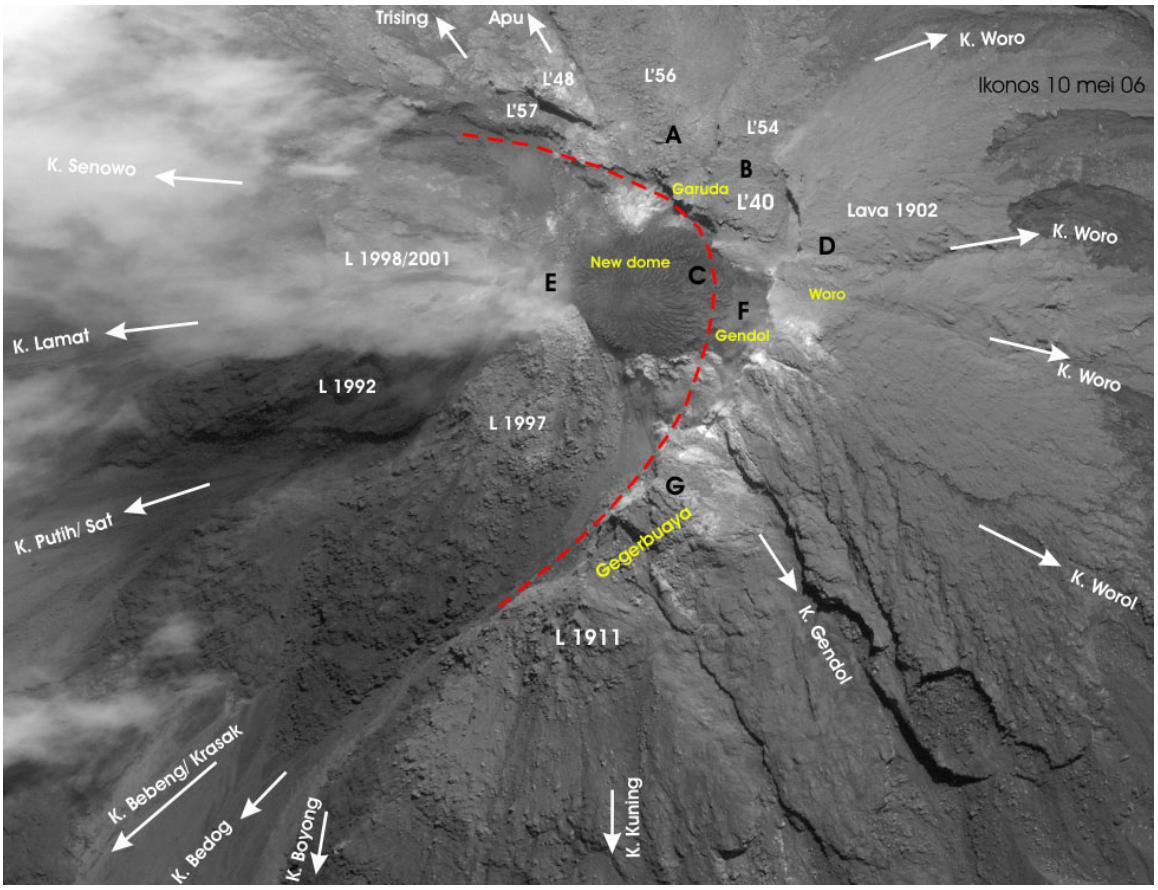

Figure 1-2. Ikonos satellite image of the Merapi summit area as of 10 May 2006. Ages of the various lavas ("L", "Lava") are indicated, including the "New dome" of 2006. Labeled arrows show the names and locations for the heads of major drainages ("K" = Kali, i.e. river). Dashed line shows approximate position of the crater wall at the start of the 2006 eruption. All annotations are by Merapi Volcano Observatory (pers. Commun., 2006).

Chapter 2

Ground Deformation at Merapi Volcano, Java, Indonesia: Distance Changes, June 1988 - October 1995

Abstract

Edifice deformations are reported here for the period 1988-1995 at Merapi volcano, one of the most active and dangerous volcanoes in Indonesia. The study period includes a major resumption in lava effusion in January 1992 and a major dome collapse in November 1994. The data comprise electronic distance measurements (EDM) on a summit trilateration network, slope distance changes measured to the upper flanks, and other data collected from 1988 to 1995. A major consequence of this study is the documentation of a significant 4-year period of deformation precursory to the 1992 eruption. Cross-crater strain rates accelerated from less than 3 x 10^{-6} /day between 1988 and 1990 to more than 11 x 10^{-6} /day just prior to the January 1992 activity, representing a general, asymmetric extension of the summit during high-level conduit pressurization. After the vent opened and effusion of lava resumed, strain occurred at a much reduced rate of less than 2 x 10^{-6} /day. EDM measurements between lower flank benchmarks and the upper edifice indicate displacements as great as 1 m per year over the four years before the 1992 eruption. The Gendol breach, a pronounced depression formed by the juxtaposition of old lava coulées on the southeast flank, functioned as a major displacement discontinuity. Since 1993, movements have generally not exceeded the 95% confidence limits of the summit network. Exceptions to this include 12 cm outward movement for the northwest crater rim in 1992-93, probably from loading by newly

erupted dome lava, and movements as much as 7 cm on the south flank between November 1994 and September 1995. No short-term precursors were noted before the November 1994 lava dome collapse, but long-term adjustments of crater geometry accompanied lava dome growth in 1994. Short-term 2-cm deflation of the edifice occurred following the November 1994 dome collapse.

2.1 Introduction

Merapi, an andesitic stratovolcano located in Central Java, Indonesia, has experienced semi-continuous extrusion of lava over the last century (Siswowidjoyo et al., 1995). The extrusions characteristically form lava domes at the summit, and these domes collapse sporadically to generate rock avalanches and pyroclastic flows. Because of this activity, Merapi volcano (Fig. 2-1) poses extraordinary hazards to people and culture. At the same time it affords an opportunity to test volcano monitoring techniques and to develop basic ideas on how volcanoes work, as illustrated by the many papers in this volume. Fundamental issues for study include dome growth and collapse, edifice deformation, and stability of the volcano's flanks.

In this paper, we present the data and analysis of our electronic distance measurement (EDM) program for the period 1988-1995. We concentrate on deformation experienced by the upper edifice of the volcano. Our study has incorporated a summit network of benchmarks, surveyed at least once per year, and a series of fixed prisms on the dome and south flank that were surveyed frequently from lower-flank benchmarks.

Distance measurements over the period 1988-1991 recorded pronounced movements of benchmarks and fixed prisms near the summit, during a substantial hiatus in dome growth. Strain of the summit area was non-axisymmetric, suggesting pressurization from a magmatic conduit at shallow depth and greater mobility of a weakened upper south flank with respect to the rest of the edifice. Episodic dome growth actively resumed in January 1992, and after this period, edifice movements were small.

2.2 Geological Background

Explosive eruptions and viscous extrusions of highly crystalline basaltic-andesite lava domes or thick lava coulées from summit vents have been typical of Merapi activity for several centuries (Berthommier et al., 1992; Andreastuti et al., 2000; Camus et al., 2000; Newhall et al., 2000). Larger-scale explosive eruptions that were typical prior to 1900 have been largely replaced with smaller dome-collapse events during the 20th century (Newhall et al., 2000; Voight et al., 2000a). Dome growth at Merapi commonly occurs within a horseshoe-shaped, open-ended summit crater formed by collapse of portions of the pre-existing dome complex (Voight et al., 2000a). Over time the summit craters and breaches have been ephemeral, as lavas partly or entirely filled such depressions. Subsequent explosive eruptions or major dome collapses have created new depressions that can differ from previous depressions in size and orientation. For example, the major eruption of 1930 formed a pronounced westward-facing crater ("Senowo" crater) that filled more or less completely with lavas during subsequent

eruptions (Neumann van Padang, 1931). The southwestward facing Batang breached crater that influenced the events during 1988-1995 (Fig. 2-2) arose from events during the 1961 eruption (Voight et al., 2000a). Though mostly filled in by lavas dating from 1984 to present, this crater retains sufficient topographic relief to continue to direct small or moderate scale volcanic activity towards the southwestern flank of the volcano.

Pyroclastic activity usually accompanies lava dome growth and destruction at Merapi, and several distinctive eruptive patterns have been recognized (Hartmann, 1935; Zen et al., 1980; Zen, 1985; Voight et al., 2000a). Partial to total collapse of the poorly vesicular lava generates the nuées ardentes referred to as "Merapi type" (Escher, 1931, 1933; Boudon et al., 1993; Voight et al., 2000a). The lethal pyroclastic currents of 22 November 1994 were typical of this type, resulting from piecemeal collapse of about 15-20% of the total 1984-94 dome volume (Abdurachman et al., 2000; Brodscholl et al., 2000).

A pronounced asymmetrical juxtaposition of a "young" Merapi forming the presently active cone upon the eroded remnants of an "old" Merapi suggests a major collapse at this volcano in the past. The timing and delineation of the associated debris avalanche deposit remain open questions that are still being debated (Newhall et al., 2000; Camus et al., 2000). Upper-flank slopes of 40^{o}-60^{o} on "young" Merapi, with extensive alteration-weakened areas around high-temperature geothermal areas such as Gendol-Woro (Fig. 2-2) highlight the possibility of future collapse events. We take seriously the possibility of moderate-size upper flank failures that would be comparable to the 1963 Little Tahoma Peak rockfalls at Mt. Rainier (Crandell and Fahnestock, 1965),

and our deformation data confirm the weakness of this portion of the edifice. Such a failure might be accompanied by a highly dangerous explosive eruption.

2.3 Summary of Recent Activity

Merapi was almost continuously active from 1967 through 1984. Previous activity is summarized by Voight et al. (2000a). A moderate explosive eruption occurred in January 1969, and substantial dome collapses accompanied by nuées ardentes occurred in 1976, 1981, and 1984. The lava dome was destroyed in the 1984 eruption (Boudon et al., 1993). Dome growth resumed shortly thereafter and continued in pulses, attaining a total volume of about 6.4×10^6 m^3 by earliest 1989. Growth rates were slow between 1987 and 1989, and minor changes of the dome profile by endogenous growth added about 0.4×10^6 m^3 through mid-1990. Following several years of accelerating deformation as discussed in this paper, active lava effusion resumed in January 1992 and was accompanied by numerous gravitationally-generated Merapi-type nuées ardentes. The intact dome volume more than doubled, to 14.5×10^6 m^3. Lava overtopped the crater rim on the northwest side in spring 1992, expanding the flank regions exposed to nuées ardentes. Further pulsed extrusion continued in late 1992 into 1993. Dome surface deformation in late December 1993 preceded breakout of a new lava lobe in February 1994, and led to nuées ardentes in March. The 1994 lava accumulation grew steadily, and collapsed on 22 November 1994, when the total dome volume had reached 16×10^6 m^3. Dome growth was again evident in December 1994 and has since continued at varying rates through 1999 (Voight et al., 2000b).

2.4 Monitoring by Electronic Distance Measurement

2.4.1 History and Organization

The Volcanological Survey of Indonesia (VSI) has the responsibility for assessing Merapi's hazards, with most efforts conducted through their Merapi Volcano Observatory (MVO) in Yogyakarta. Cooperative efforts in the early 1980's between the U.S. Geological Survey (USGS) and VSI formed the basis for the seismic monitoring program that operates today (Ratdomopurbo and Poupinet, 2000; Voight et al., 2000a). Implementation of deformation monitoring at Merapi at that time was made difficult because of eruptions at Galunggung in 1982-83. Nevertheless, preliminary EDM surveys at Merapi in the early 1980's using fixed prisms showed no movements exceeding system noise (Siswowidjoyo et al., 1985).

In 1988 a new program using EDM was established by Voight as part of a project supported by the USGS, US AID, and VSI (Voight, 1988; Voight et al., 1989). Our subsequent work operated mainly with NSF support.

Due to the steep topography of Merapi, the EDM program consists of separate *observatory* and *summit trilateration networks* (Figs. 2-1, 2-2, 2-3, 2-4). Summit measurements yield precursor displacements and strain around the vent and are closely related to high-level conduit pressure and growth or destruction of the lava dome. The observatory network measures slope distance from several VSI observation posts at the base of the cone in order to monitor movements of fixed prisms arrayed on the upper flanks of the volcano (Figs. 2-1, 2-3, 2-4).

Global Positioning System (GPS) measurements were first carried out by Institute Géographique National (France) researchers in 1993, and continue to be monitored by VSI and French survey teams (Jousset et al., 2000). The GPS technique allows mark-to-mark distances to be determined for cross-crater shots obstructed by the rising lava dome since 1992, and have supplanted the summit EDM measurements since 1995.

2.4.2 Methods

Differing approaches were used for the two types of EDM monitoring surveys conducted at Merapi. In 1988, Voight and colleagues installed a network of benchmarks and several fixed prisms around the summit of Merapi (Figs. 2-1, 2-2A, 2-4A). The benchmarks thereafter allowed the setup of EDM/theodolite instrumentation and tripod-mounted reflector stations during annual surveys that formed the basis for trilateration data adjustments. The frequency of measurements was constrained by the effort and cost associated with the surveys, as instruments, supplies, food, and water for drink and cement had to be hand-carried to the summit. The surveys usually took three or four days to complete, and required survey teams to camp out at the summit. Helicopter support was unavailable, and was replaced here by processions of dozens of torch-bearing porters surmounting the spiny ridge paths of Merapi like scattered fireflies on moonless nights. They remain indelible in our memory.

Two baseline stations were located off the cone of "new" Merapi by adapting preexisting survey monuments installed by the Dutch at Selokopo Duwur (SEL) and Pusunglondon (PUS) (Fig. 2-1). Line of site considerations from the summit constrained

these selections, but it was also believed that SEL would represent a nearly stationary point during future volcano deformation. GPS results from 1993 and later show these stations as essentially stationary within the errors of the method (Beauducel and Cornet, 1999; F. Beauducel, 1999, written communication). The resulting geometry of the base triangles is necessarily eccentric, and this influences absolute station positioning and displacement errors; relative errors for movements between station pairs are unaffected by baseline selection.

Fixed prisms for the observatory network were bolted to rock on both the lava dome and upper south flank, generally following techniques described by Doukas and Ewert (1992). Distance measurements to the prisms were shot originally from the Plawangan observation post located approximately 5 km south of the summit (Figs. 2-1, 2-4A). Between 1992 and 1995, further fixed prisms were installed for measurements from Plawangan (Fig. 2-4B), Babadan observation post on the northwest flank (4 km), and a ridge above Deles village to the southeast about 3 km from the summit (Fig. 2-1).

2.4.3 Data Processing and Error Estimates

Data were adjusted using conventional procedures to account for instrument-prism constants, setup heights to optical centers, and atmospheric corrections (at instrument site only) (Bomford, 1980). Further processing used commercial software for three-dimensional trilateration adjustment of distances and angles that minimized the sum of squares for the residual errors. In these adjustments, benchmark SEL was assumed stationary with a fixed azimuth to the other baseline benchmark PUS. A further baseline

constraint was applied to PUS using 10 ppm for horizontal coordinates and 20 ppm for elevation. Absolute positions relied on inserting the Universal Transverse Mercator (UTM) position for SEL as calculated from GPS measurements of 1993 (T. Duquesnoy, 1994, written communication).

The least squares adjustments provide some estimate of total summit network errors. Excluding 1988, when logistics spread measurements over 8 weeks, and 1991, when only part of the network was occupied, standard errors on distance and vertical angle were no greater than 3 mm (~1 ppm) and 10 arcsecond. Standard errors were combined to generate 95% confidence ellipses on location and displacement. A final step was input of the trilateration reductions into equations appropriate to infinitesimal strain analysis in order to calculate the horizontal principal strain tensors for three-station network triangles (see Appendix).

2.5 Results of the EDM Measurements

2.5.1 1988-90

Two summit surveys were conducted in late June and July of 1988 during conditions at the volcano similar to those seen in Fig. 2-4A. About two years occurred between these and the subsequent measurements. The first year (mid-1988 to mid-1999) was relatively aseismic, but accelerating volcano-tectonic (VT) energy release took place during early 1990. Low-frequency (LF) seismicity occurred in June 1990, suggesting renewed fluid migration within the edifice. Ratdomopurbo and Poupinet (2000) and Hidayat et al. (2000) discuss the classification of seismic events.

Three weeks prior to our survey of September 1990, VT energy release culminated in a seismic crisis; gas venting occurred from the upper part of the dome on 24 August 1990.

2.5.1.1. Summit network

Stations arrayed on the summit buttress from NUR to GQ4, in north and east quadrants (Fig. 2-2A), show dominantly radial movements of about 5 to 20 cm (Fig. 2-5A). Vertical components are generally negligible for these stations, but significant uplift of 9 cm and 33 cm was measured along the northwest crater rim for stations NUR and TRI, respectively. Outward displacement at station TRI is more pronounced, indicating non-axisymmetric deformation. The greater displacements here may reflect proximity to the conduit pressure source for the narrow northwest rim of the crater.

Relatively small horizontal displacements for LUL and PUN, compared to TRI, indicate non-axisymmetric deformation with greatest deformational resistance in the massive rock buttress of the upper flank and summit north of the crater. A subsidence of PUN by ~8 cm during this period, anomalous when compared to other neighboring stations, continued through 1991 and perhaps reflects localized instability of this station on the very highest part of the crater rim.

Relatively large outward movements occurred at DOZ and ALB on the south rim (Fig. 2-5A), in marked contrast to movement of GQ4 and the fixed prism YAY sited immediately north of the Gendol breach, where little or no significant displacements were detected. Displacements for DOZ and ALB were nearly identical at 63 cm directed S10^{o}-20^{o} W for the two-year period, and match those of nearby fixed prisms (discussed

below). A pronounced displacement discontinuity therefore straddles the Gendol breach (Figs. 2-3, 2-4A, 2-5A), a topographic notch that extends radially from the Gendol-Woro zone of very high temperature fumarolic alteration. The breach separates East Dome lavas extruded in 1888-1909, northeast of the breach, from West Dome on the southwest whose lavas were extruded in 1911-1913.

More precise slope distance measurements on the summit network (summarized in Fig. 2-6) reveal large movements averaging 40 cm/year on cross-crater measurements and inflationary extensions of up to 2.4 ± 1.4 cm/year for most radial and circumferential station pairs.

2.5.1.2. Observatory Network

As measured from Plawangan (PLW), prisms LAN and BUG on 1986-1988 lava inside the crater (Figs. 2-2A, 2-4A) moved outward at nearly constant rates of 25 cm and 30 cm per year ± 3 cm, respectively, between 1988 and 1990 (Figs. 2-5A, 2-7). The slope distance changes correspond to a time of minor changes in surface morphology higher on the lava dome. Displacements are comparable with trilateration stations ALB and DOZ on the south rim, each of which averaged about 32 cm/year southward movement. Fixed prism CEC on the south flank below ALB and DOZ (Fig. 2-2A) experienced accelerating outward displacement that matched ALB and DOZ and, in the short term, reached a rate of 1 m per year before it was lost in mid-1989 (Fig. 2-7). Across the Gendol breach, in contrast, little or no movement was detected by fixed prism YAY to 1989. Slope distance changes to YAY accelerated to about 13 ± 3 cm/year between 1989 and 1990 (Figs. 2-5A, 2-7).

2.5.2 1990-91

While a hiatus in eruptive activity continued, accelerating deformation and seismicity indicated enhanced edifice pressurization that presaged further activity. During 1990-91, the greatest edifice displacements and strains were measured on both the summit and observatory networks. At the same time, VT seismicity peaked, tremor increased at the beginning of 1991, and long period events occurred irregularly. Multiphase earthquakes (MP), events usually associated with lava dome growth (Shimozuru et al., 1969; Ratdomopurbo, 1995; Ratdomopurbo and Poupinet, 2000; Hidayat et al., 2000), appeared in small numbers beginning in early 1991.

2.5.2.1. Summit network

The summit network was occupied in late August 1991. Accelerating displacements characterized the horizontal movements with respect to the two preceding years at several stations (Fig. 2-5B). Notably, southwards motion of about 110 cm for stations DOZ and ALB atop the south flank for the one year period greatly exceeded the 32 cm/year mean rate detected by the 1988-90 surveys (Fig. 2-5A). Slope distance changes across the crater also uniformly accelerated from 40 cm/year in 1988-1990 to 1.0-1.2 m/year in 1990-91. The radially outward movement of 24 cm for northwest rim station TRI was a little more than the mean rate of 20 cm/year recorded in the previous two years.

Stations on the north and northeast flank showed only small horizontal displacements that are not significant with respect to their 2σ error bounds. A very small

radial outward displacement is perhaps suggested in their data. However PUN, very near the crater rim, continued a radially inward motion, and dropped -15 ± 9 cm (Fig. 2-5B). Elevation drops at a number of other stations are notable, in contrast with uplift or no elevation change observed for the same stations between 1988 and 1990 (cf. Figs. 2-5A, 2-5B). South flank stations DOZ and ALB dropped 8 cm and 25 cm, respectively, while the north rim stations dropped 9 to 15 cm (all ± 9 cm).

The large southerly displacements for the south flank stations in the summit network indicate continued, pronounced non-axisymmetric and inelastic deformation. The "stable summit" thus seemed to include nearly the complete summit region north of the Gendol breach, with large movements occurring at rim locations southwest of this feature (Fig. 2-5B).

2.5.2.2. Observatory Network

With the continuing hiatus in activity, site BUG was reestablished and three additional prisms were installed on the dome lava nestled inside the crater (Fig. 2-5B). Station NOM was installed near the apex of the south flank crater rim between trilateration benchmarks DOZ and ALB (Fig. 2-2A). The frequency at which measurements were made averaged about one set per month, lower than in 1988 and 1989, but still allowing a detection of the change in displacement rate for the fixed prisms (Fig. 2-7).

From August 1990 to August 1991, dome prisms moved 34 cm to 51 cm toward the EDM station PLW at Plawangan (Figs. 2-5B, 2-7). Progressively greater displacements generally occurred toward the summit of the dome, excepting KEE, which

displayed the greatest movement of 51 cm during this period. Shorter-term variations in displacement rate were detectable, but were not correlated to any degree between stations. Rates for these shorter periods of about 1 to 3 months varied from 3 to 70 cm/year. The style of variation also differed between stations. For example, At KEE, the rate accelerated regularly from 37 to 70 cm/year, whereas higher on the dome at station GOB, 4 months of 25 cm/year movement were followed upon by 3cm/year and 12 cm/year rates in succeeding 4 month periods.

For the uppermost south flank, NOM moved 112 cm towards Plawangan, in good agreement with the horizontal vector displacements of 117 cm and 108 cm for ALB and DOZ, respectively.

2.5.2.3. Displacement discontinuity across the Gendol breach

The YAY prism north of the Gendol breach confirms the discontinuity in deformation at Gendol. The displacement rate for YAY increased from 5 cm/year in 1989 to about 15 cm/year in 1990. The prism was "lost" by deterioration sometime in 1991, but a new fixed prism was installed at this same site in 1993 and calibrated to the previous setup. Assuming the movement trend for 1988-91 terminated with depressurization associated with dome extrusion in February1992, interpolation suggests a displacement rate for YAY towards Plawangan of 20-25cm/year during 1991 (Fig. 2-7). This is a maximum value and contrasts with the movements exceeding 1 m per year for prism NOM, and stations ALB and DOZ (Fig. 2-7).

2.5.3 1991-92

A new eruption began 20 January 1992, with a fresh lava extrusion building upon the existing dome (Ratdomopurbo and Poupinet, 2000). The volume of the dome complex by late 1992 was 14.5 x 10^6 m^3. Subsequent surges of dome growth and partial dome collapses (notably 2 February 1992) that generated nuées ardentes (Fig. 2-8) characterized the activity of Merapi through the remainder of the period considered in this paper (to 1995). The distinct change in eruptive activity that began in January 1992 correlates with a marked change in the style and magnitudes of displacements of points about the summit region.

2.5.3.1. Summit network.

The summit survey was carried out in October and November 1992. Pronounced southwards displacement continued in the upper south flank based on data from the sole-surviving south-side benchmark at ALB (Figs. 2-6, 2-9A), which moved 84 cm. Station DOZ and the fixed prisms located on the lava dome and the south flank were lost by the end of this period. Because of the long, approximately one-year interval between surveys, we can do no better than to infer that the great majority of this displacement occurred as a precursor to the eruption of mid-January and February 1992. However, this supposition is strongly supported by measurements across a radial crack that were carried out on the crater rim between PUN and LIL at frequent intervals throughout 1991 and 1992 (Fig. 2-10). These measurements indicate a sharp decline in movement rate following the January/February 1992 eruption. Seismicity at depth, furthermore, underwent substantial declines after this eruption (Fig. 2-10).

Other stations on the north and NE rim show small, statistically insignificant movements based on 2σ error ellipses (Fig. 2-9A). A 14-cm SSW movement is suggested for station IPU, but this is poorly constrained by abbreviated summit measurements taken during the 1991 survey.

A subsidence at station ALB of the order of 41 cm for 1991-92 continued a south flank trend of subsidence evident in the data of 1990-91. Vertical changes at other summit stations were not resolvable at ± 9 cm.

2.5.3.2. Observatory network

Almost no data was collected, as the fixed-prism network was lost due to deterioration and vandalism between 1991 and 1993.

2.5.4 1992-93

Eruptive activity during this time was dominated by episodic dome growth. A significant sequence of nuées ardentes was generated by dome lava effusion in February 1993. The summit EDM network was resurveyed in September 1993, and the observatory network was reestablished on the upper south flank at this time. The topography is represented in Fig. 2-11A. Additional fixed prisms were established on the northwest crater rim for measurement by EDM from benchmark BAB at the Babadan observation post (Figs. 2-1, 2-2B).

2.5.4.1. Summit network.

This first survey *interval* coming after the eruption of January/February 1992 (October 1992 to September 1993) reflects in great measure the deformation pattern that would prevail at the summit for the remainder of the study period into late 1995. The loss of TRI during the 1992 eruption, and a later gravity collapse of ALB into the crater, hampered a characterization of summit strains in subsequent months. A more stable survey point DZ2 was eventually established near, but not equivalent to, the old site DOZ, and a new station TR2 was installed on the northwest rim near the location where 1992 lava first spilled out of the crater (Fig. 2-2B).

Specific results between 1992 and 1993 show significant movements horizontally and vertically at TR2 on the northwest rim, GQ4 in the Gendol-Woro sulfataras, and DZ2 on the south flank (Fig. 2-9B). Continued mobility of the south flank is suggested by displacement of DZ2 14 cm to the southwest. However, a movement of just 3 ± 2.8 cm for fixed prism ABD situated 50 m below DZ2 (Figs. 2-9B, 2-12) urges caution in interpretation of the DZ2 displacement as a large-scale translation of the upper south flank.

North rim stations in general show eastward shifts of several cm that straddle the bounds of 95% statistical significance. It is unclear whether these apparent small movements are genuine or are artifacts arising from assumptions in the least-squares adjustment of data, e.g., the fixed position of baseline station PUS. If genuine, they might reflect loading of 1992 and 1993 dome lava against the edifice.

The NW rim station TR2 suggests significant subsidence of 37 cm during 1992-93. This perhaps resulted from loading of the crater rim by the eruption of new lavas in

late 1992 and early 1993. However, as only one sideshot to TR2 was performed in 1992 (the new lava blocked the cross-crater shot, compare Figs. 2-2A, 2-2B), we do not have full confidence in either the vertical component or the horizontal vector.

2.5.4.2 Observatory network

Significant shortening was observed between Babadan and the northwest rim (Figs. 2-9B, 2-13). Prisms on the edifice closest to the dome lava of 1992 and 1993 (SAT, DUA) moved most toward Babadan, displacing 8.8-12.0 ± 2.5 cm in slope distance. Prisms 70 m farther north and downslope showed lesser movements of 4.9 cm and 3.9 cm. We interpret this to be a displacement gradient related to loading of the crater rim by the 1992-93 lava.

Fixed prisms on the south flank remained damaged or lost in late 1992, except for reflector ABD. As mentioned above, movement of this point was 3 ± 2.8 cm towards the Plawangan observation post between July 1992 and September 1993 (Figs. 2-9B, 2-12).

2.5.5 1993-94

Eruptive activity during this time encompassed a major phase of lava extrusion and dome growth that formed the 1994 dome and coulée shown in Figs. 2-11B and 2-9C. The 1994 summit survey was performed about one month prior to the major dome collapse of 22 November 1994. In this eruption nearly the entire 1994 dome, some 2.0 to 2.6 x 10^6 m^3 in volume, was launched downslope as a succession of nuées ardentes with runouts as far as 6 km from the summit of Merapi (Voight et al., 2000b; Abdurachman et al., 2000; Brodscholl et al., 2000).

2.5.5.1 Summit network

The summit network was surveyed mid-September 1993, and again in mid-October 1994. A new benchmark, AL2, was installed for the 1994 survey near the former site of ALB, which had been destroyed in a rockfall that affected the crater rim. Overall, results detected no horizontal or vertical movements within the 95% confidence bounds on displacement (Fig. 2-9C). An exception was the vertical movement of PUN, showing a continued subsidence of 11 cm that is attributed to local gravitational instability of the crater rim. The new northwest rim station TR2 also displayed uplift of about 17 cm, although this result may be suspect due to poor constraints at the edge of the trilateration network.

Circumferential lines on the north rim show a consistent minor shortening during this period (Fig. 2-6), consistent with small amounts of north flank deflation. Cross-crater measurements to DZ2 on the south flank (Fig. 2-6), however, suggest widening of 5.0 ± 2.3 cm along this line, although reduction of the data to horizontal displacements generates errors too large to discern reliable absolute movements for DZ2. The deformation is consistent with outward squeezing of the crater walls during build-up of the new dome lava.

2.5.5.2 Observatory network

Fixed reflectors were refurbished, reinstalled, or augmented on the upper south flank in late 1993, allowing numerous measurements to again be made from PLW at the Plawangan observation post. Of particular importance were the reoccupations of sites NOM and YAY on opposite sides of the Gendol breach (Fig. 2-2B). Installation of new

prisms here were sufficiently precise to allow comparison of the new measurements with older surveys made prior to the eruption of 1992. Paired prisms were installed at several sites (PHX, RUN, ABD, YAY) to allow dual measurements of a given station from both Plawangan and a planned EDM station DEL near Deles village (Figs. 2-1, 2-2B).

Results suggest a 2-2.5 ± 2.8 cm southward movement towards Plawangan for the highest fixed prisms NOM and SUB on the upper south flank (Figs. 2-12, 2-14A) while slightly lower-elevation reflectors ABD, KAS, and RUN show negligible significant movement with respect to Plawangan. Reference prisms across the Gendol Breach at YAY and BEA show no movement (Figs. 2-12, 2-14A). No indicated displacements, however, exceed their 2σ error bounds.

Reflectors aimed at Babadan from the northwest flank were measured in August and again in October 1994. They likewise suggest shortening no greater than 2-2.5 cm, again marginal to non-significant with respect to their ± 2.5 cm 2σ errors (Figs. 2-13, 2-14A). This result suggests a decline in movements compared to 1992-1993.

2.5.6 1994-95

Surveys conducted during this period encompass the significant dome collapse eruption of 22 November 1994. A summit trilateration survey in October 1994 was followed by flank distance measurements from base stations BAB, PLW, and DEL in October and very early November. Following the dome collapse, flank measurements were performed as part of the crisis response from PLW and DEL, and

repeated again in March 1995. Full sets of summit trilateration and flank measurements were performed in late September 1995.

2.5.6.1 Nature of the eruptive activity

Most significant during this interval was the major dome collapse on 22 November 1994. Much of the lava erupted between February and November of 1994 was lost in this event, leaving an arcuate headwall (Fig. 2-9D) in the remaining dome material. The original vent for the 1994 lava extrusion controlled geometry of the headwall. The collapse followed long-term adjustments to the summit geometry (Fig. 2-6). However, no short-term precursors to the 1994 collapse were evident in the various geophysical parameters used to monitor the volcano, and none are recognized in hindsight. The first seismic events related to the eruption appear attributable to the first collapses of lava dome material (Global Volcanism Program, 1995). The collapse of the lava dome on 22 November may be substantially an "accident" of gravity developed from slowly evolving instability in downslope expansion of the lava dome and coulée. More detailed evaluations of this eruption and its precursors can be found elsewhere in this issue (Voight et al., 2000b; Abdurachman et al., 2000; Brodscholl et al., 2000).

When visual observations of the summit became possible in early December with clearer weather and a lessening density of the plume, a dome of new lava was visible within the collapse scar of 22 November. The geometry of the new dome did not at first appear to vary much, as attrition from frequent rockfalls balanced the flux of extruded lava. By the time of our summit and flank surveys in September-October 1995, changes

in the new lava dome morphology suggested at least three cycles of dome growth following the 22 November 1994 collapse.

2.5.6.2 Summit network

Absolute horizontal displacements showed no significant changes on the summit network between September 1994 and October 1995 (Fig. 2-9D), in spite of the significant changes that occurred in the lava dome volume and geometry. Minor outward displacement recorded at LUL, DZ2, and AL2 lie well within their error bounds. The more precise slope distance changes between station pairs may indicate a change from deflationary to inflationary movements between the successive surveys of 1993-94 and 1994-95. Circumferential lines show extension of up to 5.4 ± 1.1 cm (2σ) in most cases (excepting LUL-NUR, PUN-GQ4) (Fig. 2-6). Cross-crater expansion also appears significant at 2-6 ± 1.1 cm (Fig. 2-6). Lines oriented oblique or radial to the vent show small to negligible movement except for -16 cm shortening on GQ4-DZ2. The latter may reflect instability of the deteriorating GQ4 monument in the Gendol-Woro sulfatara. A more stable benchmark AYI located 4.1 m N36^{o}E from GQ4 was therefore incorporated into the 1995 trilateration adjustment.

Oblique and radial shots to baseline stations SEL and PUS (Fig. 2-6) generally show statistically insignificant changes. Shortening with respect to PUS shot from MAR and LUL on the north rim, however, may indicate minor gravity movement by PUS.

2.5.6.3 Observatory network

Three to four sets of measurements were made from flank base stations to fixed prisms between October 1994 and October 1995. As measured from Babadan (Figs. 2-

13, 2-14B), shortening of slope distance by up to 2.5 cm to fixed prisms on the NW flank continued into 1995, but 2σ errors of ± 2.5 cm on the displacement urge caution. Shortening over the two years between 1993 and 1995 is significant, however. A gradient in displacement is evident with the largest movements occurring at SAT and DUA nearest the dome lava spillover point on the crater rim (Fig. 2-2B).

For the south flank, measurements were made from a position of relative safety at DEL nine days before and over four days after the 22 November 1994 collapse (Fig. 2-15). Results suggest a slope distance lengthening of 2.1-2.6 ± 2.3 cm by 27 November, consistent with the unloading of the lava mass near the summit. A survey conducted 22 December 1994 from Plawangan observation post obtained signal returns from prisms PHX and RUN (Figs. 2-1, 2-2B). Neither showed significant change since the measurements of late October (Fig. 2-12). Repeating this effort in March 1995 detected no change more significant than a deflationary 2.0 ± 2.8 cm for ABD.

Combined results from Plawangan and Deles are more intriguing as it was possible to employ the paired prisms at sites ABD, RUN, PHX, and YAY for measurements from both PLW and DEL. The results for October-November 1994 to October 1995 provide a displacement vector for the south flank prisms with respect to the observatory stations (Fig. 2-14B).

Measurements show significant outward movement of two upper south flank prisms (Fig. 2-14B). While the lowest prisms on the south flank appear stationary (ORA, PHX at 2213 m and 2441 m, respectively), those nearer to the summit exhibit slope

distance changes as great as 6.7 ± 2.8 cm (NOM, SUB). The latter prisms were shot only from Plawangan. Using measurements from both Plawangan and Deles to the fixed prism pairs RUN and ABD suggests 1.5 and 2.5 ± 2.8 cm southward movement. In contrast, negligible movements were recorded for PHX and YAY. A gradient is evident in these displacements, with highest prisms on the south flank moving most, slightly lower prisms moving less, and mid-flank prisms and those on the northeast side of the Gendol breach showing cumulatively no change.

2.6 Deformation fields and conceptual models

2.6.1 Deformation for 1988-1992

A major consequence of this study is the documentation of a significant 4-year period of deformation precursory to the eruption of January/February 1992 (Fig. 2-10). Displacements that were observed near the summit of the south flank attained a horizontal rate of at least 1.1 m/year in 1990 and 1991. Lesser though still large rates of 0.3-0.7 m/year were observed over the same period for prisms set on the lava dome (only the component toward benchmark PLW was measured).

General aspects of summit deformation gradients are revealed by strain analysis (see Appendix). Cross-crater rates of strain accelerated from less than 3×10^{-6} /day (1988-90) to more than 11×10^{-6} /day in the period just prior to the 1992 eruption (Fig. 2-16). The movements reflect a general, though not symmetric, radial and circumferential extension (areal dilatation) over the center of the crater. Large extensions are oriented

approximately north-south in the crater area, and are linked to nearly uniaxial stretching of the adjacent summit buttress on the north and east (Fig. 2-16).

The deformation field is interpreted to be the result of slow, upward migration of a pressure source beneath the summit crater. A shallow magma chamber has been inferred to lie at roughly 1-km depth (Ratdomopurbo and Poupinet, 2000), and pressurized flow above this level – beginning at least as early as 1988 – is proposed as the cause of the surface deformations. This rising basaltic andesite magma, with phenocryst content greater than 50% by volume and with a strongly silicic interstitial liquid (Hammer et al., 2000), was highly viscous due to degassing and combined microlite and phenocryst crystallization (Hess and Dingwell, 1996). The pressure gradient was controlled by magma chamber pressure and by shallow-level pressurization due to degassing, and the resistance offered by the upper edifice to conduit propagation.

The response of the upper part of the edifice is not well explained by axisymmetric elastic models of homogeneous media with pressure sources centered beneath the crater, because markedly greater displacements occur along specific parts of the crater rim, e.g., west of DOZ on the south rim, and TRI on the northwest rim. The large differences in the magnitude of these displacements suggest that the medium was inhomogeneous. In addition, some movements were probably non-elastic, influenced by joint slip and crack widening in response to the conduit pressurization. The displacements of 1988-1992 were not recovered after the 1992 eruption relieved much of the pressure. Subsidence of parts of the upper south flank and north rim began sometime in 1990-91 at the same time as large movements were occurring on the south flank. Such

displacements are further at odds with equidimensional or cylindrical pressure sources in homogeneous elastic media (e.g., Dieterich and Decker, 1975).

Projecting the horizontal displacement vectors (Fig. 2-5A) or maximum principal strains (Fig. 2-16A) for 1988-90 backward to a hypothetical pressurization epicenter suggests a focus near the northeast part of the crater, and a displacement discontinuity within the edifice crossing the region of Gendol. The northeast crater location similarly has been identified as the epicenter for multiphase earthquakes (Hidayat et al., 2000).

We consider in general terms two deformation models. The first model consists of a dike- or elliptical-shaped pressure source. The dike (slot) or elliptical conduit model for the pressurization-induced displacement field may be a better conceptual model than axisymmetric pressure sources, for both horizontal and vertical displacements are predicted to be relatively small near the inflation center, and larger some distance away. Strain analysis of the trilateration triangles illustrate a maximum extension oriented roughly north-south (Fig. 2-16), suggesting approximately an east-west long-axis orientation for the conduit. This orientation is roughly perpendicular to the aligned foci distribution reported by Ratdomopurbo (1995) for low-frequency seismic event multiplets in a swarm that peaked in September 1991 (Fig. 2-17). The seismic data suggest the possible applicability of a dynamic fluid-filled crack model (Chouet, 1988). In this interpretation, the low-frequency seismicity could have been produced by gas streaming through cracks above the rising magma. The cracks would open in accordance with the extensional stress field, and magma might then fill and pressurize these cracks, leading to the deformation model discussed above.

Problems with this simple model include: (1) The limited lateral extent available for the dike-shaped conduit; (2) the negligible uplifts experienced at stations DOZ and ALB while these stations were experiencing marked outward, probably non-elastic horizontal displacement; and (3) the high, non-Newtonian viscosity and apparent yield strength of the magma resisting dike propagation.

In the second, alternative general model, we focus not on the symmetry of the pressure source, but rather on the asymmetry and heterogeneity of the edifice (Figs. 2-18, 2-19). While detailed and thorough analyses of slope deformation simulations are beyond the scope of this paper, Fig. 2-20 presents some relevant qualitative information based on preliminary two-dimensional finite difference modeling. Deformation is assumed to be plane strain, a simplification of actual conditions in which three-dimensional geometry and material property distributions are likely important. The models assume a pressurized dislocation high in the edifice, an assumption consistent with pressurization induced by melt degassing and microlite crystallization.

Two situations are compared. In one, the volcano is assumed homogeneous, and the resulting displacement fields are of similar magnitude on both the north and south flanks (Fig. 2-20B). This is contrary to our field observations, which indicate the clear dominance of south-flank deformation. In addition, modeled displacement vectors high on the flanks display large vertical components, also contrary to observations.

Thus, we examine a second situation, in which the south flank and summit areas are assumed to have bulk and shear moduli reduced by a factor of 5 (Fig. 2-

20C). This local reduction of modulus is justified by the numerous fumaroles in the southern sector, and the highly altered lavas locally observed. The result of this model adjustment is to enhance the deformations experienced by the south flank, in comparison to those on the summit and north flank (Fig. 2-20D). Likewise, the displacement vectors on the south flank have flattened out, and are now qualitatively similar to those observed.

In the above interpretation, which we prefer, the unequal deformations experienced by the edifice reflect mainly the compliance and steep slopes of the south flank and the thin northwest rim, in contrast to the stiff, massive buttress of the summit edifice to the north and east. The deformations observed can then be produced by non-symmetric yielding, in response to relatively uniform and possibly symmetric pressures exerted about the conduit. The displacement discontinuity observed at the Gendol breach represents a major rock mass defect that penetrates into the interior of the edifice.

2.6.2 Deformation since 1992

Movements have been much smaller since 1992, suggesting that the eruption beginning January 1992 relieved much of the pressure. With the lava breakout and a high rate of effusion, the associated edifice strains occurred at a much reduced rate of 1 to 2 x 10^{-6} /day for cross-crater measurements. For the most part, surveys from 1992 through 1995 suggest that horizontal displacements measured by the summit network do not exceed their 95% error bounds (Fig. 2-9). During this period, the upward flux of magma

through the conduit was variable but sufficiently active to maintain an effectively open vent system. Thus, following the outbreak of lava in 1992, high-level conduit pressurization was much reduced, and the edifice suffered little upper-flank deformation.

During 1992-95, EDM measurements made to fixed prisms on the upper flanks generally showed outward displacements of no greater than several centimeters per year. Unfortunately, the measurement frequency was insufficient to enable strong conclusions regarding the correlation of edifice displacement rate to pulses of magma flow.

Upper north flank prism measurements from Babadan indicate as much as 12-cm outward movement of the crater rim during 1992-93. The motions correlate with 1000 μrad outward tilt recorded by two tiltmeters within 70 m of these fixed prisms, along the northwest rim (Young et al., 1994; Young et al., 1995a, b). The deformations are a response to direct loading of the rim by the erupting dome lava during this time or, possibly in addition, tractions exerted on rock by viscous lava at the top of the conduit.

On the south flank, measurements from Deles just before and just after the 22 November 1994 dome collapse detected an associated deflation of up to 2.5 cm in the several days following the eruption (Fig. 2-15). Between October 1994 and October 1995, slope distance vectors using combined measurements from Plawangan and Deles indicate southward movement of at least several centimeters for the upper south flank (Fig. 2-14B). For the same interval, movements were negligible to the north of the Gendol breach (YAY, BEA), suggesting that this structure continued to mark a displacement discontinuity.

2.7 Summit Geology and South Flank Mobility

Mobility of the south flank likely results from the interaction of magmatic pressures, altered zones, and structural discontinuities developed in the upper edifice over the past 200 years or more (Voight et al., 2000a). In our conceptual model, the rising magma provides lateral overpressure to the south flank, via a pathway affected by earlier history (Figs. 2-18, 2-19).

The Gendol breach possibly coincides with a flow contact boundary between the steep flanks of abutting viscous lavas erupted out of vents within the now-buried Mesjidanlama crater of 1872 (Neumann van Padang, 1931; Hartmann, 1935). These lavas formed East Dome on the east flank from 1888 to 1909, and West Dome on the south flank during 1911 to 1913 (Neumann van Padang, 1931; Holcomb et al., 1982). The location of their mutual contact was itself perhaps controlled by a moderate breach of 20 meters or more in the 1872 crater rim near the current Gendol breach (Neumann van Padang, 1936). Explanation for the breach simply as a contact between lavas of different ages may be insufficient to explain its structural function as a displacement discontinuity for edifice deformation. Possibly the breach contains a *radial crack* generated by dome lavas squeezing against the wall of the 1872, 1930, or other craters, or by high-level conduit pressurization. Whatever the origin of this gap, significant fumarolic exhalations at this location during the late 19th Century indicate that the old breach lay at the top of a structure that penetrated the edifice (Neumann van Padang, 1936).

The structural discontinuities of buried crater walls and breaches, radial cracks, and the steep lateral contacts of older viscous domes and lava coulées on Merapi thus favor significant non-elastic deformation of the upper edifice during subsequent volcanic activity. Moderate-size flank failure from the continuation of such deformation on the steep 40^{o}-60^{o} slopes of the south flank seems entirely feasible, and worthy of a systematic, sustained monitoring program. A moderate-sized upper flank failure would be highly hazardous due to the long-runout capability of an avalanche toward the south, and also because of the possibility of such a failure being accompanied by a violent explosive pyroclastic flow. The latter scenario recalls the catastrophic eruption of 1930, which represented the combination of a flank failure of an old dome complex undermined by freshly extruded lava, and consequent explosive volcanism (Neumann van Padang, 1933).

2.8 Acknowledgements

A large number of people have participated in and supported our program of field-oriented observations. We particularly thank VSI Heads Dr. Wimpy S. Tjetjep, and Dr. R. Sukhyar for facilitating the collaboration of the USA authors with their Indonesian counterparts. On a day-to-day basis, VSI staff based in Yogyakarta was of indispensable help in carrying out the field campaigns, and we would especially like to thank former MVO Heads Dr. Pak Olas, Dr. S. Bronto, and current Head Dr. Ir. Mas Atje Purbawinata in this regard. The MVO staff was of tremendous help to us as they carried out difficult field assignments. They include Mas Paijo, Mas Magi, Mas Dalijo, and Mas Ahreef. Dr.

Michel Kasser provided great impetus at the beginning of the EDM campaign in 1988. Collaboration with the GPS work of Dr. Kasser and M. Thierry Duquesnoy later in our research provided a chance to compare results for two very different surveying methods. Special thanks also go to French Cooperants Dr. Philippe Jousset, M. Jacques Tondeur, Dr. Francois Beauducel, and M. Michel Dejean who assisted and collaborated with us even when pressed for time in fulfilling their own challenging duties as French-Indonesian technical liaisons. Hadley Johnson provided key assistance in the strain analysis. We are grateful also to the friendly villagers at Jrakah and Selo for essential logistics assistance. This research was funded by NSF grants EAR-91-06134, 93-16739, and 96-28413, US AID support to B. V. in 1988, and USGS support for B. V. in 1988 and all USA authors in 1995. We thank P. Delaney, E. Iwatsubo, and J. Marso for constructive reviews.

2.9 Appendix: Calculation of Strains

Reduced data from trilateration measurements are used to calculate the horizontal principal strain tensors. Linear strain is first determined from the change in distance between surveys divided by the initial length of the line. The horizontal strain tensor is defined by three independent components (ε_{11}, ε_{22}, and tensor shear strain ε_{12}). Linear strain ε_α on a specific line at azimuth α (measured clockwise from North) relates to these strain components according to:

$$\varepsilon_\alpha = \varepsilon_{11}\sin^2(\alpha) + 2\varepsilon_{12}\sin(\alpha)\cos(\alpha) + \varepsilon_{22}\cos^2(\alpha) \quad (1)$$

Three EDM lines therefore provide sufficient information to simultaneously solve three equations for the unknown strain tensor components.

Equation (1) is derived from infinitesimal strain theory (e.g., Ramsay, 1967) and is appropriate in cases where strains do not exceed 1%. A valid and simplifying assumption in such a case is that the change in azimuth for the measured lines is insignificant when comparing their initial and final states.

The azimuth of the maximum principal strain is calculated from:

$$\alpha_{e1} = 90 - (1/2)\tan^{-1}[2\varepsilon_{12}/(\varepsilon_{11} - \varepsilon_{22})] \qquad (2)$$

The signs of the numerator and denominator in the argument for the arctangent function are significant in that they provide a 4-quadrant result for the arctangent. The azimuth of minimum principal strain is then 90^{o} from (2). The values of the principal strains are determined by substituting the result from (2) into (1) using the tensor components (ε_{11}, ε_{12}, and ε_{22}) solved for earlier.

2.10 References

Abdurachman, E.K., Bourdier, J.-L., Voight, B., 2000. Nuées ardentes of 22 November 1994 at Merapi volcano, Java, Indonesia. J. Volcanol. Geotherm. Res. 100, 345-361.

Andreastuti, S.D., Alloway, B.V., Smith, I.E.M., 2000. A detailed tephrostratigraphic framework at Merapi Volcano, Central Java, Indonesia: Implications for eruption predictions and hazard assessment. J. Volcanol. Geotherm. Res. 100, 51-67.

Beauducel, F., Cornet, F.H., 1999. Constraints from GPS and tilt data on the magma chamber at Merapi volcano (Java, Indonesia). J. Geophys. Res. 104(B1), 725-736.

Berthommier, P.-C., Bahar, I., Boudon, G., Camus, G., Gourgaud, A., Lajoie, J., Vincent, P.-M., 1992. Le Mérapi et ses éruptions: importance des mécanismes phréatomagmatiques. Bull. Soc. géol. Fr. 5, 635-644 (in French).

Bomford, G., 1980. Geodesy, 4th Edition. Clarendon Press, London, 855 pp.

Boudon, G., Camus, G., Gourgaud, A., Lajoie, J., 1993. The 1984 nuée-ardente deposits of Merapi volcano, Central Java, Indonesia: stratigraphy, textural characteristics, and transport mechanisms. Bull. Volcanol. 55, 327-342.

Brodscholl, A.L., Kirbani, S.B., Voight, B., 2000. Sequential dome-collapse nuées ardentes analyzed from broadband seismic data, Merapi volcano, Indonesia. J. Volcanol. Geotherm. Res. 100, 363-369.

Camus, G., Gourgaud, A., Mossand-Berthommier, P.-C., Vincent, P.-M., 2000. Merapi (Central Java, Indonesia): An outline of the structural and magmatological evolution, with a special emphasis to the major pyroclastic events. J. Volcanol. Geotherm. Res. 100, 139-163.

Chouet, 1988. Resonance of a fluid-driven crack: radiation properties and implications for the source of long-period events and harmonic tremor. J. Geophys. Res. 93(B5), 4375-4400.

Crandall, D.R., Fahnestock, R.K., 1965. Rockfalls and avalanches from Little Tahoma Peak on Mount Rainier, Washington. U. S. Geol. Surv. Bull. 1221-A, 30 pp.

Dieterich, J.H., Decker, R.W., 1975. Finite element modeling of surface deformation associated with volcanism. J. Geophys. Res. 80(29), 4094-4102.

Doukas, M.P., Ewert, J., 1992. Installation of bench marks and permanent reflectors for geodetic deformation networks. In: Ewert, J. W., and Swanson, D. A. (Editors), Monitoring volcanoes: Techniques and strategies used by the staff of the Cascades Volcano Observatory, 1980-90. U. S. Geol. Surv. Bull. 1966, 115-124.

Escher, B.G., 1931. Gloedwolken en lahars. Vulkanische katastrophes in Nederlandsch-Indie. Tropisch Nederland 3, 291-320 (in Dutch).

Escher, B.G., 1933. On a classification of central eruptions according to gas pressure of the magma and viscosity of the lava. On the character of the Merapi eruption in Central Java. Leidsche Geol. Meded. VI-1, 45-58.

Global Volcanism Program, 1995. Merapi. Global Volcanism Net. Bull., Smithsonian Institution, 2/95.

Hammer, J.E., Cashman, K.V., Voight, B., 2000. Magmatic processes revealed by textural and compositional trends in Merapi dome lavas. J. Volcanol. Geotherm. Res. 100, 165-192.

Hartmann, M., 1935. Die Ausbrüche des Gunung Merapi (Mittel-Java) bis zum Jahre 1883. N. Jahrb. Min. Geol. U. Palaont. 75, 127-162 (in German).

Hess, K.-U., Dingwell, D., 1996. Viscosities of hydrous leucogranitic melts: A non-Arrhenian model. Am. Min. 79, 113-119.

Hidayat, D., Voight, B., Langston, C., Ratdomopurbo, A., Ebeling, C., 2000. Broadband seismic experiment at Merapi Volcano, Java, Indonesia: very-long-period pulses embedded in multiphase earthquakes. J. Volcanol. Geotherm. Res. 100, 215-231.

Holcomb, R., Djumarma, A., Suparban, F.X., 1982. Geology of the summit region, New Merapi. VSI-Merapi Volcano Observatory, unpub. report, 5 pp.

Jousset, P., Dwipa, S., Beauducel, F., Duquesnoy, T., Diament, M., 2000. Temporal gravity at Merapi during the 1993-1995 crisis: an insight into the dynamical behavior of volcanoes. J. Volcanol. Geotherm. Res. 100, 289-320.

Neumann van Padang, M., 1931. Der Ausbruch des Merapi (Mittel Java) im Jahre 1930. Zeitsch. f. Vulkanologie 14, 135-148 (in German).

Neumann van Padang, M., 1933. De uitbarsting van den Merapi (M. J.) in de jaren 1930-1931. Vulkanol. En Seism. Meded. Nr. 12 (in Dutch).

Neumann van Padang, M., 1936. Die Tätigkeit des Merapi-Vulkans (Mittel-Java) in den Jahren 1883-1888. Zeitsch. f. Vulkanologie 17, 93-113 (in German).

Newhall, C.G., Bronto, S., Alloway, B., Banks, N.G., Bahar, I., del Marmol, M.A., Hadisantono, R.D., Holcomb, R.T., McGeehin, J., Miksic, J.N., Rubin, M., Sayudi, S.D., Sukhyar, R., Andreastuti, S., Tilling, R.I., Torley, R., Trimble, D., Wirakusumah, A.D., 2000. 10,000 Years of explosive eruptions at Merapi Volcano, Central Java: archaeological and modern implications. J. Volcanol. Geotherm. Res. 100, 9-50.

Ramsay, J.G., 1967. Folding and Fracturing of Rocks. McGraw-Hill, Inc., New York, 568pp.

Ratdomopurbo, A., 1995. Étude sismologique du volcan Merapi et formation du dôme de 1994, Ph.D. dissertation. L'Univ. Joseph Fourier-Grenoble I, Grenoble, France, 208 pp. (in French).

Ratdomopurbo, A., Poupinet, G., 2000. An overview of the seismicity of Merapi volcano (Java, Indonesia), 1983-1994. J. Volcanol. Geotherm. Res. 100, 193-214.

Shimozuru, D., Miyasaki, T., Gioda, N., Matahelumual, J., 1969. Seismic observation at Merapi volcano. Bull. Earthquake Research Inst. 47, 969-990.

Siswowidjoyo, S., Tulus, Djumarma, A., Matahelumual, J., Tjetjep, W.S., Pratomo, I., Bahar, I., 1985. Kegiatan G. Merapi, Jawa Tengah, tahun 1984. Proc. PIT XIV Ikatan Ahli Geologi Indonesia, pp. 181-192 (in Indonesian).

Siswowidjoyo, S., Suryo, I., Yokohama, I., 1995. Magma eruption rates of Merapi volcano, central Java, Indonesia during one century (1890-1992). Bull. Volcanol. 57, 111-116.

Voight, B., 1988. Development of geodetic monitoring program at Merapi volcano, Java. US Geological Survey/US AID/OFDA, unpub. report, 30 pp.

Voight, B., Casadevall, T., Cornelius, R.C., 1989. Development of geodetic monitoring program at Merapi volcano, Indonesia. Proc. Gen. Assem., Inter. Assoc. Volcanol. Chem. Earth's Interior, Santa Fe, NM, USA.

Voight, B., Constantine, E.K., Siswowidjoyo, S., Torley, R., 2000a. Historical eruptions of Merapi Volcano, Central Java, Indonesia, 1768-1998. J. Volcanol. Geotherm. Res. 100, 69-138.

Voight, B., Young, K.D., Hidayat, D., Subandrio, Purbawinata, M.A., Ratdomopurbo, A., Suharna, Panut, Sayudi, D.S., LaHusen, R., Marso, J., Murray, T.L., Dejean, M., Iguchi, M., Ishihara, K., 2000b. Deformation and seismic precursors to dome-collapse and fountain-collapse nuées ardentes at Merapi Volcano, Java, Indonesia, 1994-1998. J. Volcanol. Geotherm. Res. 100, 261-287.

Young, K.D., Voight, B., Marso, J., Subandriyo, Sajiman, Miswanto, Paijo, Suharna, Bronto, S., 1994. Tilt monitoring, lava dome growth, and pyroclastic-flow generation at Merapi volcano, Java, Indonesia (abstr.). Geol. Soc. Am. Abst. with Prog. 26(7), A-483.

Young, K.D., Voight, B., Subandrio, Sajiman, Miswanto, 1995a. Ground deformation studies at Merapi volcano, Indonesia. Proc. Merapi Decade Volcano Intl. Workshop, Vol. Surv. Indonesia/UNESCO, Yogyakarta, pp. 13-15.

Young, K.D., Voight, B., Subandrio, Sajiman, Miswanto, 1995b. Deformation monitoring at a Decade volcano: G. Merapi, Indonesia (abstr.). Eos Trans. Am. Geophys. Union 76(46), F671.

Zen, M.T., 1985. Destruction, formation and growth of the Merapi domes, Buletin Jurusan Geologi, Institut Teknologi Bandung, Jilid 14.

Zen, M.T., Suparto, S., Djoharman, L., and Harto, S., 1980. Type and characteristics of the Merapi eruption. Buletin Departemen Teknik Geologi Institut Teknologi Bandung, Jilid 1, 34-46.

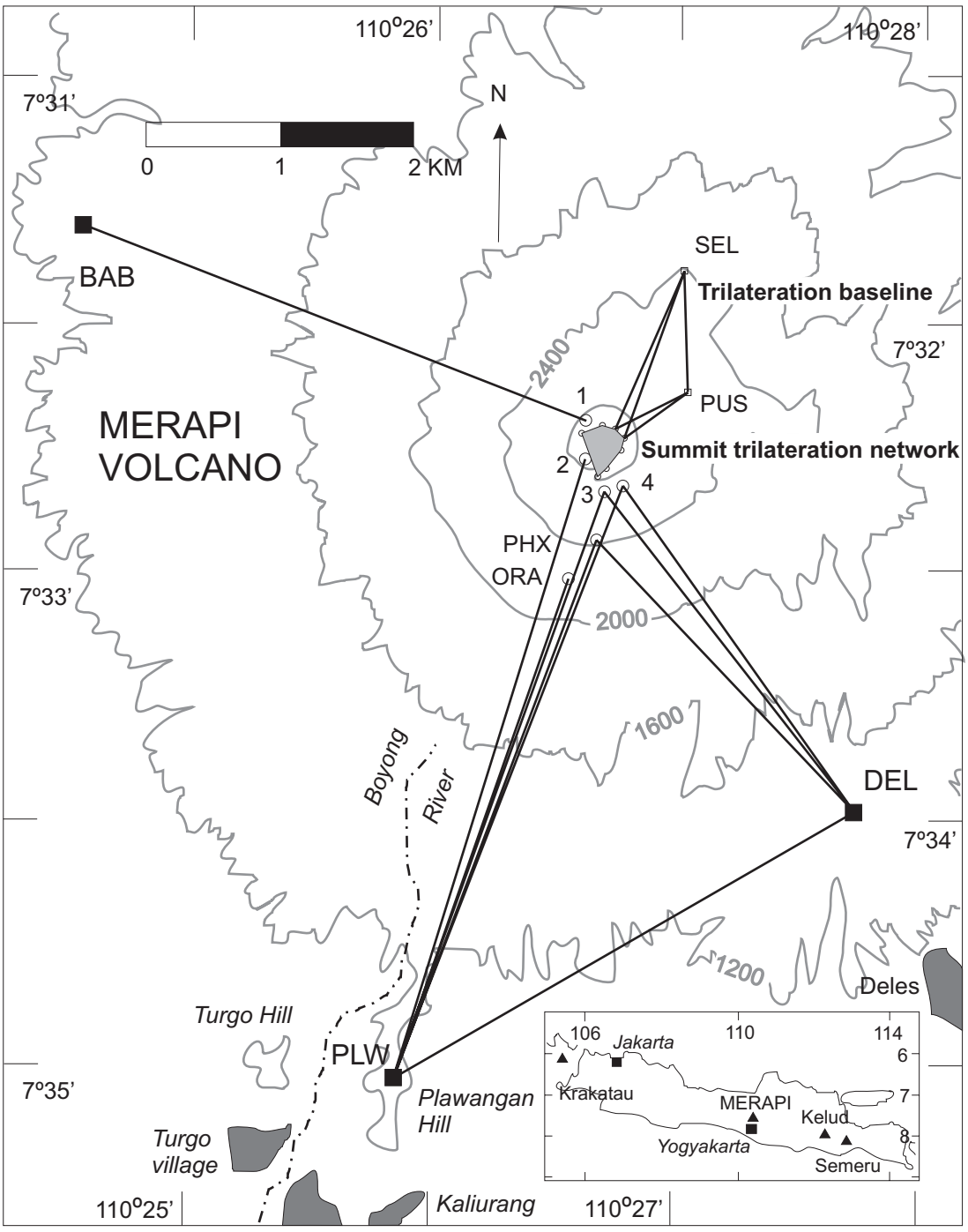

Figure **2-1**. Location of Merapi volcano and geometry of the Observatory network of fixed prisms. Baseline stations used for the Summit network are also shown. Inset shows the location of Merapi on the island of Java, Indonesia.

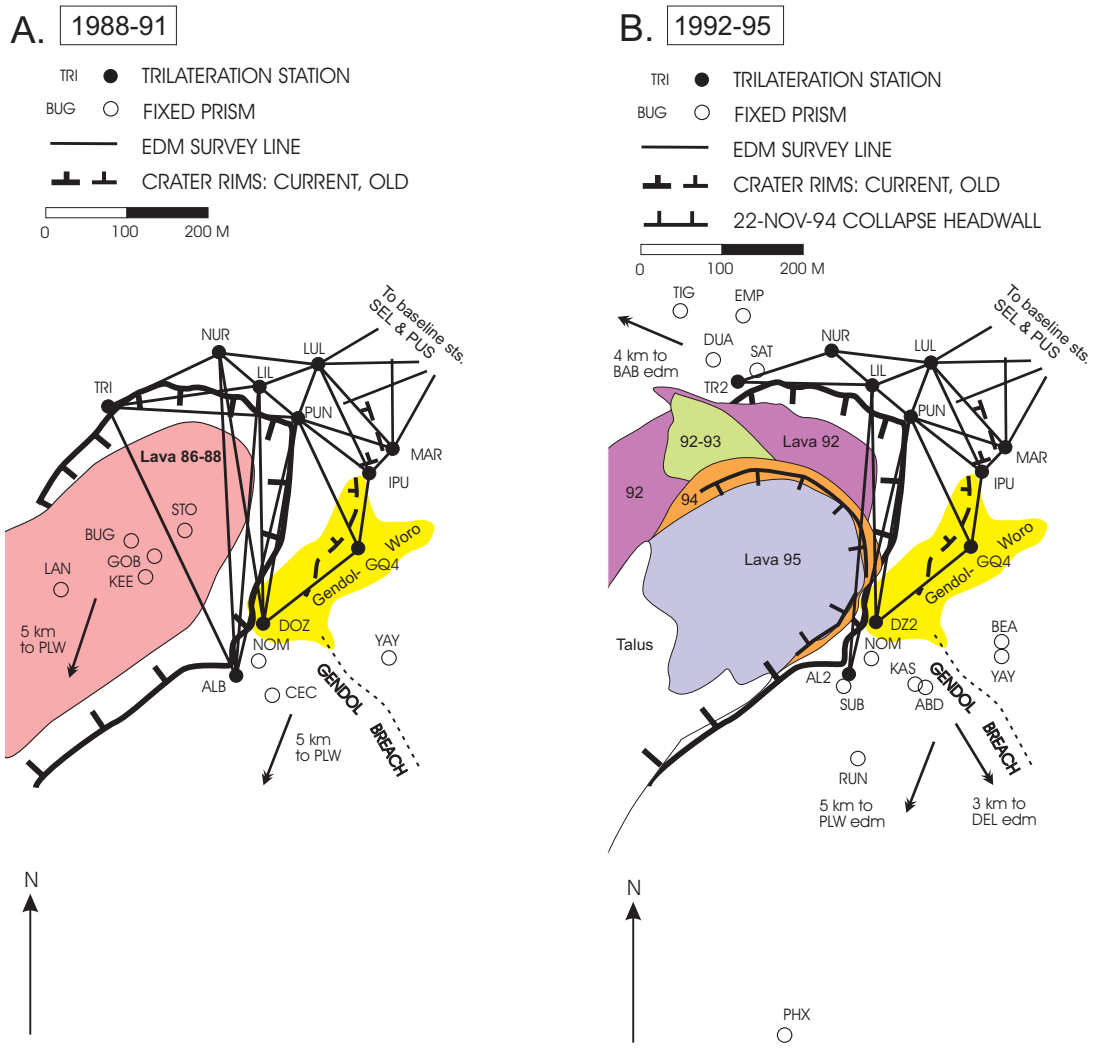

Figure **2-2**. Summit network of EDM trilateration stations and fixed prisms installed on Merapi volcano. (A) Network geometry between 1988 and 1991. (B) Same, 1992 to 1995. Most recent dome geology is shown as it existed at the end of (A) 1991 and (B) 1995. Current crater is Batang breach of 1961, old crater is remnant of Senowo breach of 1930. High-temperature fumarolic alteration dominates the surface of the Gendol-Woro area. Note alignment of the Gendol breach, a topographic notch separating the upper south flank to the SW (West Dome lava, 1911-13) from adjacent lava of the east flank (East Dome, 1888-1909) lavas.

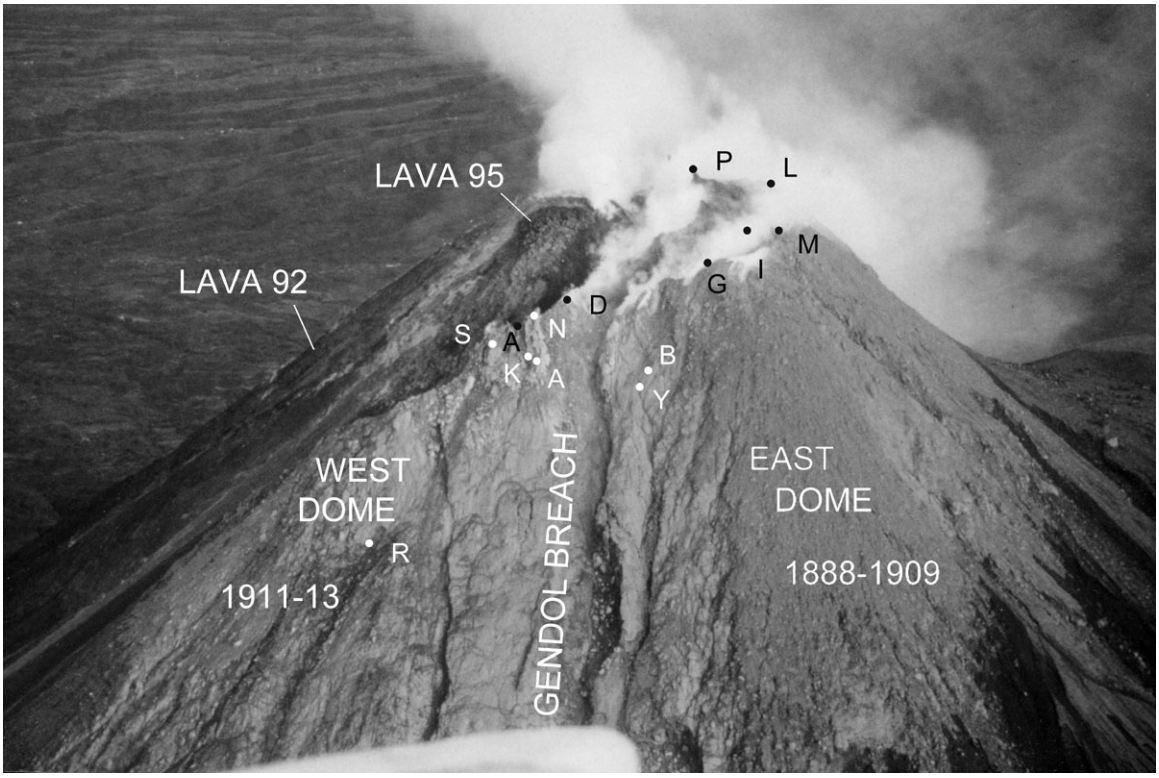

Figure **2-3**. Oblique aerial view in March 1995 of the upper south flank of Merapi, with summit crater and active 1995 lava behind. Locations of fixed prisms and most EDM trilateration benchmarks is also shown. Relief from base of the photo to top of 40o-60o slopes composing the south flank is about 350 meters. Plume rises from above the vent for 1994 and 1995 lava, adjacent 1992-1993 dome lava, and the Gendol-Woro sulfataras on the east rim. The pronounced depression down the center of photo is the Gendol breach, marking the abutment of viscous dome lavas erupted in 1888-1909 on the right, and 1911-13 on the left. (B. Voight photo).

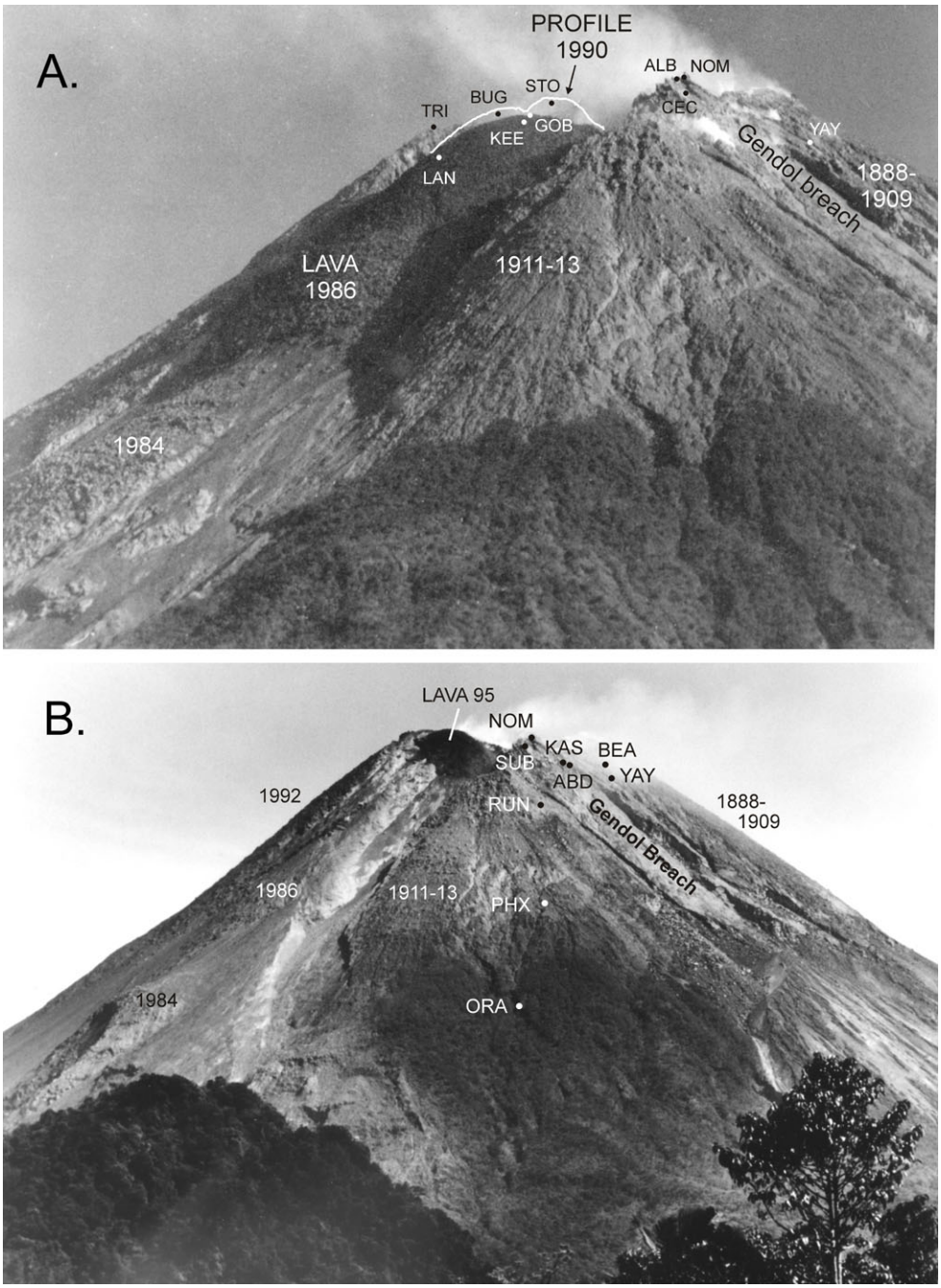

Figure **2-4**. South flank of Merapi volcano. (A) View from Plawangan observation post, December 1986, showing 1984-1986 lavas that exited the summit crater via the Batang breach, dome profile in August 1990, and locations of fixed prisms measured by EDM from 1988 to 1991. (T. Casadevall photo). (B) View from Kaliurang, December 1994, soon after the November 1994 dome collapse. The same vent was used for 1994 and 1995 lavas. Also shown are locations of fixed prisms measured by EDM from 1992 to 1995. (H. Wiyanto photo).

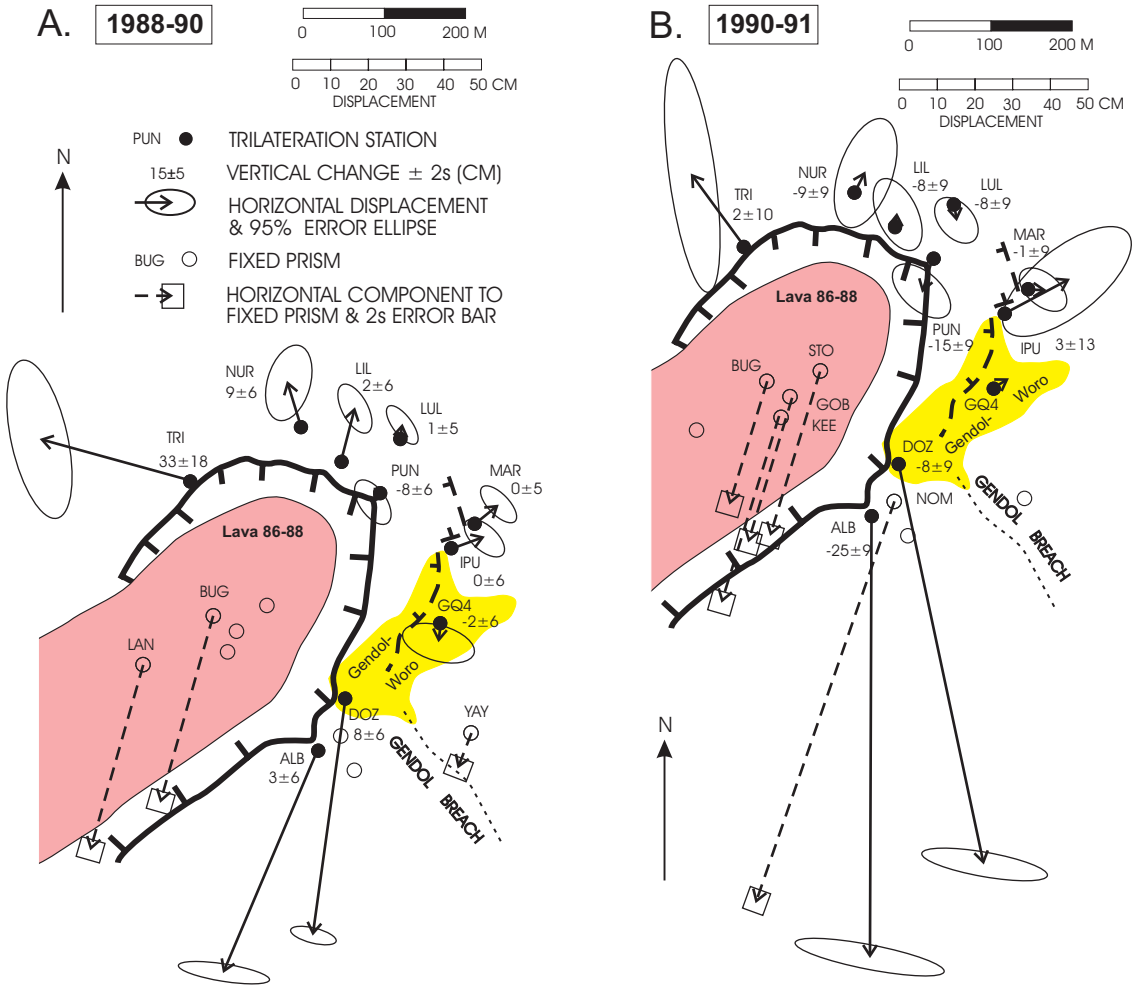

Figure **2-5**. Horizontal and vertical displacements for EDM summit network stations between surveys conducted (A) June/July 1988 - September 1990 and (B) September 1990 August 1991. 2σ errors are shown for the trilateration station movements. Dome displacements are slope distance changes measured from PLW (Fig. 2-1) to fixed prisms. Note GQ4 was a sideshot in 1991. Distribution of lava in the crater is that existing at the time of the surveys.

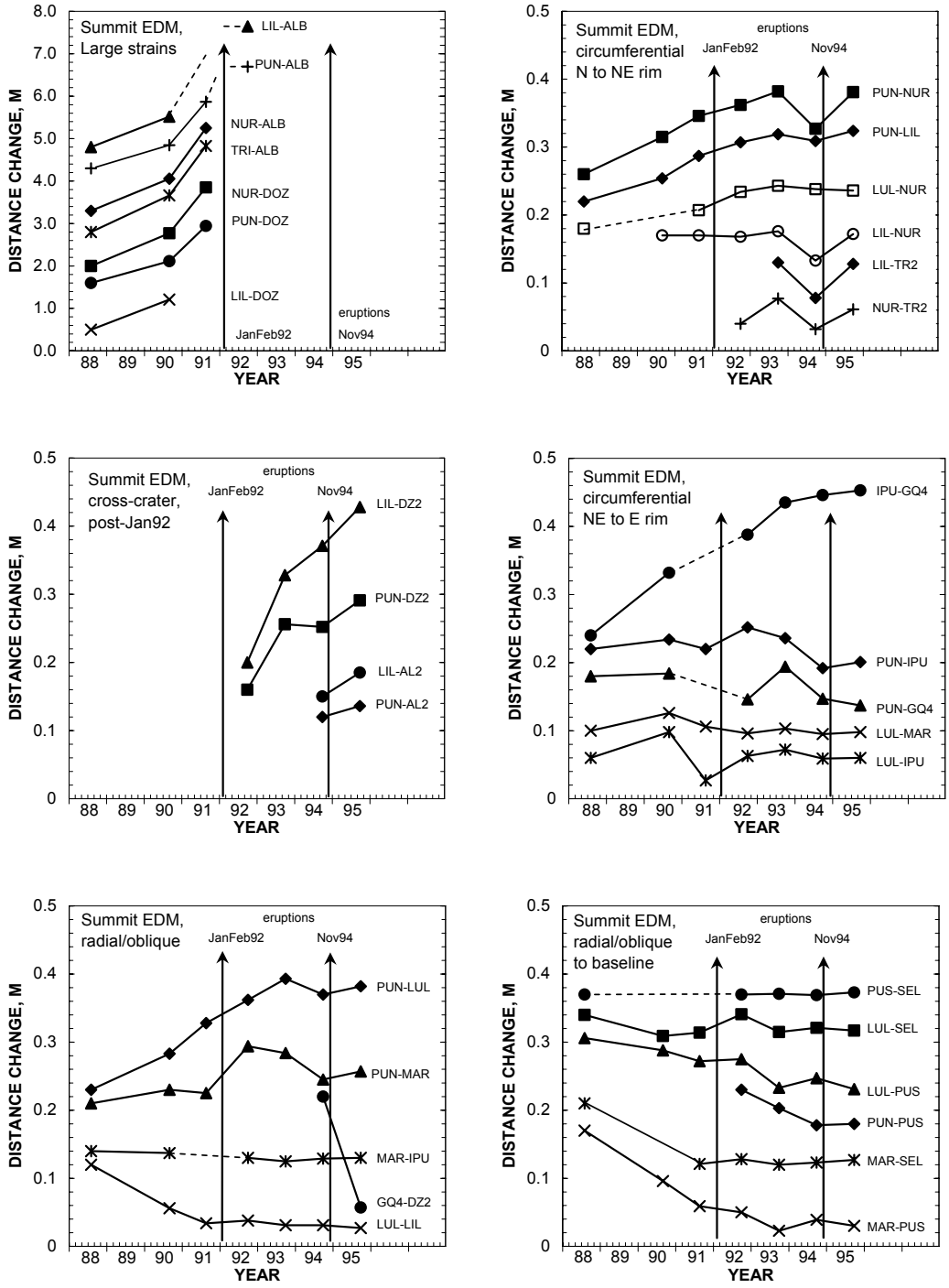

Figure **2-6**. Cumulative slope distance changes for EDM lines on the summit trilateration network. Arrows mark significant eruptions in January/February 1992 and 22 November 1994. Data shown are without error bars as their 2σ errors are no larger than the symbols.

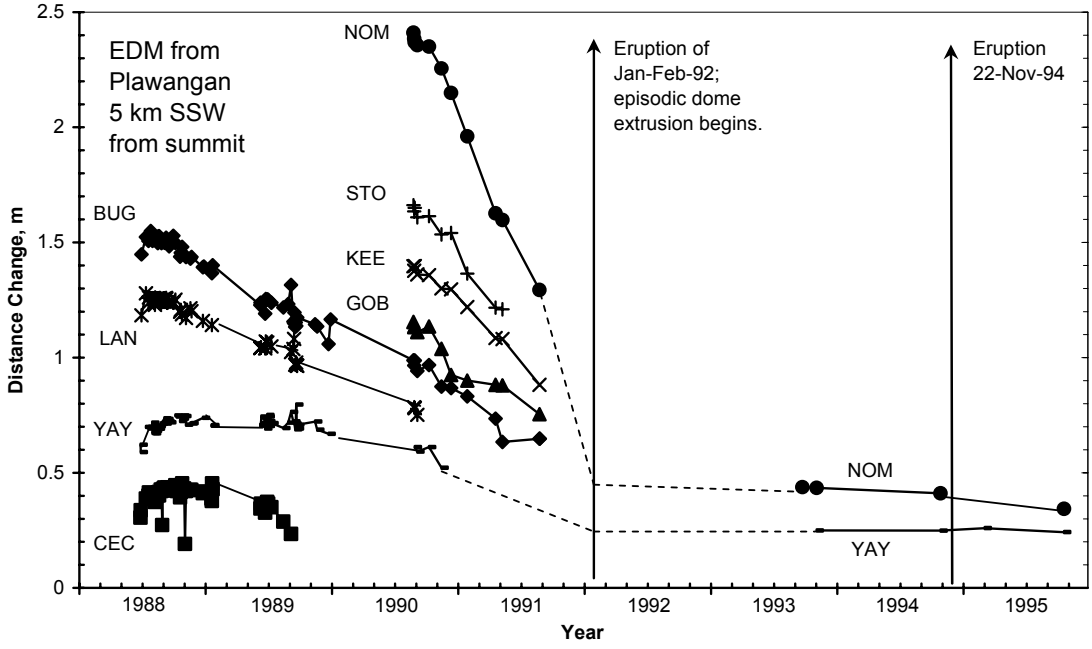

Figure **2-7**. Slope distance changes between PLW and fixed prisms, 1988-1995. Note dramatic change in displacement rate for surviving site NOM following the eruption of Jan-Feb-1992. 2σ errors are smaller than symbols.

Figure **2-8**. Merapi volcano viewed from Babadan in February 1992, soon after the outbreak of new lava. Small pyroclastic flow is seen descending to the southwest. (H. Wiyanto photo).

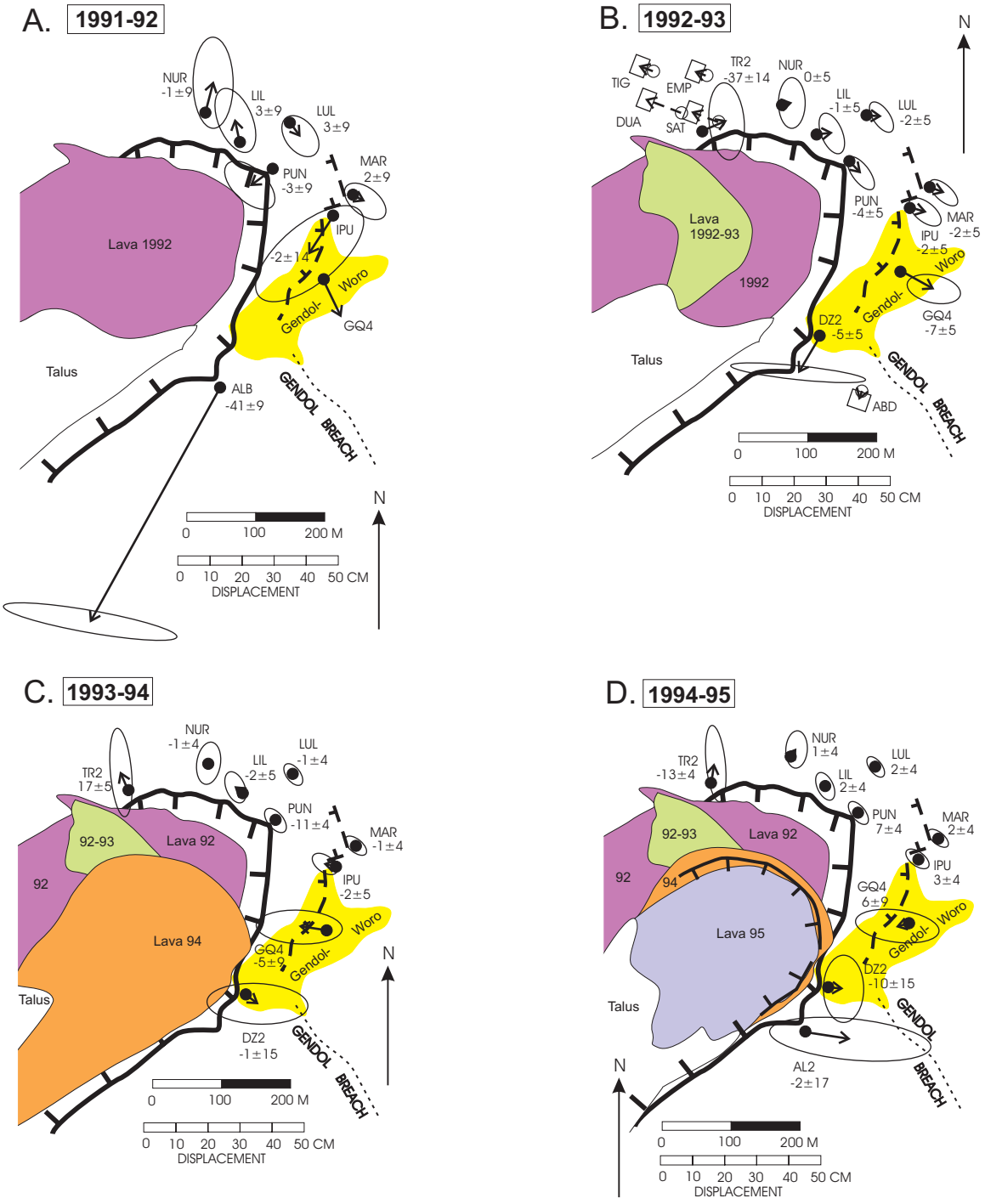

Figure **2-9**. Horizontal and vertical displacements with 2σ errors for surveys conducted on the EDM summit network (A) August 1991 October/November 1992, (B) October/November 1992 September 1993, (C) September 1993 October 1994, and (D) October 1994 September 1995. Horizontal slope distance changes to certain fixed prisms are also shown. Note GQ4 was sideshot in 1991. Age distribution of lava in the summit crater is that present at the end of the survey interval. Legend as in Fig. 2-5.

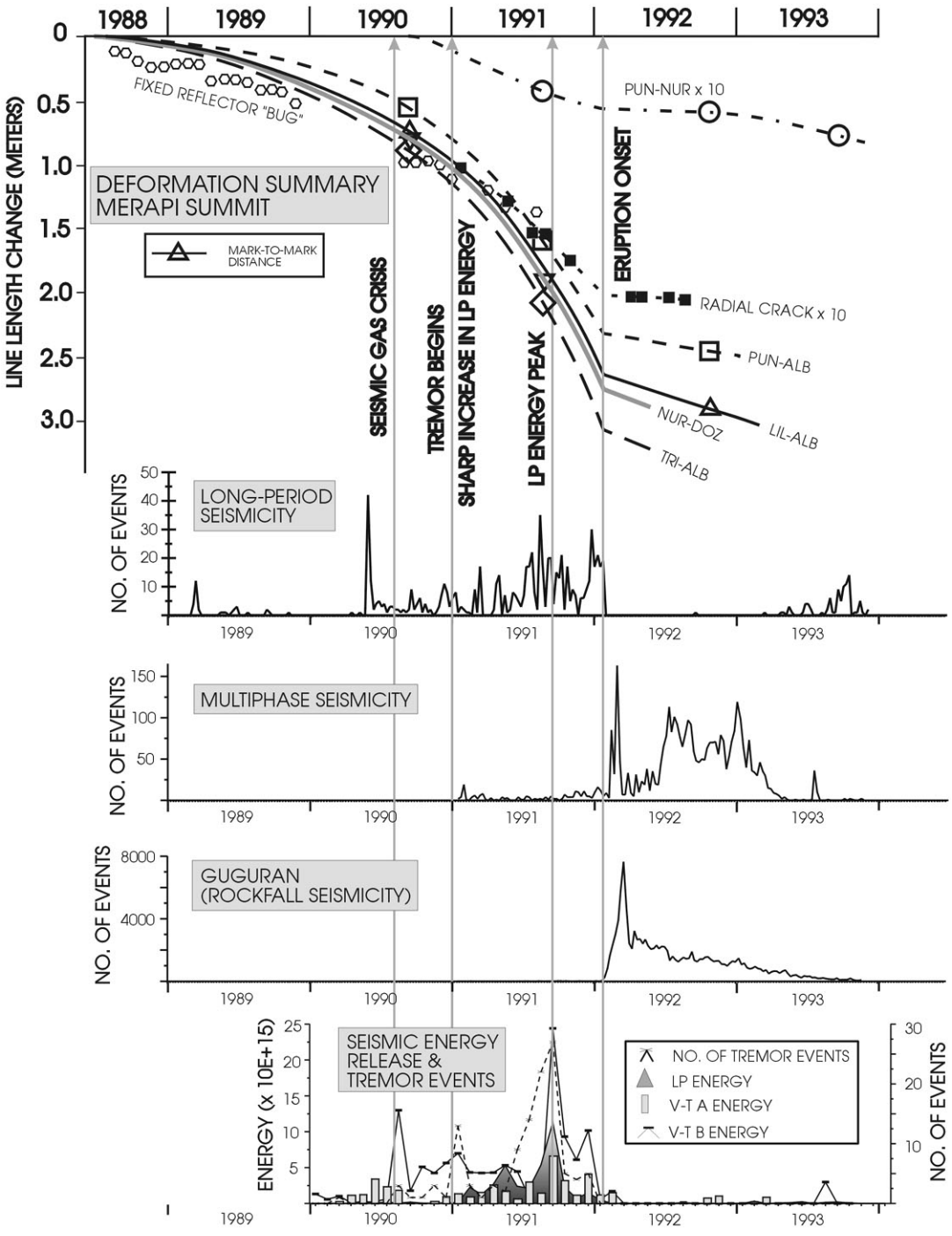

Figure **2-10**. Correlation of cumulative distance changes measured on the EDM network to seismic events and the January/February 1992 eruption at Merapi. Radial crack measurements made between trilateration stations LIL and PUN are also shown. A pronounced diminution in deformation and subsurface seismic parameters is evident with the onset of the 1992 eruption. Near-surface seismicity associated with dome growth dominates subsequently.

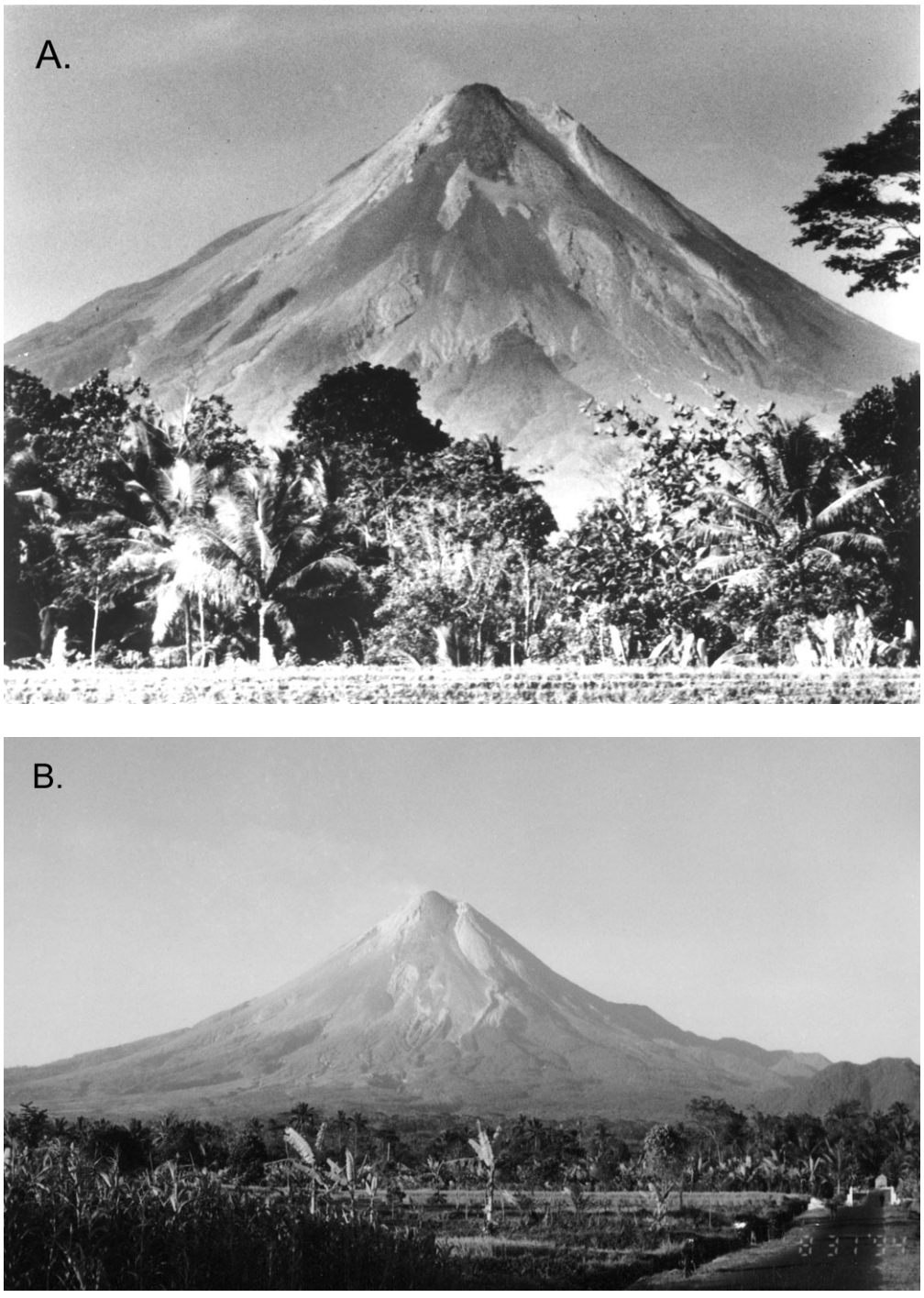

Figure **2-11**. Merapi volcano viewed from the west-southwest. (A) View from Srumbung (Magelang) in 1993. Note the high lava dome, overtopping the northwest crater rim. (B) From Ngepos observation post, August 1994. The 1994 lavas (dark) fill much of the gap between 1992-1993 lava and the south crater rim (right). Much of the 1994 lava dome collapsed on 22 November 1994.

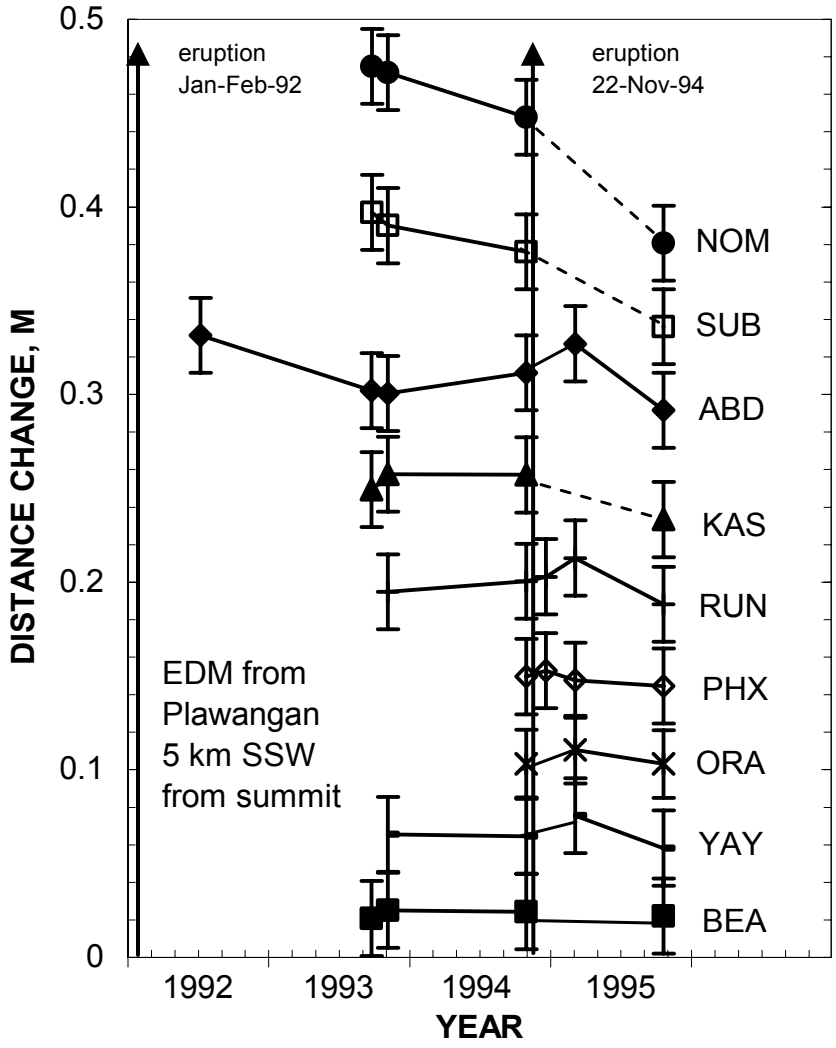

Figure **2-12**. Slope distance changes between PLW and fixed prisms, 1992-95. Note difference in vertical scale compared to that used in Figure 7. Error bars are two standard deviations (2σ) on either side of the plotted points.

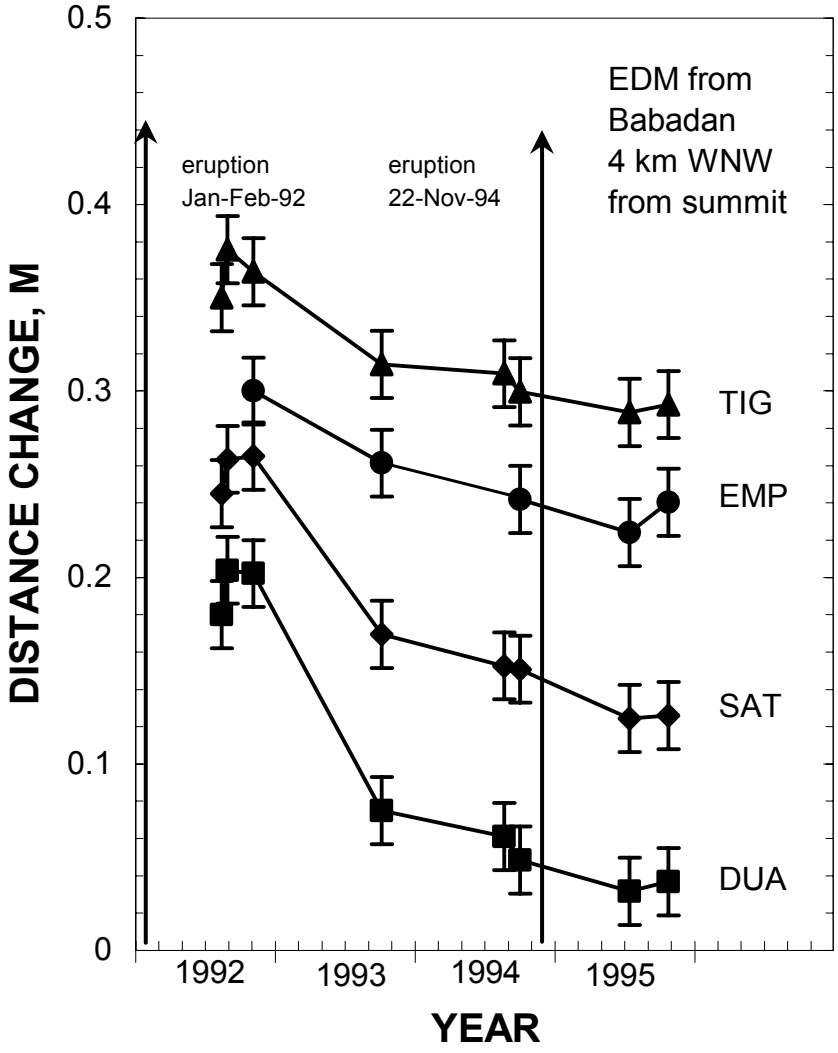

Figure 2-**13**. Slope distance changes between BAB and fixed prisms, 1992-95. Error bars are 2σ on either side of the plotted points.

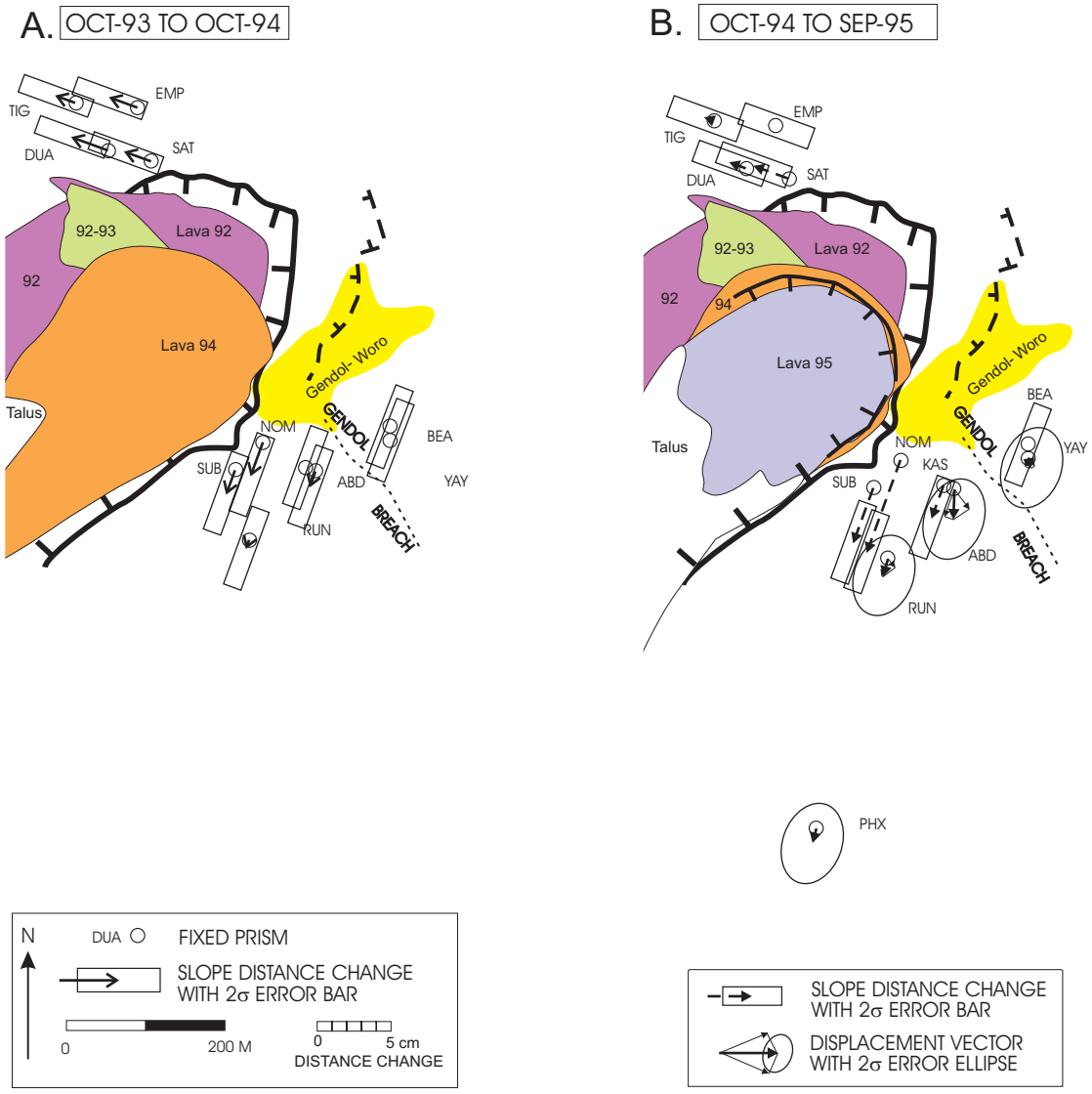

Figure **2-14**. Slope-distance changes and vector displacements for fixed prisms located on the south and southeast flanks. (A) October 1993 October 1994, (B) October 1994 - November 1995. Displacement vectors in (B) result from EDM measurements taken from PLW and DEL to fixed prism pairs at sites PHX, RUN, ABD, and YAY. Note contrast in distance-change/displacement scale with respect to Figs. 2-5 and 2-9.

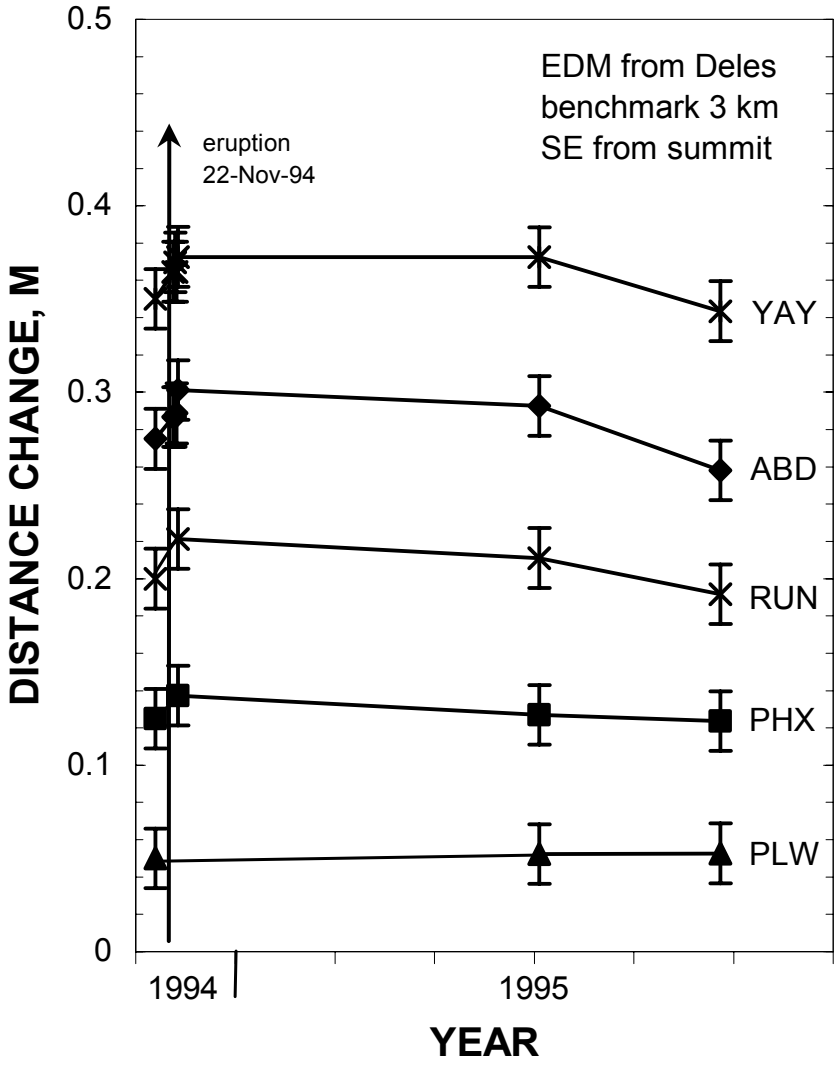

Figure **2-15**. Slope distance changes between DEL and fixed prisms, 1994-95. Error bars are 2σ on either side of the plotted points.

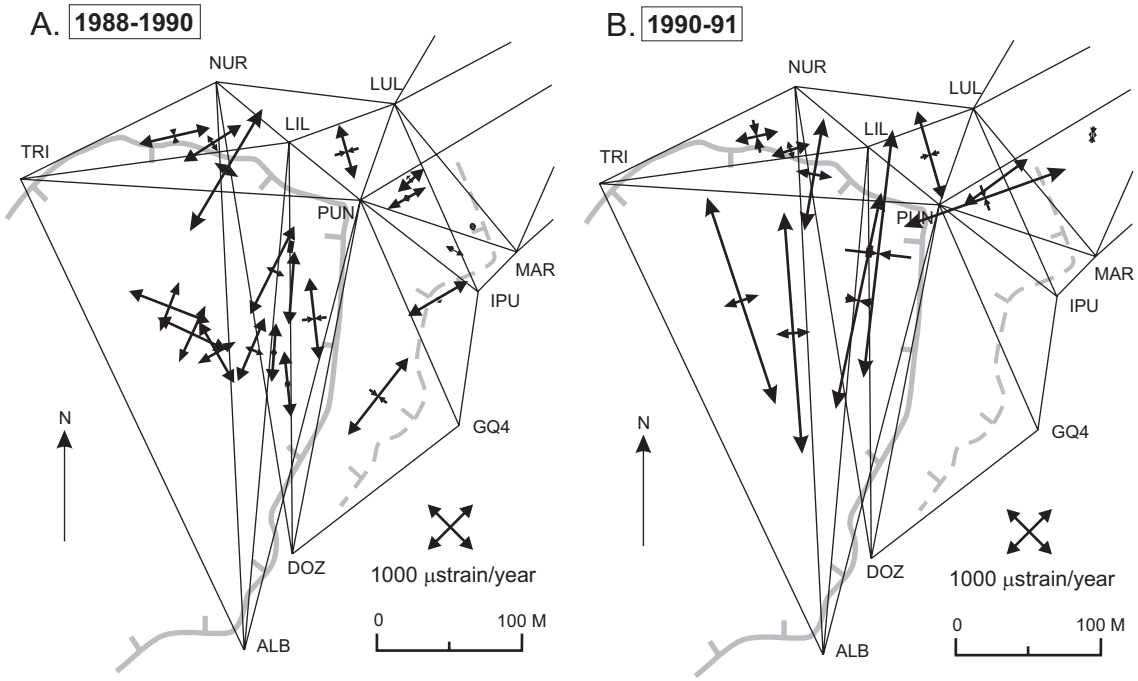

Figure **2-16**. Principal directions and values of the strain-rate tensors for selected triangles of the summit network. (A) June/July 1988 - September 1990. (B) September 1990 August 1991.

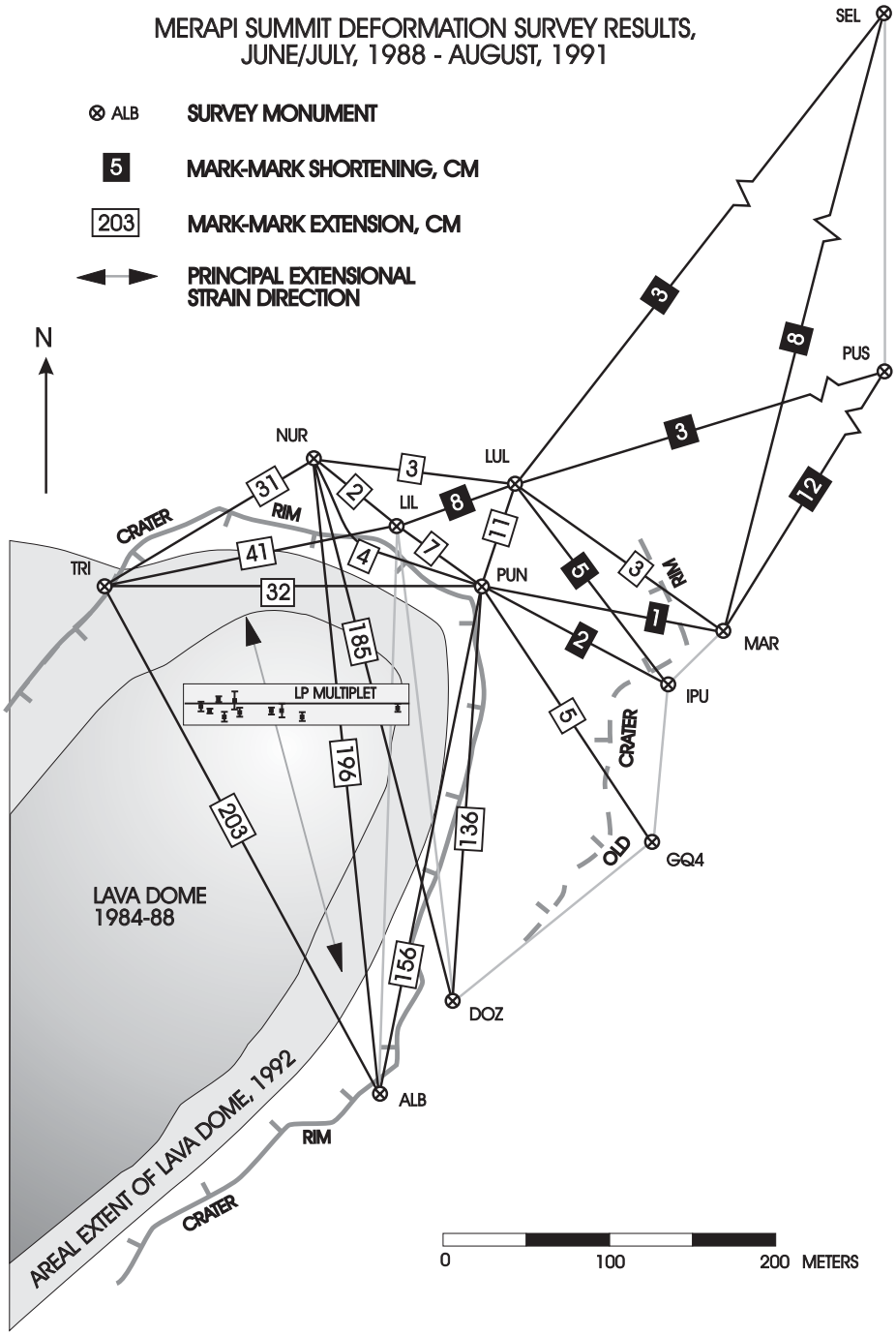

Figure **2-17**. Location of the LF multiplet recorded in 1991, and a principal extensional strain direction derived from strain analysis of the trilateration results, June/July 1988 - August 1991. Slope distance changes measured on the summit network are also shown.

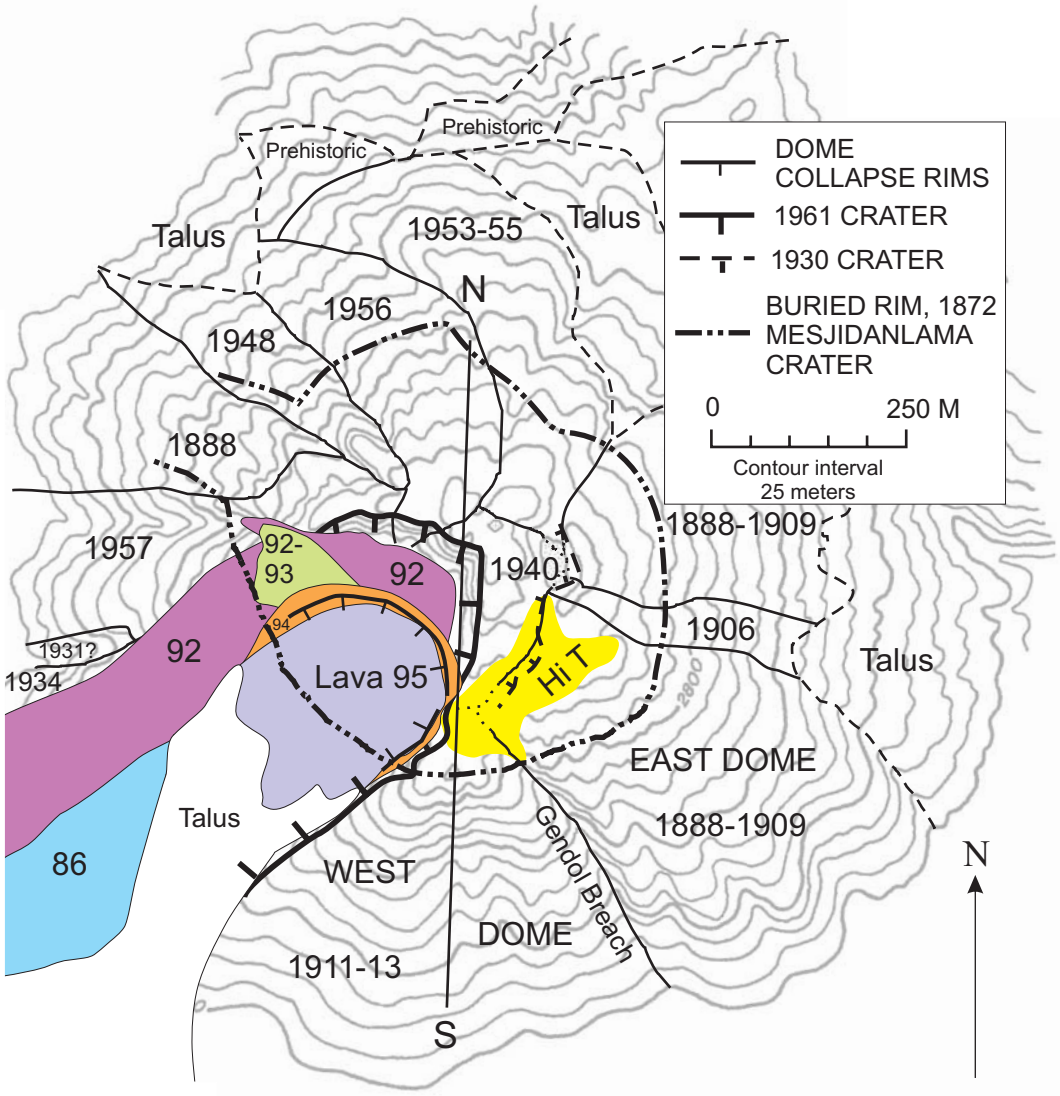

Figure **2-18**. Age distribution of lava domes and flows near the summit of Merapi volcano at the end of 1995. Locations of existing crater walls and buried 1872 crater rim also shown. Cross-section N-S is shown in Fig. 2-19.

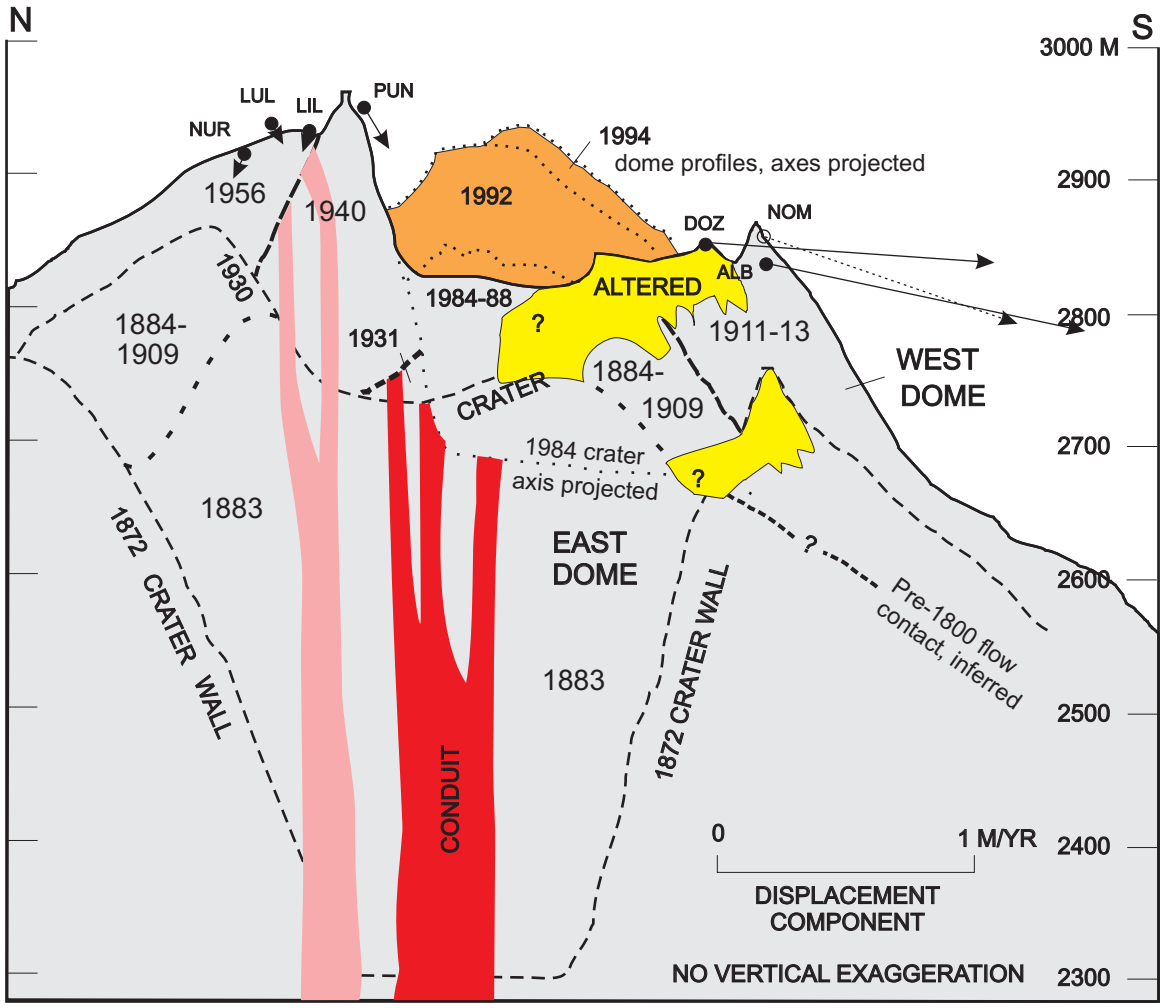

Figure **2-19**. North-south cross section through the summit and south flank of Merapi volcano, showing age distributions of lavas and buried crater walls at the end of 1995. Dome lavas found in present crater, present crater axis (dotted lines), and conduit are projections onto plane of cross-section. Displacement components in plane of cross section are shown for selected survey stations for the period September 1990 August 1991. Cross-section position shown in Fig. 2-18.

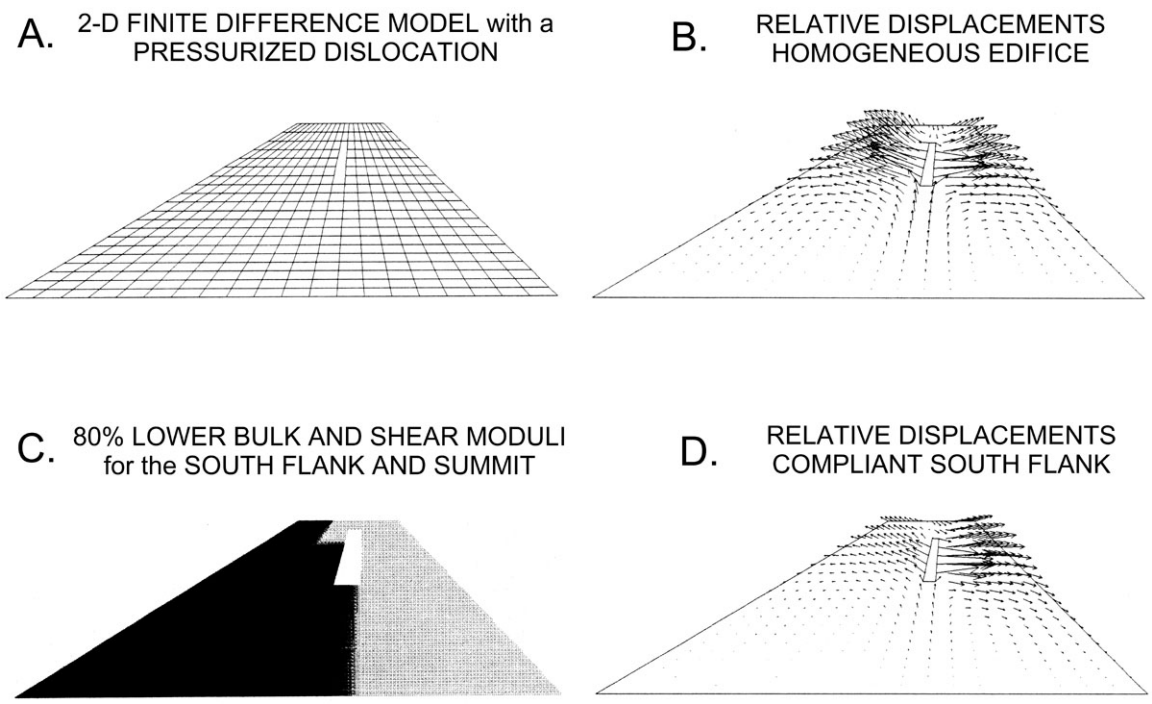

Figure 2-**20**. (A) Finite difference grid of simplified north-south section through Merapi, showing idealized high-level pressurized conduit zone. Model is plane strain. (B) Displacement vectors for homogeneous elastic volcano, uniform pressure against conduit wall. (C) Inhomogeneous model, showing compliant summit area and south flank (stippled area) with moduli reduced by 5X. (D) Displacement vectors for inhomogeneous model, showing concentration of deformation on south flank, and reduced inclination of displacement vectors.

Chapter 3

Deformation, Lava Dome Evolution, and Eruption Cyclicity at Merapi Volcano, Central Java, Indonesia

Abstract

An elevated phase of magma production with respect to the long-term rate for the 20th Century characterizes the activity at Merapi volcano, Central Java/Yogyakarta, Indonesia, for the period 1992-2006. Some 224,810 recorded seismic events were identified as rockfalls and/or pyroclastic flows between January 1992 and December 1998. Of these, 820 pyroclastic flows specifically were reported, mainly from field observatory posts. Most of nine large (0.2 - 3.4 x 10^6 m^3) dome collapses or dome collapse episodes in the 1990s were initiated during elevated short-term extrusion rates, typically 0.2 m^3 s^{-1} or greater, rates that are large for Merapi but not for volcanoes worldwide**.** Large collapses were often preceded by variable inflationary tilt of the crater rim, by increasing numbers of rockfalls and their associated seismicity, and by intensifying multiphase earthquake activity. In such cycles, a modestly gas-rich volume of magma extruded onto or intruded into a pre-existing lava dome, leading to rockfalls and eventual partial dome collapses from the headwalls of developing lava flow fronts. While gas pressure build-up within the dome may have played some role, similar effects in some cases may have been generated or intensified by intense monsoon rainfall on still hot lava. Multiphase earthquakes, rockfall counts, and amplitude-duration data established from seismic records show varying positive correlations with extrusion rate. Pyroclastic flow and rockfall seismic amplitude-duration data have been calibrated as proxies to enable estimates of collapsed lava volume. When combined with calculations

of dome volume estimates over time, and deposit volumes from major dome collapses, an overall magma flux of 0.1 m^3 s^{-1} between 1992 and the end of 1998 has been obtained. This rate is significantly greater than the long-term 0.04 m^3 s^{-1} magma flux calculated for Merapi over the first nine decades of the 20th century (Siswowidjoyo et al., 1995), but that calculation did not include volumes lost to rockfalls and is therefore misleading. Thus the real long-term flux rates may have been roughly 25% or greater than those calculated. For the 20th Century as a whole, observed magma production rates have suggested long-term cycles of ca. 30 years spacing that began with heightened magma flux over two to eight years with greater potential for explosive eruptive activity during these phases, followed by much-diminished mean magma flux in the concluding ~25 years of the cycle. The data examined up through 2006 suggest that if similar periodicity were to continue into more of the 21st Century, activity at Merapi would likely experience lower magma production in the next decade and a half as compared to the most recent eruptive phase(s) during the 1990s and 2000s. Of note, the resumption of activity in 2006 was surprising in its vigour, with extrusion rates exceeding 2.3 m^3 s^{-1} for several months, illustrating the caution necessary in believing too strongly in specific long-term forecasts based on prior volcanic activity.

3.1 Introduction

Merapi, an andesitic stratovolcano located in Central Java, Indonesia (Fig. 3-1), has experienced episodic extrusion of lava over the last century (Siswowidjoyo et al., 1995; Voight et al. 2000a). Typically, lava domes and lava tongues formed within or near the summit crater (Fig. 3-2), and gravitational collapses of portions of these domes have

produced numerous rockfalls, and 'Merapi-type' pyroclastic flows (Escher, 1933; Voight et al., 2000a**).** On occasion Merapi also has experienced relatively violent explosive eruptions as well, including Plinian and sub-Plinian activity, with the larger events occurring at intervals of a few centuries (Andreastuti et al., 2000; Newhall et al., 2000).

The Merapi volcanic edifice rises to some 2962 m elevation a.s.l. at its crater rim, with relief above surrounding agricultural lands of at least 1800 m (Fig. 3-2). Major population centers within 30 km of Merapi are the cities of Yogyakarta and Surakarta, comprising a total population of at least one million people (Thouret et al., 2000). More significant is the high population density of rural areas that include hundreds of villages, with at least one million people living within 20 km of Merapi, a distance attainable by the largest pyroclastic flows and debris avalanche deposits based on historical and stratigraphic records. Some 80,000 rural inhabitants live within a proximal zone defined somewhat arbitrarily 60 years ago as the "forbidden zone" (Voight et al., 2000a).

Because of the proximity of a high population density and the frequent and potentially violent nature of its volcanic activity, Merapi poses extraordinary hazards to people and culture. It receives considerable attention from the Volcanological Survey of Indonesia (VSI, officially referred to as the Center of Volcanology and Geological Hazard Mitigation or CVGHM), and has been designated a '*Decade Volcano*' as part of the *International Decade for Natural Disaster Reduction*, one of sixteen volcanoes worldwide identified as deserving of special attention by volcano researchers and hazard managers. Scientists from numerous countries have thus been drawn to Merapi. A compilation of results from many of these projects appeared in a special issue of the *Journal of Volcanology and Geothermal Research* (Voight et al., 2000c).

In this study we report on a broad range of geophysical parameters measured at Merapi since 1992. These data are cross-correlated and compared to the observed eruptive activity to assess eruption precursors (in hindsight), and to improve our understanding of the mechanisms of dome collapse and other activity. Data were taken from our own fieldwork, from selected published results of other researchers, and from unpublished observations and the monitoring database of the VSI Merapi Volcano Observatory.

The paper is organized in the following way. First we summarize the activity of Merapi since 1992. Next we examine the various phenomena or parameters monitored, including rockfalls and pyroclastic flows, seismicity, and tilt deformation, and estimate the variation in lava extrusion rates (magma flux). These new flux estimates include an important allowance for dome volume loss due to rockfalls, and are considered more accurate than previous assessments of magma flux in which this factor had been ignored**.** The geophysical monitoring data and magma flux data are compared to the occurrences of major dome collapse events. Next, the cyclicity of magma flux variation is assessed for the period since 1992, and compared to prior estimates of the long-term cyclicity of lava extrusion. The eruptive episode of 2006 is noted, and its implications on cyclicity are considered. Finally we provide further discussion, and present conclusions.

3.2 Eruptive Activity, 1992-2006

An important phase of eruptions at Merapi volcano began 20 January 1992, after several years of steady and pronounced deformation (Young et al., 2000). The fresh lava extrusion built upon an existing dome dating from a previous growth episode in 1984-89

(Ratdomopurbo and Poupinet, 2000; Voight et al., 2000a). Growth of the new dome was sufficient within days to generate small pyroclastic flows that culminated in a peak of pyroclastic flow activity on 2 February 1992 (Ratdomopurbo, 1995; Voight et al., 2000a; Ratdomopurbo and Poupinet, 2000; Ratdomopurbo et al., 2000). The eruption followed an effective hiatus of at least 3 years, a time characterized by accelerating widening of the summit crater, based on EDM measurements begun in 1988 (Young et al., 2000).

The dome continued to grow following the early February collapse, and overtopped a section of the western crater wall in March. Deterioration of the lava tongue, with an unstable dome headwall emplaced on the steep upper flank, expanded the lower flank region subjected to rockfalls and pyroclastic flows off the dome. (In this paper we consider a *rockfall* as a collapse of fragmenting lava dome material with runout < 0.5-1 km; larger collapses are pyroclastic flows, with further distinctions between the two types considered in a subsequent section.) Relatively high extrusion rates continued until May 1992, and the extrusion was accompanied by numerous small pyroclastic flows and rockfalls through late April. Subsequently, the rate of dome growth waned although pulses of more rapid growth took place in June-July and October-November 1992. During these pulses, rockfalls of incandescent, blocky, dome fragments were numerous; however, at no time were there more than several minor pyroclastic flows per month.

Renewed, relatively vigorous dome growth began in January 1993, and culminated on 3 February in a series of 36 pyroclastic flows with runouts as great as 5 km. Frequent pyroclastic flows continued through March 1993, but by May, dome growth rate had declined and no pyroclastic flows took place during the remainder of 1993.

Activity re-energized in December 1993, as evidenced from visual observations of deformation in the 1993 lava lobe, and a new site of dome extrusion was detected by 14 February 1994. Eruptive activity during this time encompassed a major phase of lava extrusion and dome growth that formed the 1994 dome lobe and lava coulée (Fig. 3-3A). Long-term inflationary tilt, with few rockfalls after August, preceded a major dome collapse on 22 November 1994 (Voight et al., 2000b). In this eruption nearly all of the 1994 lava, some 2.6 x 10^6 m^3 in volume, was launched down slope as a succession of pyroclastic flows in the form of block-and-ash flows and ash-cloud surges (Fig. 3-4), with runouts as far as 6.5 km from the summit of Merapi (Voight et al., 2000b; Abdurachman et al., 2000; Brodscholl et al., 2000). There were many casualties (Shelley and Voight, 1995). Left behind was an arcuate headwall (Fig. 3-3B), with geometry controlled by the original vent for the 1994 lava extrusion, and the steep break-off slope at the mouth of the crater. The November collapse followed long-term adjustments to the summit geometry. However, no short-term precursors to the 1994 collapse were evident in the various geophysical parameters used to monitor the volcano, and none are recognized in hindsight (Voight et al., 2000b).

Dome extrusion within the collapse scar was vigorous following the 22 November events, and proceeded into at least early 1995. Growth slowed significantly by the latter half of 1995, but nevertheless led eventually to a concentration of some 28 pyroclastic flows that, in total, shed some 0.18 x 10^6 m^3 off the lava dome during 23-27 November (the basis for the volume estimate is discussed subsequently). Growth continued at a much reduced rate throughout 1996, and January 1997 marked the beginning of yet another cycle of heightened extrusion rates, with the appearance of a new dome on or

around 11-13 January. Significant partial collapses on 14-24 January, and a vulcanian explosion on 17 January, generated numerous pyroclastic flows that travelled as far as 6 km from the vent.

Yet another cycle of dome extrusion initiated around 30 June 1998, especially significant because of an eventual redirection of lobe growth from the southwest to the west (Kelfoun, 1999; Voight et al., 2000b**)**. This redirection led to collapses of portions of the 1957- and 1934-age crater wall lava during events on 11 and 19 July 1998. The pyroclastic flows generated by these collapses travelled beyond the base of the cone, as far as ~5.5 km from the summit on 11 July, and a similar distance again on the 19th. Vigorous growth of the 1998 lobe proceeded throughout the rest of 1998 and into earliest 1999.

After the cessation of magma extrusion by early 1999, a roughly 15 month hiatus ensued before activity commenced again by May 2000, with deformation of 1998 dome lava, incandescence, crater rim crack widening, and increasing numbers of deep and shallow volcano-tectonic earthquakes (types VT-A and VT-B, respectively) (Smithsonian Institution, 2000a). Field observations on 31 October 2000 finally confirmed new lava having shoved aside portions of the 1998 lobe. A culmination in VT seismicity was reached the week of 1 January 2001, and incandescence and glowing rockfalls were observed in the following days, heralding formation of a 2001 lobe of dome lava in the area of the 1998 activity (Smithsonian Institution, 2000b). Instability of the 2001 lava was reflected in increasing numbers of pyroclastic flows in subsequent days, which led to a substantial dome collapse on or about 16 January 2001 (Smithsonian Institution, 2001). Lava continued to be extruded in subsequent days within the collapse scar, and larger

collapses occurred on 27 and 31 January, with pyroclastic flows reaching as far as 4.5 km from the summit. In the following week, improved weather allowed an estimate of total dome volume for the 2001 lobe of 1.0 x10^6 m^3 on 6 February. Instability continued in the following days, culminating on 10 February with a dome collapse sufficiently large to incorporate portions of the surviving 1998 lava. Resulting events included pyroclastic flows as far as 7 km from the summit, an ash plume as high as 5 km above the summit, and ash fall as far as 50 km from the volcano. In spite of attrition by the collapse events, the overall size of the 2001 lobe was estimated at 1.4 x 10^6 m^3 by 14 February (Smithsonian Institution, 2001).

Activity after February 2001 waned significantly, though partial collapses off the 2001 lobe occurred on 17-20 August 2001. Little activity was observed from late 2001 to 2004. Subsequent monitoring data suggested that magma rose abortively in June-July 2005.

Following a slow increase in unrest after October 2005, new magma broke out in April 2006, likely by the 10^{th} of that month, between the 1997 lava and the 1961 scarp. About 3.8 m of summit deformation preceded the breakout (C. Newhall, written commun., 2006). The dome grew rapidly by Merapi standards, with a rate exceeding 1.7 m^3 s^{-1} (150,000 m^3/d). Activity was similar to that of the 1990's eruptions, but with a new vent location and a *prolonged* rapid extrusion rate. A second dome lobe developed simultaneously on the NW. SO_2 output was around 200 t/day as measured by COSPEC, a rate considered anomalously low for the amount of volume extruded.

The unusually high extrusion rate occurred between early May and late June. An escalation of activity was perceived after the shallow (10 km) and damaging Yogyakarta

M_w 6.3 earthquake of 27 May, with significant increases in daily numbers of rockfalls and pyroclastic flows, especially on 2-5 June (C. Newhall, written commun., 2006). A substantial crisis developed as rockfall and pyroclastic flow activity threatened drainages to the south and southeast for the first time in a century. A dome-collapse pyroclastic flow on 14 June extended to 7 km in the Gendol River valley, killing two people in Kaliadem village. The eruption wound down in July and August after 12-13 x 10^6 m^3 of lava in total had been extruded (C. Newhall, written commun., 2006).

3.3 Geophysical and Observational Data

3.3.1 Dome-collapse phenomena

The structural collapses at Merapi include rockfalls, relatively simple 'gravitational' collapses that generate 'Merapi-type' pyroclastic flows (Escher 1933; Voight *et al.* 2000a, p. 72-74), and more complex events involving both newly extruded lava with variable gas content, and older lavas making up the cone. *Rockfalls* represent the smaller-scale end-member of collapse phenomena, and range from assemblages of cool, discrete blocks (sometimes up to 20 m diameter or more) that roll, bounce and slide downhill, to avalanches of incandescent blocks with substantial fines generated from block attrition. Rockfalls can be passively generated, occurring during periods of little apparent growth, and relatively low activity; or actively generated, occurring during periods of new or vigorous growth, or following changes in the locus of active growth (cf. Calder et al., 2002). Passively generated rockfalls at Merapi occur typically as isolated events with relatively little elutriation of fine, comminution-generated ash. Small, mildly convecting clouds that form above passive rockfalls soon deteriorate into

diffuse, drifting clouds that travel only a few hundred metres. Some of these rockfalls are initiated by discrete blocks that descend with little fragmentation, remobilizing loose talus along the flow path and creating a slow grain flow of talus material. The rockfalls are dramatically observable at night during dome growth, recorded as bright orange streaks of light in long-exposure photography. A. Ratdomopurbo noted in 2006 that new cracks exposed incandescent magma several minutes before some collapses (C. Newhall, written commun., 2006).

Actively generated rockfalls are derived from headwall failures in rapidly growing parts of the dome or lava lobe, and are composed of hot, incandescent blocks that have broken away. Associated ash clouds are hot and buoyant and commonly rise as small coherent plumes, several hundred meters to one km high. This ash is formed by spontaneous comminution during the collapse process. These actively generated rockfalls grade readily into pyroclastic flows when larger volumes of nevertheless similar material collapse. During periods of active magma extrusion between 1992 and 1999, 100-500 rockfalls per day were typically produced, with a maximum of 1765 per day reported in early March 1992.

A. Ratdomopurbo of MVO in 2006 noted distinct pulsing in the frequency of rockfalls as seen on the drums and in real-time seismic amplitude measurements (RSAM, e.g., Murray and Endo, 1989; Endo and Murray, 1991), with peaks occurring a little more than a day apart (C. Newhall, written commun., 2006). Possible explanations are (1) that the pulses reflect simply the time required for the lava lobe front to get into an unstable position after a series of rockfalls had caused retreat of the front, or (2) that the pulses

reflect episodic pressurization via pulsed degassing (C. Newhall, written commun., 2006). If (2) is correct, one might expect possible correlations with MP or LP events.

Pyroclastic flows are distinguished from rockfalls by their larger size, longer runouts (minimum runouts ~0.5-1 km), more fine ash generated, and strongly buoyant hot ash clouds. The smallest pyroclastic flows, however, are completely gradational with the large actively generated rockfalls. Qualitatively, pyroclastic flows form when there is a larger proportion of ash produced by rapid, spontaneous disintegration of the collapsing dome material (Sato et al. 1992). The pyroclastic flows comprise a basal *block-and-ash flow* of dense lava blocks, lapilli, and ash and typically an overriding, dilute *pyroclastic surge* component (Bourdier and Abdurachman, 2001), with the surge component derived by separation from the underlying avalanche. The basal block-and-ash flow is poorly sorted (Boudon et al., 1993; Abdurachman et al., 2000), and commonly incandescent, with temperatures at Merapi reported at about 550^{o}C (Voight and Davis, 2000). The pyroclastic surges have (by definition) a significant lateral component of motion, but those associated with small pyroclastic flows can be weak. The surges are generated sequentially along the flow path and rise a few hundred meters to several km or more during large collapses (Voight et al., 2000b, their figs. 5 and 6), producing high-rising thermal plumes with further separation of fines (Woods and Kienle, 1994). The thermal plume generated in the 22 November 1994 eruption rose to 14 km.

In practice, because there is a continuum of collapse phenomena, it can be difficult to define rigorously whether a particular event is a rockfall or a pyroclastic flow. A continuous bulbous plume rising above the avalanche of material is perhaps a simple yet effective criterion. Runout distance is a somewhat less distinctive observation given

the changing geometry of the talus apron over time. At Merapi, recognition of a collapse event off the lava dome as a "*pyroclastic flow*" is made by trained observers stationed at the various field observation posts distributed about the base of the volcano (Fig. 3-1). Their observations of the number of pyroclastic flow events per day, and the maximum runout seen each day, are recorded at MVO in a multi-parameter database that is updated at least weekly. Recognition criteria at the field observatory posts places emphasis on a coherent ash cloud above the avalanche of material, with total runout distance a secondary criterion. The result of such observations at Merapi records a maximum runout of at least 0.5 km on all but two days between 1992 and 1999 on dates where pyroclastic flows were observed.

The relatively large dome collapses at Merapi volcano, defined here as those with deposit volumes $>0.2 \times 10^6$ m^3, occurred on nine occasions throughout the eruptive cycle of 1992-1999 (Table 3-1). At least six additional events occurred in the eruptive phases of 2000-2006 (16 Jan 2001, 28 Jan 2001, 10 Feb 2001, 19 Aug2001, 4 Jun 2006, and 14-Jun 2006; these are events not considered in detail here). Many collapses were prolonged events, with individual failures occurring over many hours. The largest of these collapses, derived from purely an active lobe of dome lava, occurred over a 7-hour period on 22 November 1994 (Fig. 3-4), and produced flow runouts as great as 6.5 km (Abdurachman et al., 2000). An even larger collapse occurred in July 1998, but this included, in addition to active lava, the incorporation of portions of the pre-existing edifice. Large collapses represent significant events in the eruption chronology and therefore are periods when MVO is on heightened alert, and events are best reported.

3.3.2 Seismicity

The seismic signals on Merapi have been monitored predominantly by 7 short-period seismometers (Mark L4C 1-Hz sensors) with the signals transmitted by VHF directly to Merapi Volcano Observatory (MVO) in Yogyakarta, 25 km from the volcano (Ratdomopurbo and Poupinet, 2000). The signals are continuously recorded on paper drums using an amplification of 800 mm/mm/s. In addition, beginning in 1991, a PCEQ digital recording system digitized analogue signals with a sampling frequency of 100 Hz. More recent upgrades include the Earthworm/Seisan data acquisition and analysis package which was restored and upgraded by the USGS Volcano Disaster Assistance Program early in the eruption crisis of 2006. Nevertheless, paper seismograms continue to be examined every day in order to classify and record the number and magnitude of the various seismic events. Digital records are later processed for detailed analysis and for hypocenter location. In addition an RSAM (Real-time Seismic Amplitude Monitoring) system was supplied by Penn State beginning in 1993 with NSF support (Endo and Murray, 1991; Voight et al., 2000a), SSAM (Seismic Spectral Amplitude Monitoring) from Penn State was in rudimentary operation by 1994, and both systems have been maintained, if sporadically, and later upgraded in-house or with external help at various times up to the present.

The seismic data used in this study relies on the unpublished MVO multi-parameter database, which incorporates daily summations of the varying earthquake types in terms of the number of events, energy release, and in the case of surficial rockfall seismicity, the mathematical product of maximum *Amplitude x Duration* (*AxD*). Seismic data stored in the database are based on drum and digital records from the

vertical component sensor at the short-period seismic station Pusunglondon (PUSZ) located on the north flank of Merapi approximately one km from the summit (Fig. 3-1).

Volcanic earthquakes at Merapi have been categorized into volcano-tectonic (*VT*) types A (S and P arrivals easily resolvable, >2.5 km depth) and B (<2.5 km depth), low frequency (or long period) (*LF*), tremor, and multiphase (*MP*) seismicity (Ratdomopurbo and Poupinet, 2000; Hidayat et al., 2000). Collapses of the lava dome (rockfalls, glowing avalanches, pyroclastic flows), vulcanian explosions (17 January 1997), and lahars also generate characteristic seismic signals (Ratdomopurbo and Poupinet, 2000; Voight et al., 2000b; Brodscholl et al., 2000; Lavigne et al., 2000).

Rockfalls and pyroclastic flows are associated with emergent, spindle-shaped seismic envelopes that have frequencies much greater than 1-2 Hz, resembling high-frequency noise (Ratdomopurbo and Poupinet, 2000). Source mechanisms and signal properties have not been examined at Merapi but, at Montserrat, using broadband seismometers, Luckett et al. (2002) reported two source mechanisms that contributed to these seismic signals, namely (i) a moving surface source generating a high-frequency component with amplitude somewhat dependent on the magnitude (volume) of the event, and (ii) a long-period (LP) component (peak in spectral amplitude at 1-2 Hz) occurring near the onset of most rockfall signals, and likely related to gas venting or jetting in association with the generation of the event (Calder et al., 2002). In comparison, at Unzen Volcano, Japan, Uhira et al. (1994) identified three phases in rockfall and pyroclastic-flow signals. They observed wedge-shaped blocks of lava falling from a steep face and distinguished (i) block fall, (ii) collision with the ground, and (iii) flow transport, as the essential components in exciting the seismic signals.

Yamasoto (1993) and Uhira et al. (1994) reported that the volumes of pyroclastic flows shed from the Unzen dome (estimated by visual observation) were proportional to the maximum amplitude of seismic waves generated by the pyroclastic flow. Likewise, Norris (1994) used maximum seismic amplitude to investigate single-block edifice failures at Cascade volcanoes. However, the *area* of the spindle-shaped seismic amplitude envelopes on a seismic record may be a more appropriate measure where pyroclastic flow events are prolonged or discrete events merge into one another (Brodscholl et al. 2000). The relationship between volume of pyroclastic flow and signal amplitude is not necessarily a simple one, as suggested by work at Montserrat where late-stage pyroclastic flows travelled over a surface of newly accumulated, unconsolidated pyroclastic deposits, a substrate which dampened the amplitudes of the associated seismic signals. However the surface characteristics of the southwest sector of Merapi have not changed markedly during 1992-1998, thus supporting use of a correlation between seismic amplitude and Merapi dome collapses. The *Amplitude x Duration* parameter measured traditionally by MVO therefore serves as a proxy for area of the rockfall seismic envelope.

Multiphase earthquakes, a prominent type of dome-growth-related seismicity, have generally emergent first arrivals of 3-4 Hz and a long-period coda (Ratdomopurbo and Poupinet, 2000; Hidayat et al., 2000, 2003). They resemble somewhat the "hybrid events" of Chouet (1996a,b) and Miller et al. (1998). For a given MP amplitude, the duration is about twice that of a VT event (Ratdomopurbo and Poupinet, 2000), with strong attenuation of the amplitude as a function of distance from the summit. Their (commonly) emergent envelopes make it difficult to pinpoint arrival times and therefore

the location of the MP hypocenters. Nevertheless, Hidayat et al. (2000) were able to estimate their source location at shallow depth at Merapi, within several hundred meters of the surface.

Data regarding seismicity and major dome collapses are summarized in Table 3-1. These results and further detailed data plots are discussed below.

3.3.3 Tiltmetry

Summit and flank tiltmeters were installed mainly by Penn State researchers with the collaboration of VSI since 1990 (Fig 3-5, 3-6). The high-gain tilt sensors are electrolytic bubble-type, either the uniaxial Applied Geomechanics model 800 at summit sites, or biaxial Model 701 at flank sites, with resolutions of 2.3 and 0.1 μrad/mV, respectively. Model 800's at the summit were affixed to rock using stainless steel mounting studs cemented into drill holes of 2-3 cm depth. The digital data telemetry platforms used in the 1990s were designed and built by the USGS Cascades Volcano Observatory. Power was provided by automobile batteries coupled to solar panels. The telemetry systems were weather protected, with radio communication provided by a planeless whip antenna placed within sealed PVC tubing for protection from acidic gases in the volcanic plume. Analog inputs were digitized and transmitted by radio to the MVO receiving site at typically 15-min intervals. Transmissions took less than 10 s, allowing several transmitters to share the same frequency. The tilt data were received by radio and relayed through the modem port of a computer for decoding and data storage. The data were stored in an unfiltered form in a database format amenable to rapid visual and quantitative analysis using the interactive, command-driven program BOB (Murray,

1992). For this paper the data were converted using BOB and processed to eliminate time gaps and noise spikes due to transmission difficulties. The tilt data are presented here exclusively as magnitudes for the radial direction, because the key stations utilized uniaxial instruments oriented to record radial deformation with respect to the center of the dome complex.

Tiltmeter stations about the summit consisted of paired high- and low-gain tilt sensors, independently mounted to provide some redundancy for data interpretation. The uniaxial high-gain instruments provided ~2 μrad resolution, thus provided a relatively small dynamic range of one angular degree before going off-scale. Conversely, the low-gain instruments provided lower resolution (e.g., <200 μrad), but a much greater dynamic range of 60^{o} and even 180^{o} in some setups. The two-fold sensitivity and range levels were designed to give each site the flexibility to handle movements over a wide range. At certain times, it was deemed practical and sufficiently safe to attempt tilt monitoring on the lava dome itself (T7) (Fig. 3-5A), where large deflections were reasonably anticipated. Thus, low-gain sensors served not only as redundant checks of high-gain monitoring, but as back-up systems to monitor high and/or accelerating tilt rates should the high-gain sensors go off-scale. Further, it was anticipated that, in many circumstances, re-leveling at the sites could prove impractical due to reasons of safety, logistical problems, or exceptional rates of deformation.

Flank stations were set up without low-gain sensors because large deformations were not expected in these far-field locations. The higher-precision, biaxial sensor available with the Model 701 was thus selected as the instrument of choice at flank stations.

The number of tilt stations operating has varied through the time of this investigation, the main factors being maintenance issues, limited hardware availability, and ultimately site destruction during volcanic activity (Fig. 3-5B). The main installations were first installed at the summit in October 1992 at three locations (Fig. 3-5A). The summit network was expanded or stations shifted in October-November 1993 and November 1994 so that data was acquired at various times at three additional sites. Among all summit sites, stations T2 and T3 eventually proved most reliable as monitors of near-vent deformation on the uppermost flanks.

Flank locations T4, T8, and T9 (Fig. 3-6) employed in our telemetry network were designed to most effectively monitor pressure sources at greater depth. T4, at a radius of about 1 km (Pusunglondon ridge), is most sensitive to changes near 1-km depth, coinciding approximately with the top of a hypothesized magma chamber located within the edifice (Ratdomopurbo and Poupinet, 2000). (This interpretation is based on seismicity and seismic wave travel time delays in the 1-3 km depth range.) Stations T8 (Klatakan) and T9 (Babadan), located at 3- and 4-km distance from the summit, respectively, most effectively monitor processes originating at deeper levels.

A typical site design for the summit installations consisted of placing the high- and low-gain tiltmeters beneath a cover that provided protection from weather and afforded a small amount of temperature insulation. Telemetry unit and battery were placed in the protection of a larger box.

The response of tilt to volcanic activity can be interpreted as either a response to changed magma pressure in the conduit or the outward load of the lava dome bearing on

the crater wall, or to change in shear stress related to lava flux change in the conduit (Voight et al., 2000b; Beauducel et al., 2000; Green et al., 2006).

3.3.4 Magma Extrusion Rates

Rockfall events were recorded by MVO using the Merapi seismic network, with daily *Amplitude x Duration* (*AxD*) data compiled from the vertical component records of the short-period station PUS (Fig. 3-1). As direct surveys of fragmental deposit volumes were logistically difficult, we use rockfall *AxD* data as a proxy for rockfall volume. Use of such a proxy is somewhat similar to, and supported by, the results of Brodscholl et al. (2000) at Merapi, and also by Norris (1994) at Cascades volcanoes, and Yamasoto (1993) and Uhira et al. (1994) at Unzen**.** An improved seismic proxy can be envisioned for future monitoring, for example, using the square of seismic amplitude and coda values or, more conveniently by digital RSAM/SSAM values or RSAM/SSAM energy. The existing database covering the time considered in this study limits use of the seismic proxy for collapse volume to the *AxD* method.

The calibration was based on unpublished Volcanological Survey of Indonesia (VSI) survey measurements of rockfall deposit volumes, the first taken prior to the onset of eruptive activity on 20 January 1992, and the second on 26 August 1992 (Suharna, personal commun.). The cumulative volume change over this period was 2.9×10^6 m^3.

An additional volume of ~10% of the rockfall volume is assumed to have been lost to ash clouds (Sparks et al., 1998), for a total of 3.2×10^6 m^3. It was further assumed that the dense rock equivalent (DRE) volume equaled ~80% of deposit and ash volume, yielding a final estimate of ~2.6×10^6 m^3.

The cumulative *AxD* for the same period is 8.2 x 10^7 mm-s. The resulting calibration factor is, therefore, 0.032 m^3 DRE/mm-s *AxD*, or, 31 mm-s *AxD*/m3 DRE.

We use this factor in estimating DRE volume lost as implied by measured *AxD*, for various periods in the span of activity occurring between 1992 and 2000. However, we recognise that caution is needed in using it. Uncertainties include the measurement of volume of rockfall deposits in the field and the assumption of the magnitude of dispersed ash cloud volume. Also assumed is a linear relationship between DRE event volume and *AxD* at any instant in time, irrespective of event size, or its direction. The calibration factor is also assumed to be invariant over the longer term, even as rockfalls and large dome collapses modified the flank geometry and impacted different sectors.

Despite these caveats, the estimates of lava production are surely improved by the consideration of lost rockfall volume, rather than ignoring the process (Beauducel and Cornet, 1999). For several prolonged periods of time (e.g., December 1994-1995), the appearance and overall geometry of the lava dome from the south flank remained apparently unchanged, thus suggesting zero growth, and yet rockfalls continually fell from the headwall overlooking the steep southwest slope. The lava lobe was in a dynamic equilibrium, continually moving outward with continued effusion – yet repeated geodetic surveys of the dome would have implied nearly zero growth. Thus, the use of rockfall data in some fashion is essential for estimating more accurately the true extrusion rate.

We have used the calibration only to deal with progressive loss due to rockfall-sized events. This is because the *AxD* vs. volume relationship demonstrably breaks down with larger pyroclastic flow events, and in reality the relation is non-linear, although we do not have the full field data to quantify the non-linearity. For example the equivalent

values for PUSZ for the 22 November 1994 pyroclastic flows are 2.6-3.1 *AxD* mm-s/m^3 as compared to our calibration value of 31 mm-s/ m^3 (calculations discussed below), implying an order of magnitude less seismic energy release than for rockfalls. A possible explanation for this is the reduction in flow resistance and increased efficiency and mobility of gas-rich pyroclastic flows.

Dome volume and major dome collapse estimates were compiled from our own data and many other studies (Abdurachman et al., 2000; Brodscholl et al., 2000; Kelfoun, 1999; Ratdomopurbo and Poupinet, 2000; Ratdomopurbo et al., 2000; Voight et al., 2000a, b; Zlotnicki, et al., 2000; VSI, various unpublished data files). Keeping in mind the caveats noted above, we proceeded with estimates of the volume changes over specific time periods, and determined corresponding rates of lava extrusion. Cumulative lava extrusion and extrusion rates are compiled in Figs. 3-7 to 3-13 and compared to the various geophysical parameters recorded at Merapi volcano.

Cumulative magma extrusion volume for any specified period was calculated as follows:

$$M_e = D_v + PF_v + R_v,$$

where

M_e = magma extrusion volume (DRE),

D_v = cumulative volume of all dome growth phases (lobes) adjusted for DRE,

PF_v = cumulative pyroclastic flow volumes from field measurements, adjusted also for associated dispersed ash clouds (~10% of flow deposit volumes), and for DRE,

R_v = cumulative rockfall volume (DRE) as deduced from seismic *AxD*.

3.3.4.1. Magma extrusion rates during the 2006 eruption

The compilations noted above served as a basis for further studies of extrusion rate during the 2006 eruption. During the 2006 crisis MVO estimated dome lava changes from photographs taken from their observatory posts and satellite images. Based upon the ideas expressed in an earlier draft of this Chapter that was provided to MVO during the eruption crisis, MVO scientists took data from Deles (DELZ) and Pusunglondon (PUSZ) seismic stations and attempted a calibration to collapse volume of seismic *AxD*, and also seismic spectral amplitude measurements (SSAM) recorded at frequencies greater than 2.9 Hz (Table 3-2). They used two reference deposit volumes, specifically the November 22, 1994 dome collapse, and the volume of 2006 deposits estimated in K. Krasak/Bedog as of May 20, 2006 (C. Newhall, written commun.). Data from DELZ had the advantage that large events remained on scale. PUSZ, on the other hand, while suffering data clipping in many of these same large events, had the advantage of being the only station with a regular calculation of *AxD* values.

The bulk volume of deposit for 22 November 1994 was about 2.5 - 3.0 x 10^6 m^3 (Abdurachman and others, 2000), and these authors further estimated DRE volume for the deposit at 2.0 – 2.5 x 10^6 m^3. The resulting DELZ calibration is 2.5 - 2.9 m^3 / *AxD* unit (cf. data in Table 3-2). This includes a variety of event sizes, many of them relatively large, and predominately pyroclastic flows versus rockfalls. MVO monitoring for the eruption in April-May 2006 shows *AxD* for PUSZ on 22 May 2006 was 7.8 times that obtained from DELZ (data from C. Newhall, written commun., 2006). If we assume the same relation would have held on 22 November 1994 (i.e., PUSZ seismic records had not been clipped), then we infer from the DELZ data for that eruption, as calculated recently

by MVO, that the PUSZ *AxD* calibration would be 2.6-3.2 *AxD* mm-s/m^3. This contrasts with our 1992 estimate for rockfalls recorded at PUSZ of 31 *AxD* mm-s/m^3; as noted above, rockfalls make more seismic noise than larger events.

Results of calibrations specifically from observations of the 2006 eruption are as follows: The volume of 2006 collapse deposits to the southwest was estimated roughly to be 0.8 x 10^6 m^3 for May 20, yielding the calibrations 7.7 *AxD* mm-s/m^3 at PUSZ, or about 1.0 *AxD* mm-s/m^3 at DELZ (C. Newhall, written commun., 2006).

This is ~5x less than our 1992 calibration. Somewhat mitigating is that the rockfall/pyroclastic flow paths were somewhat different between 1992 and 2006, and the 2006 calibrations included some pyroclastic flows also, which would tend to raise the number.

These and similar data and calculations were used by MVO to estimate an overall effusion rate (as of 20 June 2006) of as much as 210,000 m3/d (2.4 m^3/s), of which ~75,000 m^3/d is growth of the lava dome, and 130,000 m^3/d DRE is attributed to rockfalls and pyroclastic flows via seismic estimation (C. Newhall, written commun.). The estimate for May 2006 was 150,000-175,000 m^3/d. These numbers are matched in the 20th Century only by 1930, 1961, and very early 1992 (e.g., Fig. 3-13).

The analyses above raise questions regarding the uncertainty in a linear calibration assumption. Using the PUSZ calibration for 2006 in a re-examination of the 1990s data would perhaps be an upper bound estimate. The result of course would be to increase significantly the calculated fluxes for the 1990s, and by analogy, to early episodes of the 20th Century.

3.4 Correlations of Geophysical Data with Volcanic Activity

Of prime importance in this study is the correlation of the various geophysical parameters and geological field observations to the major dome collapse events. In addition, consideration is given to estimates of the dome collapse volume, active lobe volume at the time of collapse, and lava extrusion rate, when determinable. Summaries of such correlations and precursors are outlined in Table 3-1.

3.4.1 Relation of major collapses to extrusion rates

The major dome collapse events recognized during 1992-1999 are in bar graph form in Figs. 3-12 and 3-13. Bar lengths are proportionate to estimated collapse volumes, calculated for the most part by volume loss from the dome itself. The timing of these events is compared to extrusion rate.

Results for the period 1992-1999 clearly show that the magma extrusion was periodic, ranging from $3x10^6$ m^3 to $12x10^6$ m^3 DRE of magma extruded, for active phases that lasted from 6 to 12 months (Table 3-3). The associated extrusion rates over the same multiple-month periods ranged from 0.19 m^3 s^{-1} (16,700 m^3/d) to 0.49 m^3 s^{-1} (42,000 m^3/d) (Table 3-3). Periods of low extrusion rate (<0.07 m^3 s^{-1}, i.e. <6000 m^3/d), or true hiatuses lasted one to two years.

Most major dome collapse events occurred during periods of elevated extrusion rate in the (relatively) very short term of days or weeks. For example, the dome collapse that began in February 1992 occurred with growth rates as high as 2.5 m^3 s^{-1} (220,000 m^3/d), very large for Merapi, but short lived. Again, in 2006, a high rate (for Merapi) of 2.3 m^3 s^{-1} (200,000 m3/d) was achieved in association with the large pyroclastic flows

and dome collapse of that eruption. These cycles are notable in that they followed hiatuses of about 3 to 5 years (Young et al., 2000; C. Newhall, personal commun., 2006).

Of the major dome collapse events considered in detail here (Table 3-1), most occurred during extrusion rates of at least 0.12 m^3 s^{-1} (~10,000 m^3 /d). This correlation is somewhat similar to the observation of van Bemmelen (1949) for the eruption period 1942-1943, when a high pulse of effusion (~30,000 m3/d maximum) was followed by pyroclastic flows (Voight et al., 2000a, their Fig. 22). The devastating 22 November 1994 dome collapse was a notable exception to the general correlation of large collapses with enhanced extrusion rates. The best estimates for extrusion rate preceding this 1994 event have been calculated at less than 0.012 m^3 s^{-1} (1000 m^3/d) , prior to gravitational collapse of the metastable 1994 dome lobe (Figs. 3-3, 3-4).

Looking at the pattern of lava flux to collapse events (Figs. 3-12, 3-13), the events in 1993 occurred during a period of low declining extrusion rate, and those in 1996-1998 occurred with rising effusion rate. However in 1994, 1997, and 1998 the extrusion rates that followed the collapses exceeded substantially the corresponding rates before or at the time of collapse. This suggests that marginally unstable domes are sensitive to modest increases in extrusion flux, such that small increases in flux can create instability. Further, once the dome mass has collapsed, back-pressure on the conduit is reduced, leading to an overall decrease in resistance to flow, and therefore an increase in flux. This increased flux generally declines over weeks to months, as the collapse cavity is filled with new lava and back-pressure to the conduit increases, or driving pressure diminishes.

3.4.2 Eruption precursors

High-gain tiltmeter results are compared to the occurrence of pyroclastic flows and the various seismic events at key times between 1992 and 1997 in Figs. 3-14 to 3-16. Precursory high- and low-gain tilts recorded prior to the July 1998 eruption are shown in Figure 3-17. Of greatest reliability from November 1992 to July 1998 was the nearly continuous recording of tilt from station T3 on the crater rim, located just a few meters from the 1992 lava dome spillover margin on the crater rim as it existed at that time.

No single picture of correlation emerges when the various dome collapses are viewed in total. However, most moderate to large dome collapses described here correlate with varying precursory inflationary tilt at the summit. For example, T3 experienced tilt of 530 μrad in the 12 days preceding the 3 Feb 1993 collapse, and 240 μrad prior to the onset of multiple collapses in March and April 1994. In the first case, tilt peaked several days after the collapse, whereas in the second case it peaked 7 days before the onset of the collapses, and thus the collapse phenomena correlates with some post-peak (deflationary) tilt. However, we distinguish between a deflation as a detectable variation from background, and a post-peak deflation, which marks a return *toward* background level following a prominent inflation. In the latter instance, one can also interpret the collapse as related to peak inflation with a time lag, or as a sub-peak inflation compared to background level.

The increase of tilt can be interpreted as a response to an increase in magma system pressure, as an increase in extrusion velocity (which in a viscous system leads to an increase in conduit wall shear stress; e.g., Beauducel et al., 2000; Green et al., 2006),

and/or changes of morphology of the dome within the crater, such as movement of a lava lobe toward, or against, a crater rim.

Pyroclastic flow and rockfall activity occurring during post-peak (deflation) stages, as measured by tilt, normally comprised relatively small events e.g., February 1994. The large-volume, commonly prolonged dome-collapse events with multiple pyroclastic flows usually occurred near the beginning of a cycle of dome growth. During this time the increased rate of lava extrusion caused the older dome lava to deform, frequently destabilized it, and pushed a shear lobe (e.g., Watts et al., 2002) of fresh lava into critically unstable configurations (e.g., 2-3 February 1993; 14 March-2 April 1994; 14-17 January 1997; mid-July 1998).

The largest (prolonged) dome collapse of 22 November 1994, however, appears to reflect the gradual imposition of gravitationally induced shear stresses acting within the southwest sector of the 1994 lobe (Fig. 3-14). No clear short-term precursors were detected prior to the eruption (Ratdomopurbo and Poupinet, 2000; Voight et al., 2000b), although, unfortunately, tiltmetry from operating stations was lost due to electronic interference on the telemetry network in the 34.5 h prior to the collapse. Only rockfall and pyroclastic-flow seismicity took place during the several hours of retrogressive collapses comprising the 22 November eruption (Voight et al. 2000b).

Over the longer term leading up to this eruption, an average 3.5 μrad/day inflation had occurred at T3 over 210 d. The rate of rockfalls had declined since August 1994, yet tilt and MP seismicity suggested continuous growth at a slow rate. Our interpretation is that the mass within the dome was gradually increasing, shear stresses tending to cause slip were gradually increasing, and instability was very gradually decreasing. Failure

occurred when the critical limit of stability was reached, resulting in small collapses. These small collapses created an increasingly oversteepened, unstable headwall, and the dome collapsed in additional increments, each collapse generating a pyroclastic flow, until a stable configuration was achieved.

During the January 1997 eruption, a vulcanian explosion generated a 4-km high plume that generated a fountain-collapse pyroclastic flow (Voight et al., 2000b). While MP seismicity and visual observations of dome volume suggested little or no dome growth in the month preceding this eruption, crater-rim tilt showed marked accelerating inflation beginning in December, reaching 600 μradians of inflation in the week prior to the eruption (Figure 3-15); the data suggests the rise of a pulse of gas-enriched magma.

Glowing rockfalls visually indicated a new phase of dome growth was occurring by the end of December 1996. Beginning 7 January 1997, over 100 MP events took place over the course of the day, and over 500 MPs occurred on 11 January. Total energy release for all volcanic seismicity peaked 13 January (Fig. 3-16), and as seismicity began to decline the following day, the first of many dome-collapse pyroclastic flows rolled down the southwest flank, as far as 4.5 km from the summit. During the next 10 h, 80 more pyroclastic flows followed a similar path to emplacement (Fig 3-1).

During the next two days the rate of MPs declined, tilt inflation peaked and a slight post-peak deflation occurred. A burst of MPs then occurred over a 10-h period, culminating in a vulcanian explosion at 1035 h on January 17. Subsequent column collapse generated a pyroclastic flow (Fig. 3-1 map). High frequency tremor had

appeared one hour before, and continued until, the explosion (Ratdomopurbo and Suharna, 1997).

Dramatic accelerating tilt also occurred in July 1998, as recorded by the sole remaining tiltmeter of our original summit network (Fig. 3-17). The tilt achieved a rate more than an order of magnitude greater than that of January 1997. Tilt on T3 was sufficiently extreme to put the high-gain sensor off-scale after 19,500 μrad. In fact, SEAN (Smithsonian Institution, 1998) concluded that the data were not reporting geologically meaningful tilt, but rather were an artefact of heat radiated by the new dome! This explanation was incorrect, as the author did not understand the truly proximal position of the T3 site with respect to the active dome and the northwest crater rim (Fig. 3-5). Further, low-gain tilt tracked the high-gain data before the high-gain sensor went off-scale – thus proving that the high-gain data were genuine – and continued to record accelerating deformation for another five days between 3 and 8 July (Fig. 3-17), recording an additional 40,000 μrad. During the same period, inflations were also recorded at other stations, but at much lesser tilt rates that indicated less sensitive positions. Finally, a single flank EDM re-measurement from Babadan was made successfully at midnight to one of the four reflectors located near T2 and T3 on 7 July. The result of that measurement was a shortening of the slope distance by about one meter! The EDM result further demonstrated the accelerating instability of the north-western uppermost flank, consisting of exposures of 1957 lava.

Loss of data on July 8 from T3 likely was caused by local collapse of the portion of crater rim holding T3, or damage to the site (tiltmeter and/or antenna) by falling rocks, as the first major collapse did not occur until July 11. Observers from the VSI Babadan

post reported that a large rockfall event raised a dust cloud that obscured the summit after the EDM measurement had been made. Probably not coincidently, the last T3 data was recorded at 00:45 (8 July). A portion of the 1957 lava therefore apparently collapsed on 8 July, shoved aside by a new lobe of emerging lava that would later experience the large dome collapses on 11 and 19 July.

No vulcanian activity was documented by observers during the July 1998 collapse, but at least one photograph suggests at least a small laterally-directed explosion (Ratdomopurbo et al., 2000). Tilt changes in both the January 1997 and July 1998 eruptions were qualitatively similar in their accelerating character (though differing by an order of magnitude), and perhaps arose from fundamentally similar processes. These processes were of sufficient magnitude to impart significant permanent strain on the tilt station locations during at least the January 1997 eruption, preventing elastic deflation following the culmination of activity.

3.5 Eruption Cyclicity over the Long Term, and the 2006 Eruption

Based on the study of lava production rates at Merapi in the first nine decades of the 20th century, Siswowidjoyo et al. (1995) noted three periods of elevated extrusion took place during this period. Their lava production results, shown in Fig. 3-18, suggest heightened extrusion portions of each cycle during the periods 1902-1913, 1930-1934, and 1961-1969. Note that cumulative extrusion and thus extrusion rates determined by Siswowidjoyo et al. (1995) are minimum values in that losses by rockfalls were not considered in their calculations.

Adding our data and resulting estimates of cumulative lava extrusion for the period 1992 to April 2004 onto the long-term results of Siswowidjoyo et al. (2005) suggested that the period 1992-1999 represented yet another period of elevated extrusion that continued the pattern of ~30-year cyclicity (Young et al., 2003, 2004). We interpreted the eruption of 2001, given the length of preceding hiatus and the marked presence of precursory VT seismicity, as suggestive that this phase of activity was related to the beginning of a period of reduced long-term lava production found in a typical 17 to 27 year interlude between heightened phases of each cycle (Young et al., 2003, 2004).

Integrating the new data since 1992 to the long-term lava production rates of Siswowidjoyo et al. (1995) yields an adjusted 20th century mean lava extrusion rate of 0.042 m^3 s^{-1} (~3600 m^3/day) for the last 100 years. It should be noted that in this integration of data, no allowance has yet been made for the fact that we have incorporated estimates of rockfall volumes based on the seismic *AxD* data into the calculations of cumulative lava erupted, whereas such data were not available prior to 1992. For the decade of the 1990's such an allowance increased estimates of cumulative magma production by about 25% for a DRE adjustment of ~0.8. If a similar adjustment is assumed for pre-1992 data, the resulting mean lava extrusion rate is raised to about 0.05 m^3 s^{-1} (~4300 m^3/day), and even this may be too small, by a factor of 2x or more.

Documentation of the previous cycles suggested that lava effusion in the future might be 'forecast' (Young et al., 2003, 2004). For example, if the 30-year cyclicity continued at Merapi, Young et al. (2003) noted that lava production should be diminished over the next 20 years, compared to the activity witnessed between 1992 and 1999. On this basis a return to elevated lava production was expected around 2020-2028 (Fig. 18).

The eruption of 2006 indicates the difficulty in specific quantitative forecasts of volcanic activity in the long term. New magma broke out in April 2006, and the dome grew rapidly by Merapi standards, with a rate exceeding 150,000 m3/d, and overlapped the 1997 dome and 1961 scarp (Fig. 3-5B). The dome took the form of a pancake roughly 200 m in diameter over most of the summit region, with a volume of 2.5-3 x 106 m^3, and with growth nearly balanced after early May by release of rockfalls and dome-collapse pyroclastic flows off its edges, on southwest (K. Krasak and K. Boyong) and south margins (K. Gendol). Dome volume and geometry were sufficient to overtop the southeast-oriented Gendol breach, allowing pyroclastic flows and rockfalls to impact that sector for the first time since ~1913. Because the rate of extrusion only slightly exceeded loss by collapse towards the multiple sectors, the external form of the dome did not change much. But over 12-13 x 10^6 m^3 lava was extruded (C. Newhall, written commun., 2006).

Given the reality of the 2006 activity and lava production, and acknowledging the tenuous nature of long-term forecasts, we nevertheless have revised our forecast for the future eruptive activity at Merapi, based on the cyclicity observed empirically in the previous one hundred years (Fig. 3-18). In this revised interpretation, we incorporate the 2006 activity into the prolonged phase of elevated magma flux that began in 1992 (Table 3-4). The revised forecast is therefore that 2006 marks the end of this 15-year period of overall elevated extrusion rate, and will be followed by a return to a time of generally lower magma flux in the next ~16 years. Following the general observation that a cycle of high and low flux is repeated about every 30 years, it is still forecast that the next extended period of high flux will then manifest itself in about the year 2022.

3.6 Discussion and Conclusions

We have investigated correlations of various measurable and observable geophysical parameters at Merapi volcano in order to ascertain potential precursory behavior, and how such behavior reflects instability of the lava dome and dome collapse events. This study leads to the following points:

Rockfalls or pyroclastic flows generated by collapse of unstable portions of the growing lava dome occurred frequently, often on a daily basis from January 1992 to at least early 2002, and again in 2006.

Large ($> 0.2 \times 10^6$ m^3) dome collapses and their accompanying pyroclastic flows were typically generated during periods of elevated extrusion rate, > 0.17 $m^3 s^{-1}$ (15,000 m^3/d), heightened MP seismicity, and inflationary crater-rim ground deformation as measured by proximal tiltmeter stations. The elevated extrusion rate exceeds the long-term 20th century rate of 0.042 $m^3 s^{-1}$ (3600 m^3/d), as recalculated here, by nearly an order of magnitude.

The characteristics of lava extrusion were affected by extrusion rate. Lava domes and tongues have grown mainly via the extrusion of so-called shear lobes, which then played an important structural role in the generation of rockfalls and pyroclastic flows. The morphology of the lobe is influenced by viscosity and flux rate; the pancake-shaped lobe of early 1992 and 2006 corresponded to an unusually high lava flux. The direction of the extruding lobe and the location of the active headwall controlled the locations and directions of subsequent collapses. Similar observations have been reported from Montserrat (Watts et al., 2002). Collapse volumes and collapse scar shape are probably

also controlled by lobe structures. Pyroclastic flows were commonly generated from collapses of active shear lobes, where material was hot, and gas-rich, and disintegration of the microvesicular andesite lava in collapsed blocks occurred readily.

Smaller collapses may not have necessarily correlated to elevated extrusion rate or to discrete shear-lobe formation, and even the large collapse of November 1994 did not manifest itself by precursory seismic activity or measurable tilt deformation. In some cases, environmental factors such as rainfall likely have played a roll in localized instability, such as in scattered rockfalls during rainy periods, and in the relatively lesser November 1995 collapse. For the case of the large dome collapse on 22 November 1994, slow continuing growth and impeded rockfalls led to increased dome mass and gradually decreasing gravitational stability.

Elevated extrusion rates at Merapi were periodic over 6 to 48 month periods, in the period 1992-2006. These relatively medium-term eruptive cycles together comprise an overall period of heightened magma production that continued the pattern of ~30-year cyclicity observed for the first nine decades of the 20th century. A similar ~30-year cyclic period has been identified on Montserrat, and also, medium-term cycles of enhanced activity (Sparks and Young, 2002; Voight et al., 1999). The activity at Merapi in 2001, though vigorous, was interpreted initially to possibly reflect the beginning of a new phase of generally lower activity when viewed on a decadal time scale. However, the 2006 eruption has demonstrated the fallacy of this forecast.

The medium-term cycles of 6-48 months may be a response to shallow-level magma chamber processes within the volcano, possibly linked to conduit behaviour such as crystallization at conduit boundaries and impeded or blocked flows. The chamber is

postulated to lie about 1.5-2.5 km under the summit (Ratdomopurbo and Poupinet, 2000). Long-term cycles of 30 years length may represent possibly analogous processes, but at greater depth (>>5km, the limit of observed seismicity), and involving influxes of mafic magma.

The causes of localized tilt deformation are uncertain. The response of tilt to activity can be interpreted as either a response to changed magma pressure in the shallow conduit, to change in conduit wall shear stress related to lava flux change in the conduit (Sparks, 1997; Voight et al., 2000b; Beauducel et al., 2000), or to the outward load of the spreading lava dome bearing on the crater rim wall (certainly, the latter mechanism is part of the story for January 1997 and perhaps also 1998).

A multidisciplinary approach to Merapi monitoring is necessary. Seismology only sees a small fraction of the events that occur in the volcano interior and as 22 November 1994, has shown, can be blind to an exceptional event. Long-term deformation measurements near the summit and on the flanks are extremely important to understand the physics of the volcano.

There is not a clear relation between observed gas emissions and lava flux. If the lava being extruded were really fresh, we should be seeing around 900 t/d of SO2 (C. Newhall, written commun.). Instead, we are seeing 200-300 t/d, much less than anticipated for periods of really high magma flux, although over the span of decades, much more SO2 has been emitted than possible for the volume of lava erupted (Voight et al., 2000a). The simplest explanation is that magma erupted was significantly degassed over preceding years or decades (C. Newhall, written commun., 2006). Satellite data in June 2006 suggested higher rates than previously.

On petrologic grounds it has been postulated that magmas rising faster than about 10 cm/s tend to produce explosive eruptions (Rutherford and Hill, 1993; Devine et al., 1998). Considering Merapi in 2006 with a maximum but persistent lava extrusion rate of ~200,000 m3/d, and assuming a conduit of cross-section area ~350-700 m^2 (corresponding to ~10-15 m diameter; C. Newhall, written commun., 2006; Siswowidjoyo et al., 1995), the ascent rate is rising less than 1 cm/s -- an order of magnitude less than the threshold suggested for explosivity. This, coupled with the apparent lack of gas, explains the general lack of explosivity over the last Century. An intriguing question therefore is what factors caused the explosion noted in 1997, and other times such as 1961.

More to the point, why have eruptions of the 20^{th} Century been so relatively non-explosive, compared to bigger and more dramatic events that characterized previous centuries (Voight et al., 2000a)? The answer appears to be that magmas erupted during the 1900's and more recently have already lost much of their gas before they reached the surface (C. Newhall, written commun., 2006; Voight et al., 2000a). This has implications for hazards. First, degassed magma is less explosive than fresh magma and tends to erupt as viscous lava domes. Second, because magma is always present in the conduit, the transport system rarely gets obstructed and magma surges can rise aseismically and without significant deformation. Seismic and geodetic precursors, although notable in 1992, 2001, and 2006, were otherwise minimal, making the forecasting of eruptions, and changes in eruptions, relatively difficult.

Explosive eruptions can develop in two different ways with different precursors. Relatively small explosive eruptions can occur after degassing magma clogs up the

plumbing and a small amount of gas is trapped and eventually "bursts" (C. Newhall, written communication, 2006). Precursors to this could be a decrease in seismicity and gas emission, followed by a short re-escalation of both and then a small explosion. Possibly this explains the explosion during the January 1997 dome growth. Larger and more dangerous explosive eruptions can occur if there is a fast and voluminous influx of fresh magma from depth. Gas cannot bleed off fast enough and a sizeable explosive eruption occurs (tens to hundreds of million m^3 of magma). Such explosions occurred in 1822 and 1872 and swept wide areas around the volcano with pyroclastic flows larger than those of the 20^{th} Century (C. Newhall, written commun., 2006; Voight et al., 2000a; Hartmann, 1934). The great extrusion rate of the 2006 eruption made the latter possibility a substantial concern for such an event, at least on the scale of 1930 or 1961, raising substantially the mitigation concerns.

3.7 Acknowledgements

I thank the many scientists of VSI (*Center for Volcanology and Geological Hazard Mitigation, CVGHM),* for their collaboration and assistance, in particular Dr. Wimpy S. Tjetjep, Dr. R. Sukhyar, Dr. Mas Olas, Dr. Sutikno Bronto, Dr. Suparto Siswowidjoyo, and Dr. Ir. Mas Atje Purbawinata. Staff at the MVO (*Balai Penyelidikan dan Pengembangan Teknologi Kegunungapian, (BPPTK)* provided technical, logistical, and field support, and in this regard thanks are due Paijo, Suparban, and Ahreef. Telemetry for tiltmeters and seismic amplitude monitoring equipment was developed by U.S. Geological Survey scientists at Cascades Volcano Observatory, Alaska Volcano Observatory, and Menlo Park, and aid was provided by R. LaHusen, T. Murray, W. Lee,

J. Rodgers, and J. Marso. Logistical activities were aided by French Cooperants Philippe Jousset, Jacques Tondeur, Francois Beauducel, and Michel Dejean.

3.8 References

Abdurachman, E. K., Bourdier, J.-L., Voight, B., 2000. Nuées ardentes of November 22 1994 at Merapi Volcano, Java, Indonesia. J. Volcanol. Geotherm. Res. 100, 345-361.

Andreastuti, S.D., Alloway, B.V., Smith, I. E.M., 2000. A detailed tephrostratigraphic framework at Merapi Volcano, Central Java, Indonesia: implications for eruption predictions and hazard assessment. J. Volcanol. Geotherm. Res. 100, 51-67.

Beauducel, F., Cornet, F.H., 1999. Collection and three-dimensional modeling of GPS and tilt data at Merapi volcano, Java. J. Geophys. Res. 104(B1), 725-736.

Beauducel, F., Cornet, F.-H., Suhanto, E., Duquesnoy, T., Kasser, M., 2000. Constraints on magma flux from displacements data at Merapi volcano, Java, Indonesia. J. Geophys. Res. 105(B4), 8193-8203.

Boudon, G., Camus, G., Gourgaud, A., Lajoie, J., 1993. The 1984 nuée-ardente deposits of Merapi Volcano, Central Java, Indonesia: Stratigraphy, textural characteristics and transport mechanisms. Bull. Volcanol. 55, 327-342.

Bourdier, J.-L., Abdurachman, E.K., 2001. Decoupling of small-volume pyroclastic flows and related hazards at Merapi volcano, Indonesia. Bull. Volcanol. 63(5), 309-325.

Brodscholl, A., Kirbani, S.B., Voight, B., 2000. Sequential dome-collapse nuées ardentes analyzed from broadband seismic data, Merapi Volcano, Indonesia. J. Volcanol. Geotherm. Res. 100, 363-369.

Calder, E.S., Luckett, R., Sparks, R.S.J., Voight, B., 2002. Mechanisms of lava dome instability and generation of rockfalls and pyroclastic flows at Soufriere Hills Volcano, Montserrat. In: Druitt, T.H., Kokelaar, B.P. (eds) The eruption of Soufrière Hills Volcano, Montserrat, from 1995 to 1999. Geological Society, London, Memoirs 21, 173-190.

Chouet, B.A., 1996a. New methods and future trends in seismological volcano monitoring. In: Tilling, R. I., Scarpa, R. (eds.), Monitoring and Mitigation of Volcano Hazards. Springer, Berlin, 23-97.

Chouet, B.A, 1996b. Long-period volcano seismicity - its source and use in eruption forecasting. Nature 380, 309-316.

Devine, J.D., Rutherford, M.J., Gardner, J.E., 1998. Petrologic determination of ascent rates for the 1995-1997 Soufriere Hills Volcano andesite eruption. Geophys. Res. Lett. 25 (19), 3673-3676.

Endo, E.T. Murray, T.L., 1991. Real-time seismic amplitude measurement (RSAM), a volcano monitoring and prediction tool. Bull. Volcanol. 53, 533-545.

Escher, B.G., 1933. On a classification of central eruptions according to gas pressure of the magma and viscosity of the lava. Leidsche Geol. Mex. 6, 45-49.

Green, D.N., Neuberg, J., Cayol, V., 2006. Shear stress along the conduit wall as a plausible source of tilt at Soufrière Hills volcano, Montserrat. Geophys. Res. Lett. 33, L10306, doi:10.1029/2006GL025890.

Hartmann, M.A., 1934. Der grosse Ausbruch des Vulkanes G. Merapi (Mittel-Java) im Jahre 1872 [The large eruption of Mt Merapi volcano (Central Java) in 1872]. Natuurk. Tkjdschr. Ned. Indie 94, 189-210, in German.

Hidayat, D., Voight, B., Langston, C., Ratdomopurbo, A., Ebeling, C.,2000. Broadband seismic experiment at Merapi Volcano, Java, Indonesia: very-long-period pulses embedded in multiphase earthquakes. J. Volcanol. Geotherm. Res. 100, 215-231.

Hidayat, D., Voight, B., Mattioli, G., Young, S.R., Linde, A.T., Sacks, I.S., Malin, P.E., Shalev, E., Elsworth, D., Widiwijayanti, C., Herd, R., Thompson, G., Bass, V., 2003. Seismo-acoustics, VLP and ULP signals, and other comparisons of surface broadband and CALIPSO borehole data at Soufrière Hills Volcano, Montserrat, B.W.I.. Eos Trans. AGU 84(46), Fall Meet. Suppl., Abstract U31B-0002.

Kelfoun, K., 1999. Processus de croissance et de destabilisation des domes de lave du volcan Merapi (Java Centrale, Indonesie) [Lava dome growth and destabilization at Merapi volcano (Central Java, Indonesia)]. PH.D. dissertation, Universite Blaise Pascal Clermont-Ferrand II, 245pp, (in French).

Lavigne, F., Thouret, J.-C., Voight, B., Young, K., LaHusen, R., Marso, J., Suwa, H., Sumaryono, A., Sayudi, D.S., Dejean, M., 2000. Instrumental lahar monitoring at Merapi Volcano, Central Java, Indonesia. J. Vol. Geotherm. Res. 100, 457-478.

Luckett, R., Baptie, B. Neuberg, J., 2002. The relationship between degassing and rockfall signals at Soufrière Hills Volcano, Montserrat. In: Druitt, T.H., Kokelaar, B.P. (eds.), The eruption of Soufrière Hills Volcano, Montserrat, from 1995 to 1999. Geological Society, London, Memoirs 21, 595-602.

Miller, A.D., Stewart, R.C., White, R.A., Luckett, R., Baptie, B.J., Aspinall, W.P., Latchman, J.L., Lynch, L.L. Voight, B., 1998. Seismicity associated with dome growth and collapse at the Soufrière Hills Volcano, Montserrat. Geophys. Res. Lett., 25, 3401-3404.

Murray, T.L., 1992. A System for acquiring, storing, and analyzing low-frequency time-series data in near-real time. In: Ewert, J.W., Swanson D.A. (eds.), Monitoring Volcanoes: Techniques and Strategies Used by the Staff of the Cascades Volcano Observatory, 1980-90: USGS Bulletin 1966, 223pp.

Murray, T. L., Endo, E.T., 1989. A real-time seismic amplitude measurement system (RSAM): U. S. Geological Survey Open File Report 89-684, 21pp.

Newhall, C.G., Bronto, S., Alloway, B., Banks, N.G., Bahar, I., del Marmol, M.A., Hadisantono, R.D., Holcomb, R.T., McGeehin, J., Miksic, J.N., Rubin, M., Sayudi, S.D., Sukhyar, R., Andreastuti, S., Tilling, R.I., Torley, R., Trimble, D., Wirakusumah, A.D., 2000. 10,000 Years of explosive eruptions at Merapi Volcano, Central Java: archaeological and modern implications. J. Volcanol. Geotherm. Res. 100, 9-50.

Norris, R. D., 1994. Seismicity of rockfalls and avalanches at three Cascade Range volcanoes: Implications for seismic detection of hazardous mass movements. Bull. Seism. Soc. Am. 84(6), 1925-1939.

Ratdomopurbo, A., 1995. Étude sismologique du volcan Merapi et formation du dôme de 1994 [Seismology of Merapi volcano and formation of the 1994 dome]. Ph.D. dissertation. L'Univ. Joseph Fourier-Grenoble I, Grenoble, France, 208 pp. (in French).

Ratdomopurbo, A., Poupinet, G., 2000. An overview of the seismicity of Merapi volcano (Java, Indonesia), 1983-1994. J. Volcanol. Geotherm. Res. 100, 193-214.

Ratdomopurbo, A., Suharna, 1997. Seismicity before, during and after the January 17, 1997 eruption of Merapi Volcano, In: Proc. Merapi Decade Volcano International Workshop II, Yogyakarta, 14.

Ratdomopurbo, A., Sulistiyo, Y., Suharna, 2000. (eds.) Prekursor erupsi Gunung Merapi [Eruption precursors at Mt Merapi], Direktorat Vulkanologi, Maret 2000, 72pp (in Indonesian.

Rutherford, M.J, Hill, P.M., 1993. Magma ascent rates from amphibole breakdown: an experimental study applied to the 1980-1986 Mount St. Helens eruption. J. Geophys. Res. 98, 19,667-19,685.

Sato, H., Fujii, T., Nakada, S., 1992. Crumbling dacite dome lava and generation of pyroclastic flows at Unzen Volcano. Nature, 360, 664-666.

Shelley, I., Voight, B., 1995. Medical effects of nuée ardente eruptions: the November 1994 eruption at Merapi Volcano, Indonesia. In: Proc. Merapi Decade Volcano International Workshop, UNESCO/Volcanological Survey of Indonesia, Yogyakarta, 9pp.

Siswowidjoyo, S., Tulus, Djumarma, A., Matahelumual, J., Tjetjep, W.S., Pratomo, I., Bahar, I., 1985. Kegiatan G. Merapi, Jawa Tengah, tahun 1984 [Activity at Mt. Merapi, Central Java, during 1984]. Proc. PIT XIV Ikatan Ahli Geologi Indonesia, pp. 181-192 (in Indonesian).

Siswowidjoyo, S., Suryo, I., Yokohama, I., 1995. Magma eruption rates of Merapi volcano, central Java, Indonesia during one century (1890-1992). Bull. Volcanol. 57, 111-116.

Smithsonian Institution, 1998. Merapi. Bull. Global Vol. Network 23, no. 8.

Smithsonian Institution, 2000a. Merapi. Bull. Global Vol. Network 25, no. 11.

Smithsonian Institution, 2000b. Merapi. Bull. Global Vol. Network 25, no. 12.

Smithsonian Institution, 2001. Merapi. Bull. Global Vol. Network 26, no. 1.

Sparks, R.S.J., 1997. Causes and consequences of pressurisation in lava dome eruptions. Earth Plan. Sci. Lett. 150, 177-189.

Sparks, R.S.J. Young, S., 2002. The eruption of Soufrière Hills Volcano, Montserrat (1995-1998): overview of scientific results. In Druitt, T.H. Kokelaar, B.P. (eds.), The Eruption of Soufriere Hills Volcano, Montserrat, from 1995 to 1999. Geological Society, London, Memoirs 21, 45-69.

Sparks, R.S.J., Young, S.R., Barclay, J., Calder, E.S., Cole, P., Darroux, B., Davies, M.A., Druitt, T.H., Harford, C., Herd, R., James, R., Lejeune, A-M., Loughlin, S., Norton, G., Skerrit, G., Stasiuk, M.V., Stevens, N.S., Toothill, J., Wadge, G. and Watts, R., 1998. Magma production and growth of the lava dome of the Soufrière Hills Volcano, Montserrat, West Indies: November 1995 to December 1997. Geophys. Res. Lett., 25, 3421-3424.

Thouret, J.-C., Lavigne, F., Kelfoun, K., Bronto, S., 2000. Toward a revised hazard assessment at Merapi volcano, Central Java. J. Vol. Geotherm. Res. 100, 479-502.

Uhira, K., Yamasato, M. Takeo, M., 1994. Source mechanism of seismic waves excited by pyroclastic flows observed at Unzen volcano, Japan. Journal of Geophysical Research 99, 17757-17773.

Van Bemmelen, R.W., 1949. The Geology of Indonesia, 1A, Martinus Nijhoff, The Hague, 732 pp.

Voight, B., Davis, M.J., 2000. Emplacement temperatures of the November 22, 1994 nuees ardente deposits, Merapi Volcano, Indonesia. J. Vol. Geotherm. Res 100, 371-377.

Voight, B., Sparks, R.S.J., Miller, A.D., Stewart, R.C., Hoblitt, R.P., Clarke, A., Ewart, J., Aspinall, W.P., Baptie, B., Calder, E.S., Cole, P., Druitt, T.H., Harford, C., Herd, R.A., Jackson, P., Lejeune, A.M., Lockhart, A.B., Loughlin, S.C., Luckett, R., Lynch, L., Norton, G.E., Robertson, R., Watson, I.M., Watts, R., Young, S.R., 1999. Magma flow instability and cyclic activity at Soufrière Hills Volcano, Montserrat, British West Indies. Science 283 (5405), 1138-1142.

Voight, B., Constantine, E.K., Siswowidjoyo, S. Torley, R., 2000a. Historical eruptions of Merapi Volcano, Central Java, Indonesia, 1768-1998. J. Volcanol. Geotherm. Res. 100, 69-138.

Voight, B., Young, K.D., Hidayat, D., Subandrio, Purbawinata, M.A., Ratdomopurbo, A., Suharna, LaHusen, R., Marso, J., Murray, T.L., Dejean, M., Iguchi, M., Ishihara, K., 2000b. Deformation and seismic precursors to dome-collapse and fountain-collapse nuées ardentes at Merapi Volcano, Java, Indonesia, 1994-1998. J. Volcanol. Geotherm. Res. 100**,** 261-287.

Voight, B., Sukhyar, R., Wirakusumah, A.D., 2000c. Introduction to the special issue on Merapi Volcano. J. Volcanol. Geotherm. Res. 100, 1-8.

Watts, R.B., Sparks, R.S.J., Herd, R.A. Young, S.R., 2002. Growth patterns and emplacement of the andesitic lava dome at Soufrière Hills Volcano, Montserrat. In: Druitt, T.H. Kokelaar, B.P. (eds), The eruption of Soufrière Hills Volcano, Montserrat, from 1995 to 1999. Geological Society, London, Memoirs 21, 115-152.

Woods, A. Kienle, J., 1994. The dynamics and thermodynamics of volcanic clouds: theory and observations from the April 15 and April 21, 1990 eruptions of Redoubt Volcano, Alaska. J. Volcanol. Geotherm. Res. 62, 273-299.

Yamasoto, H., 1993. Seismic and acoustic signals excited by pyroclastic flows at Unzendake. In: Proc. Workshop on Volcanic Disaster Prevention, Palo Alto: Panel on Volcanic Disaster Prevention under Japan-US Science and Technology Agreement, pp. 303-304.

Young, K.D., Voight, B., Subandriyo, Sajiman, Miswanto, Casadevall, T.J., 2000. Ground deformation at Merapi Volcano, Java, Indonesia: distance changes, June 1988—October 1995. J. Volcanol. Geotherm. Res. 100, 233-259.

Young, K.D., Voight, B., Ratdomopurbo, A., Andreastuti, S.D., Subandriyo, Suharna, Sajiman, Miswanto, 2003. Pyroclastic flows, rockfalls, and heightened magma flux associated with the Merapi volcano eruption of 1992-1998, Central Java, Indonesia. Eos Trans. AGU 84(46), Fall Meet. Suppl., Abstract V42B-0361.

Young, K.D., Voight, B., Ratdomopurbo, A., Andreastuti, S.D., Subandriyo, 2004. Multiple extrusion cycles and lava flux since A.D. 1900 at Merapi Volcano, Central Java, Indonesia, IAVCEI General Assembly Abstracts, Pucon, Chile.

Zlotnicki, J., Bof, M., Perdereau, L., Yvetot, P., Tjetjep, W., Sukhyar, R., Purbawinata, M.A., Suharno, 2000. Magnetic monitoring at Merapi volcano, Indonesia. J. Volcanol. Geotherm. Res. 100, 321-336.

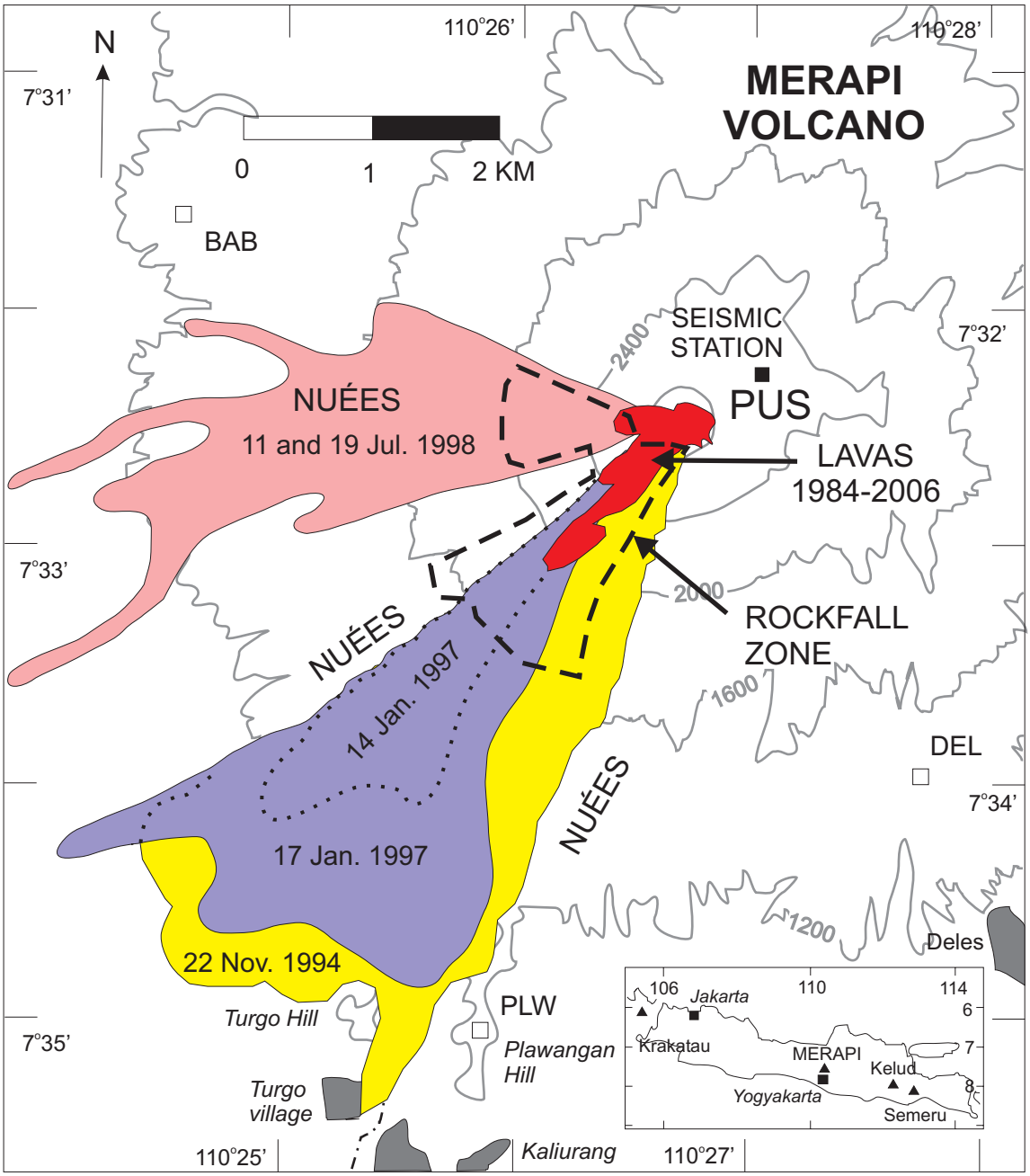

Figure **3-1**. Merapi volcano, showing the distribution of summit lava domes and tongues dating from 1984 to 2006, and debris and pyroclastic flow aprons of significance formed during 1994-2002. Pyroclastic deposits of the 2006 eruption are not shown. Short-period seismic station PUS (vertical component referred herein as PUSZ) is the source of long-term seismic data records maintained by Merapi Volcano Observatory. Inset shows the location of Merapi on the island of Java, Indonesia.

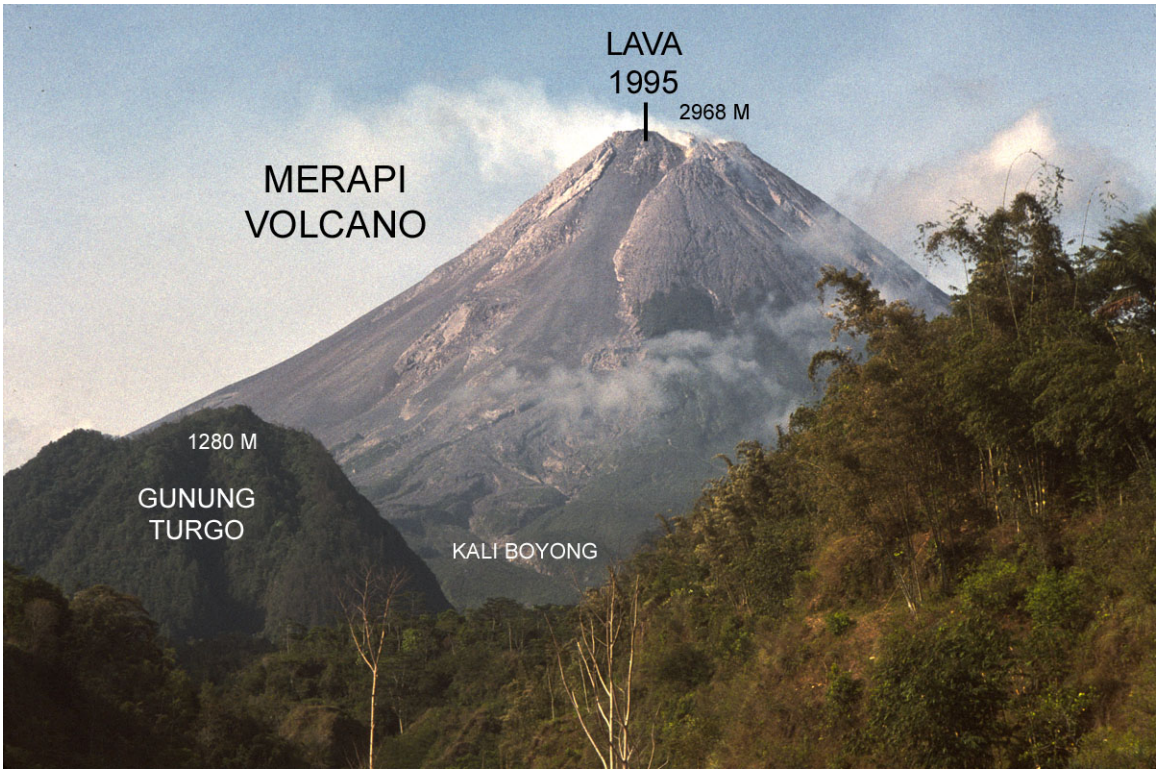

Figure **3-2**: A ground-based view in March 1995 of Merapi volcano from the edge of the Boyong river gorge, near Kaliurang. White plume emanates from summit sulfataras and the active dome shear lobe of 1995. Relief from base of the cone to summit is about 1800 meters. Gunung Turgo (Turgo Hill) rises on the left, the slopes of Gunung Plawangan on the right.

Figure **3-3**: Crater rim view of the lava dome from (A) EDM station DOZ in November 1994, and (B) a similar but not identical location in March 1995 following the 22 November 1994 dome collapse. Field of view spans approximately 200 m.

Figure **3-4**: Example of dome growth and collapse: The 22 November 1994 eruption. Shown is a distal south flank view, in profile, of a later stage nuée several hours after onset of the eruption. M. Mongin photo.

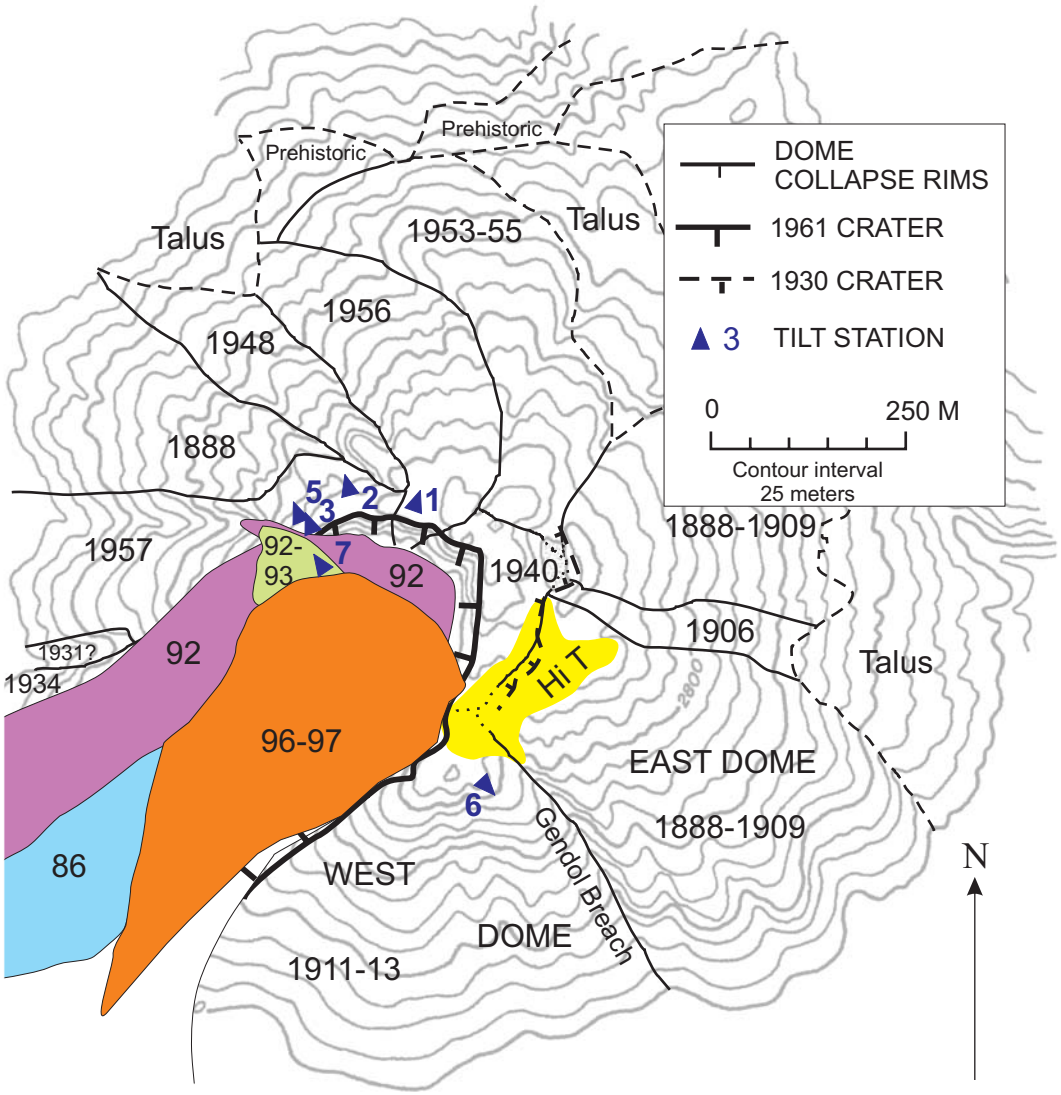

Figure **3-5A**. Summit lava dome and lava tongue distribution and location of the summit tilt stations T1, T2, T3, T5, T6, and T7. Situation as of May 1998, with summit tilt stations in operation at various times between 1992 and 1998 marked.

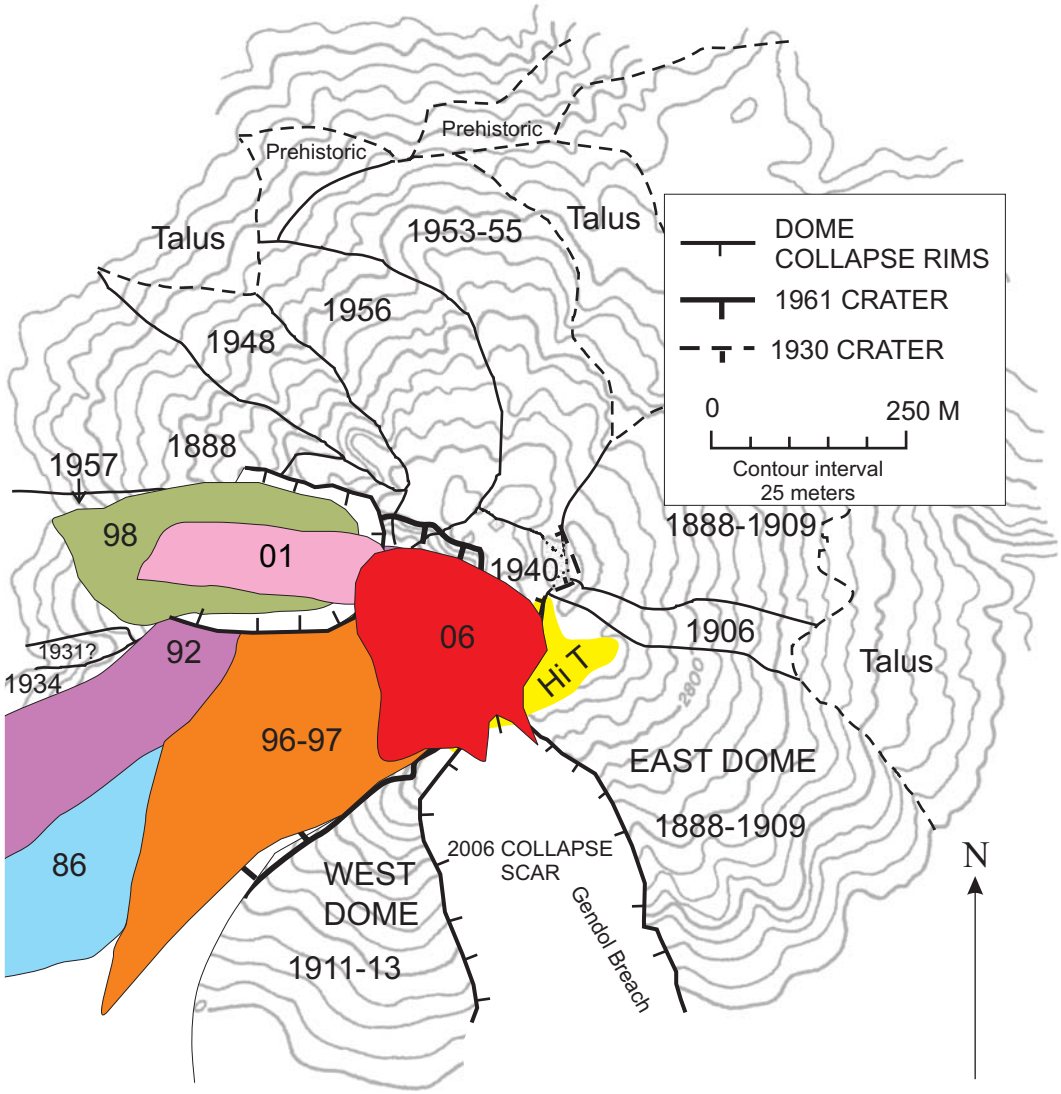

Figure **3-5B**. Situation as of July 2006. The last operating tilt station was lost in July 1998. Note that all tilt sites except T1 were either overrun by lava or lost to dome collapses by this time.

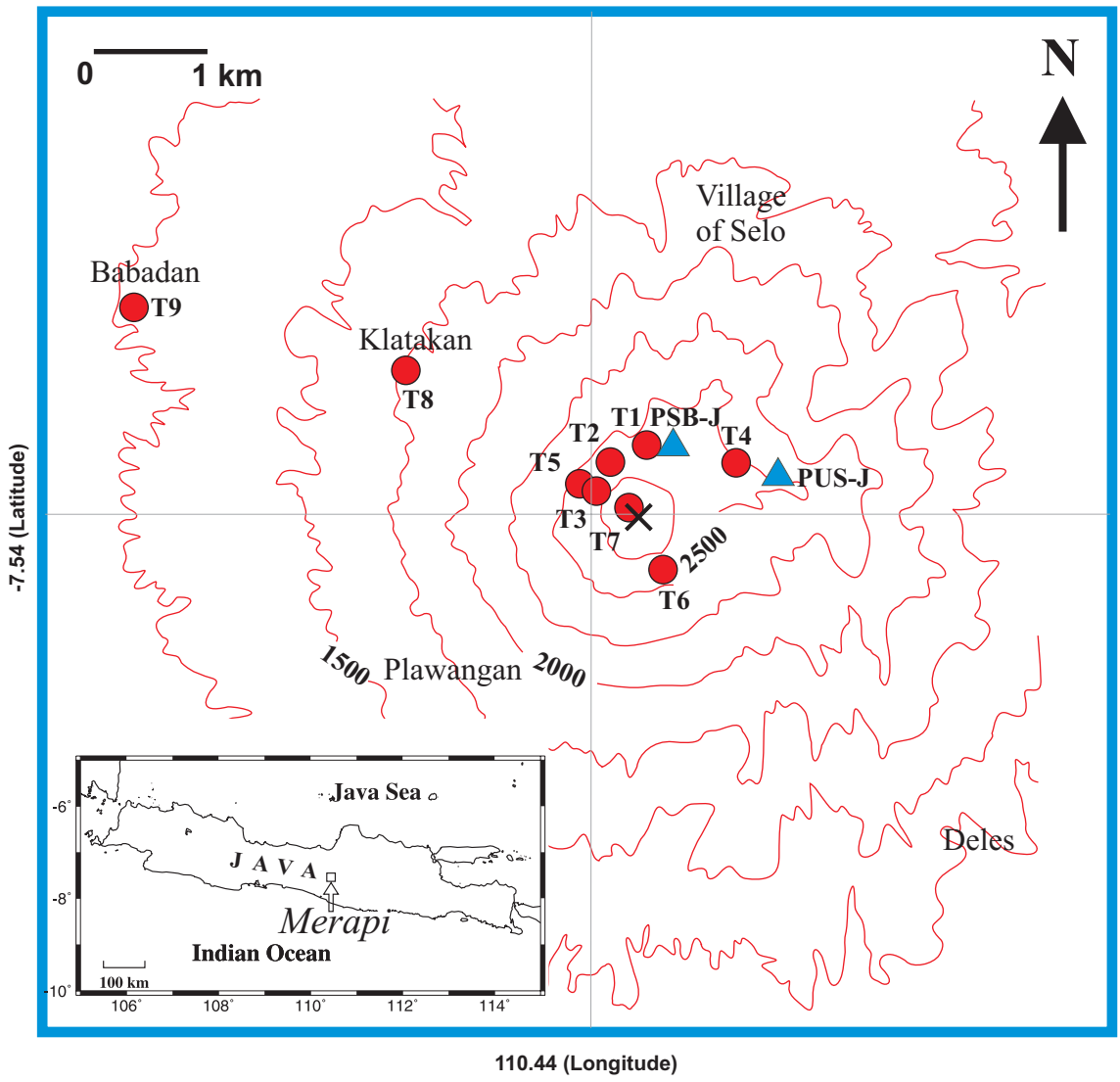

Figure **3-6**. Relationship of summit to lower flank tiltmeter station locations. Tiltmeters provided by Penn State operated at various times during the period 1992-1998, with station T3 ultimately providing the most complete data set of the stations shown here.

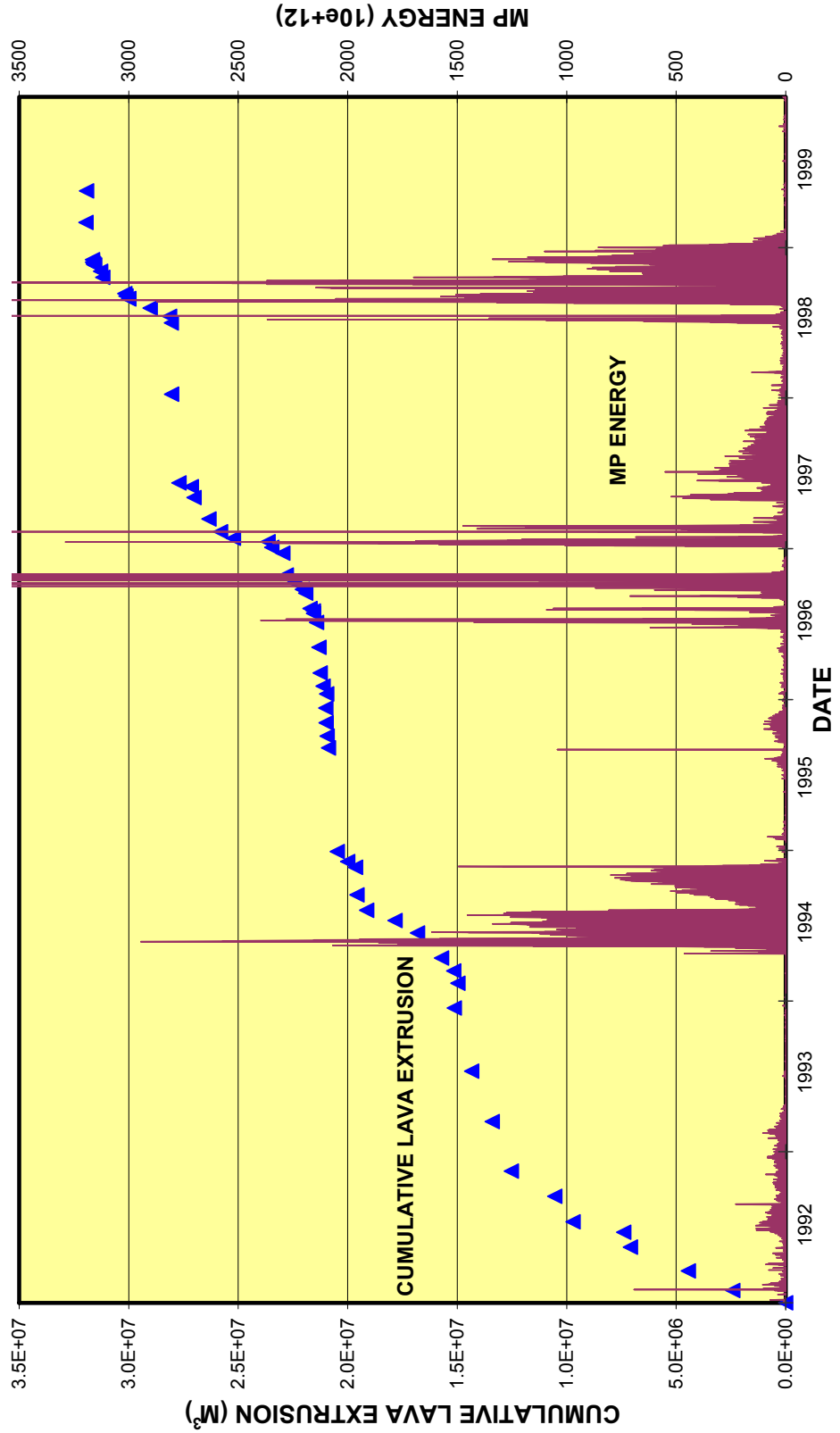

Figure **3-7**: Cumulative lava extrusion (DRE) calculated using dome volumes, collapse volumes, and AxD proxies for rockfall and PF volumes (see text) during the period 1992-1999. Comparisons in this and in Figs. 3-8 to 3-13 are made to various geophysical parameters measured or observed at Merapi. Here cumulative lava extrusion is shown versus seismic energy recorded by multiphase (MP) seismic events.

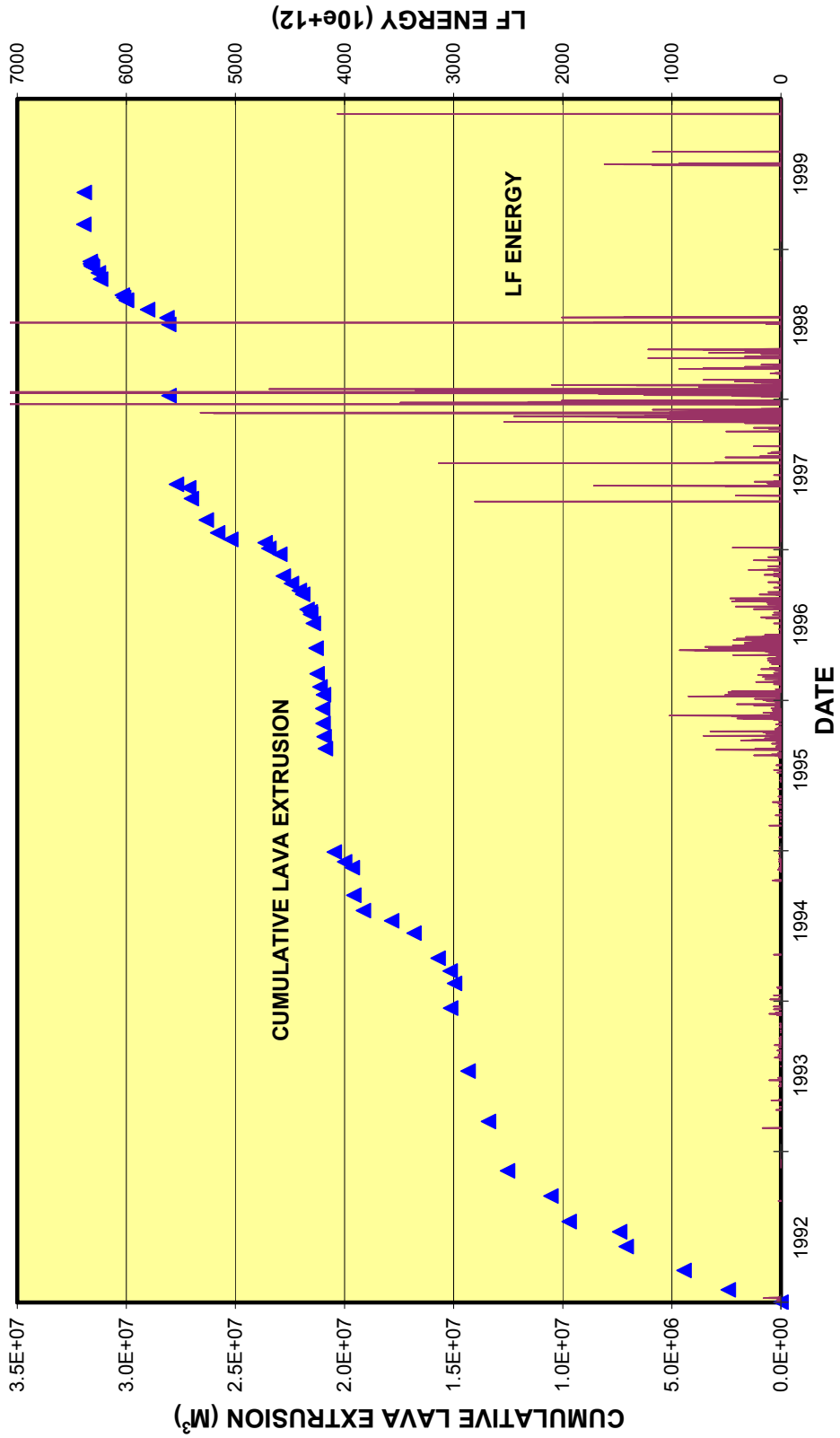

Figure **3-8**: Cumulative lava extrusion (DRE) versus the seismic energy recorded by low-frequency (LF, or long-period) events during the period 1992-1999.

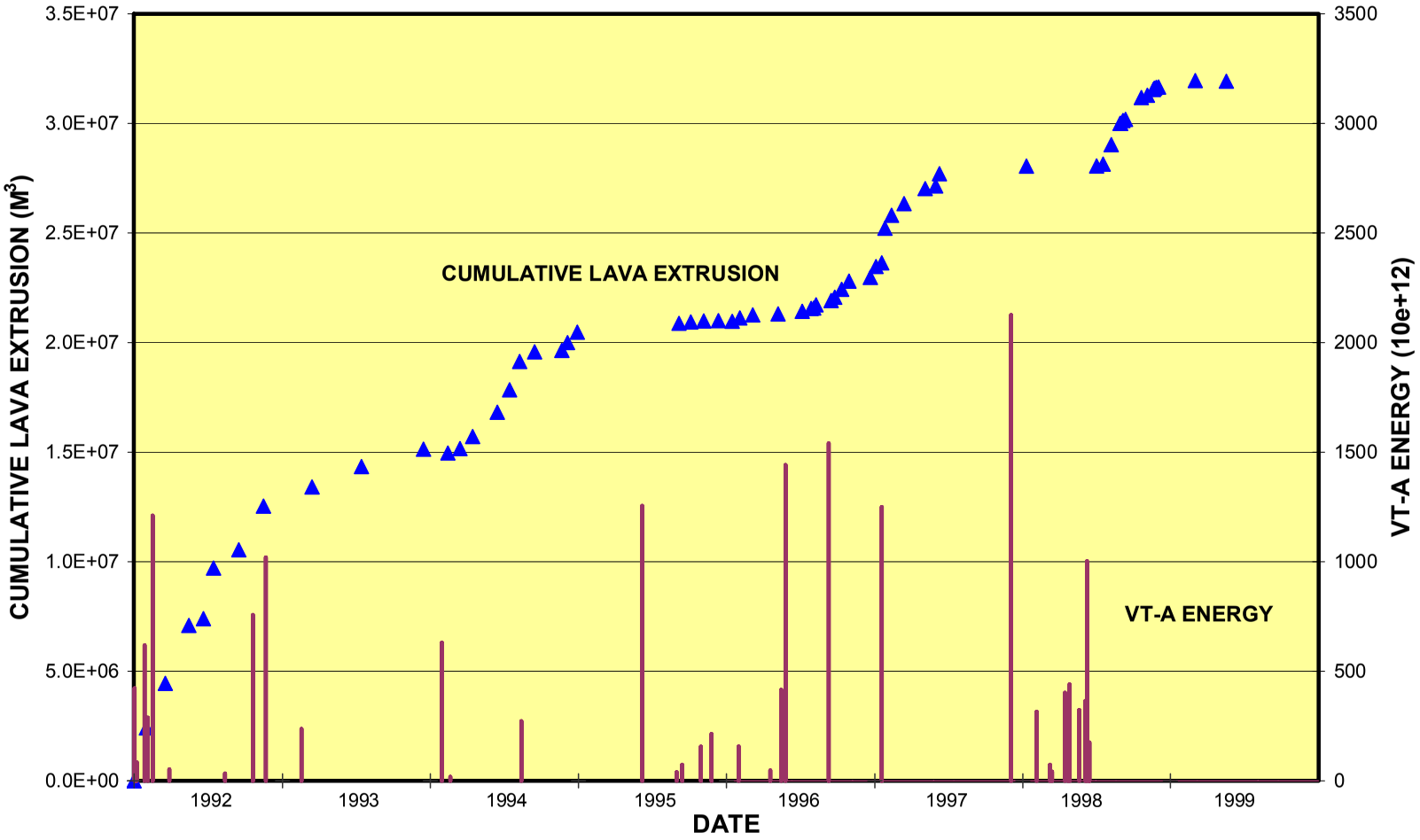

Figure **3-9**: Cumulative lava extrusion (DRE) versus the seismic energy recorded by A-type volcano-tectonic events (VT-A) during the period 1992-1999. At Merapi, VT-A is distinguished from B-type events by a clear separation of S and P first arrivals, generally >0.5 s, equating to a depth >2.5 km beneath the summit of the volcano (Ratdomopurbo and Poupinet, 2000).

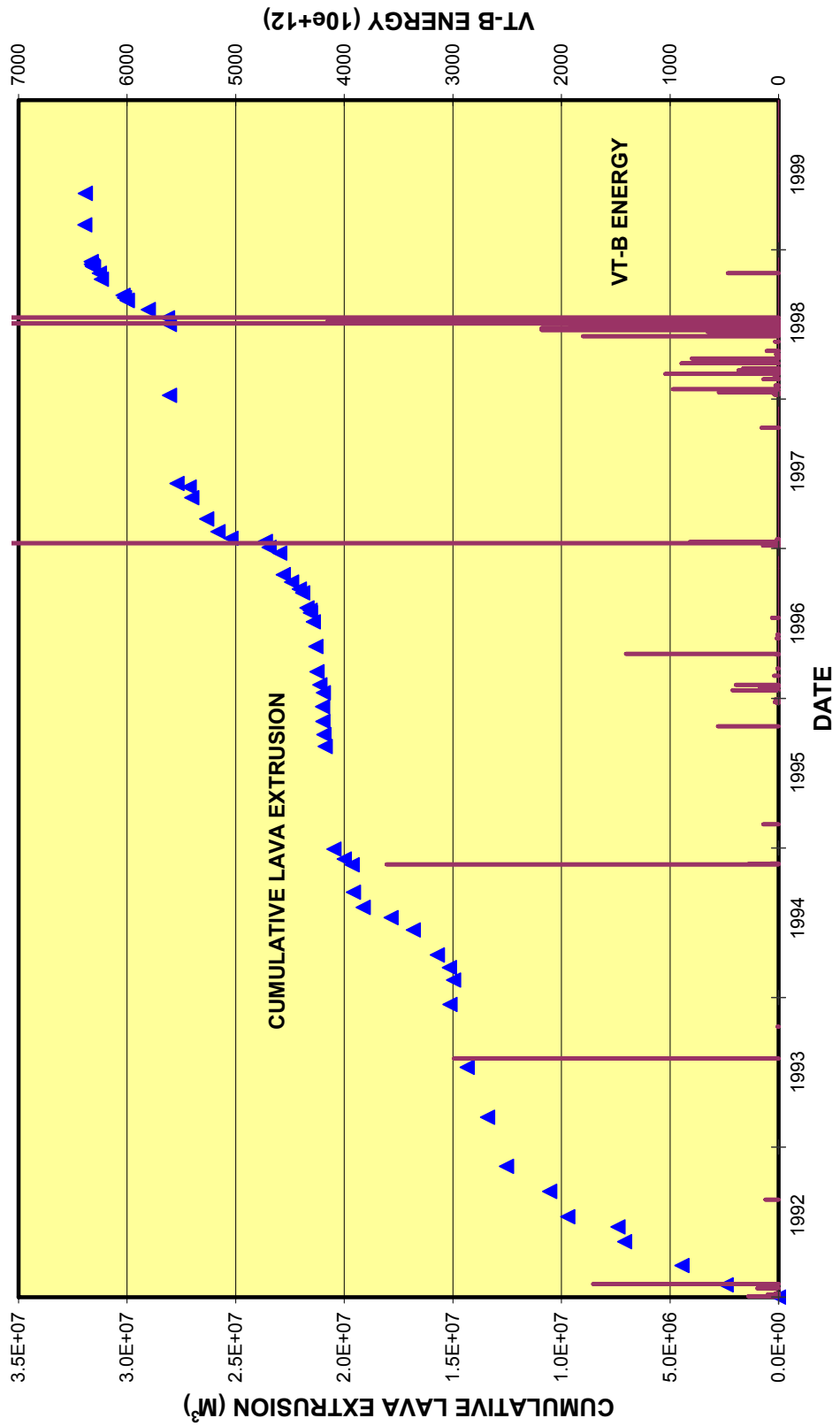

Figure **3-10**: Cumulative lava extrusion (DRE) versus seismic energy recorded by B-type volcano-tectonic events (VT-B) during the period 1992-1999. At Merapi a VT event is B type if it has poorly resolvable S and P first arrivals, generally <0.5 s apart, and a depth of <2.5 km beneath the summit of the volcano (Ratdomopurbo and Poupinet, 2000).

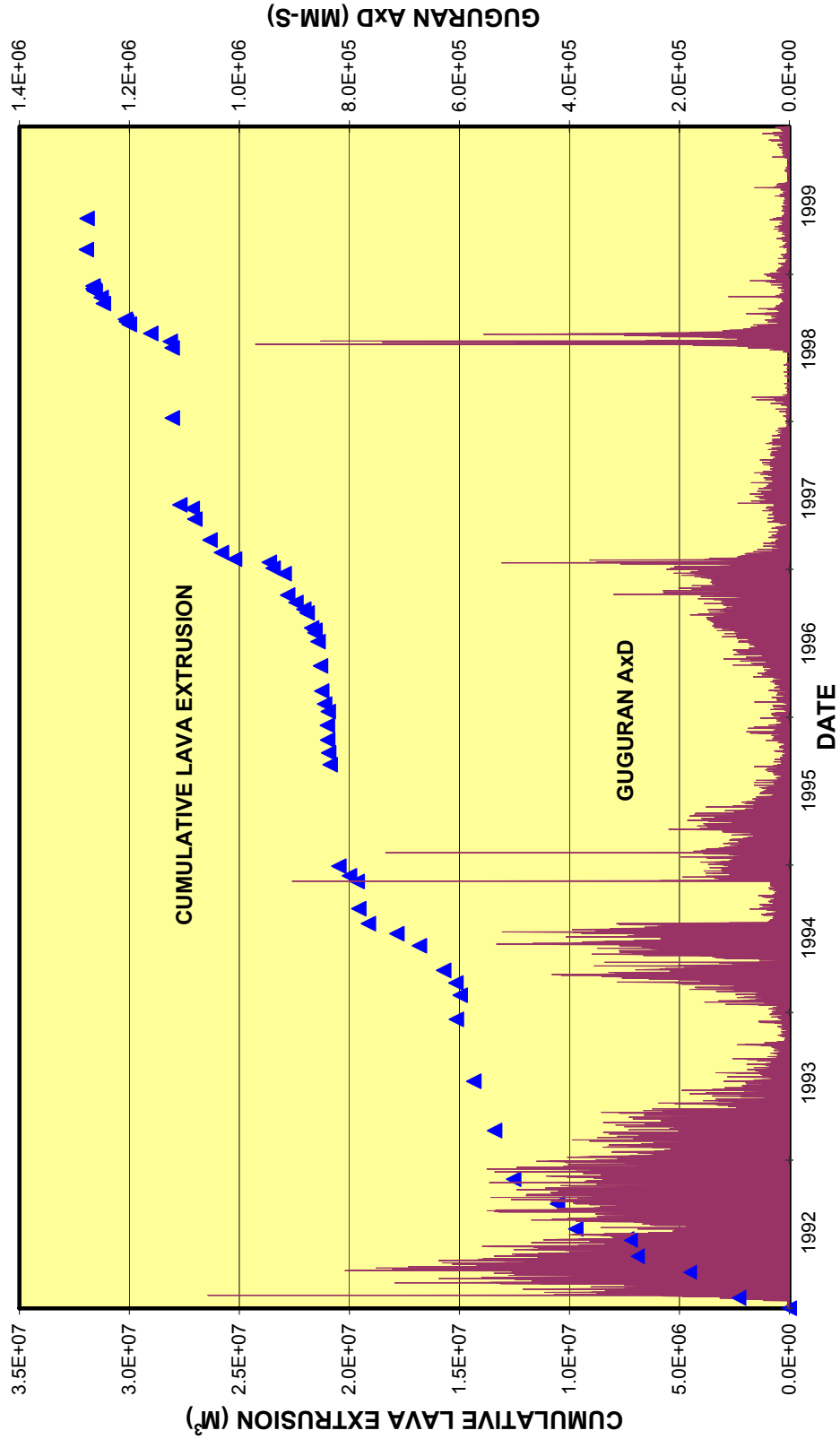

Figure **3-11**: Cumulative lava extrusion (DRE) versus rockfall seismicity, expressed here as amplitude x duration (AxD), in mm-s, during the period 1992-1999.

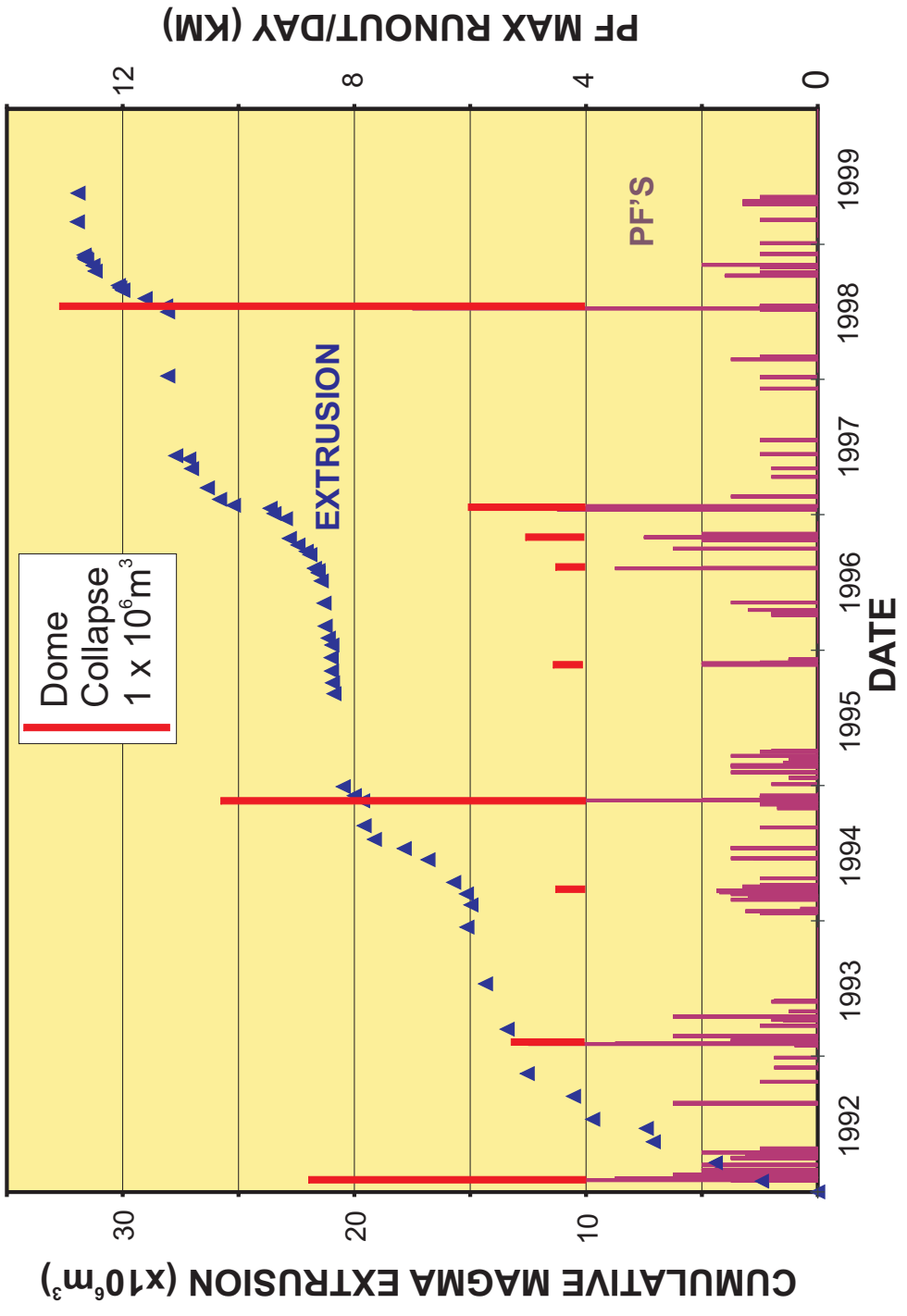

Figure **3-12**. Cumulative lava extrusion (DRE) versus pyroclastic flow runout and major dome collapse volumes during the period 1992-1999. PF runout is expressed as the maximum distance observed per day.

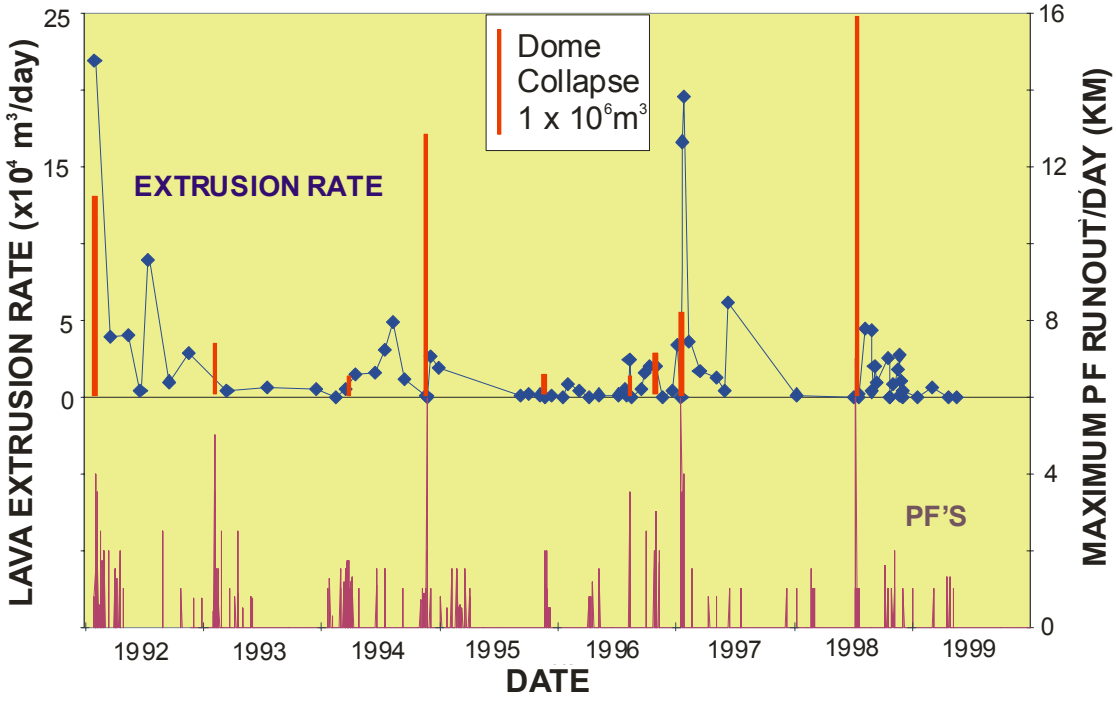

Figure **3-13**. Lava extrusion rate (DRE-adjusted) compared to pyroclastic flow runout distances (maximum seen per day) and major dome collapse volumes, during the period 1992-1999.

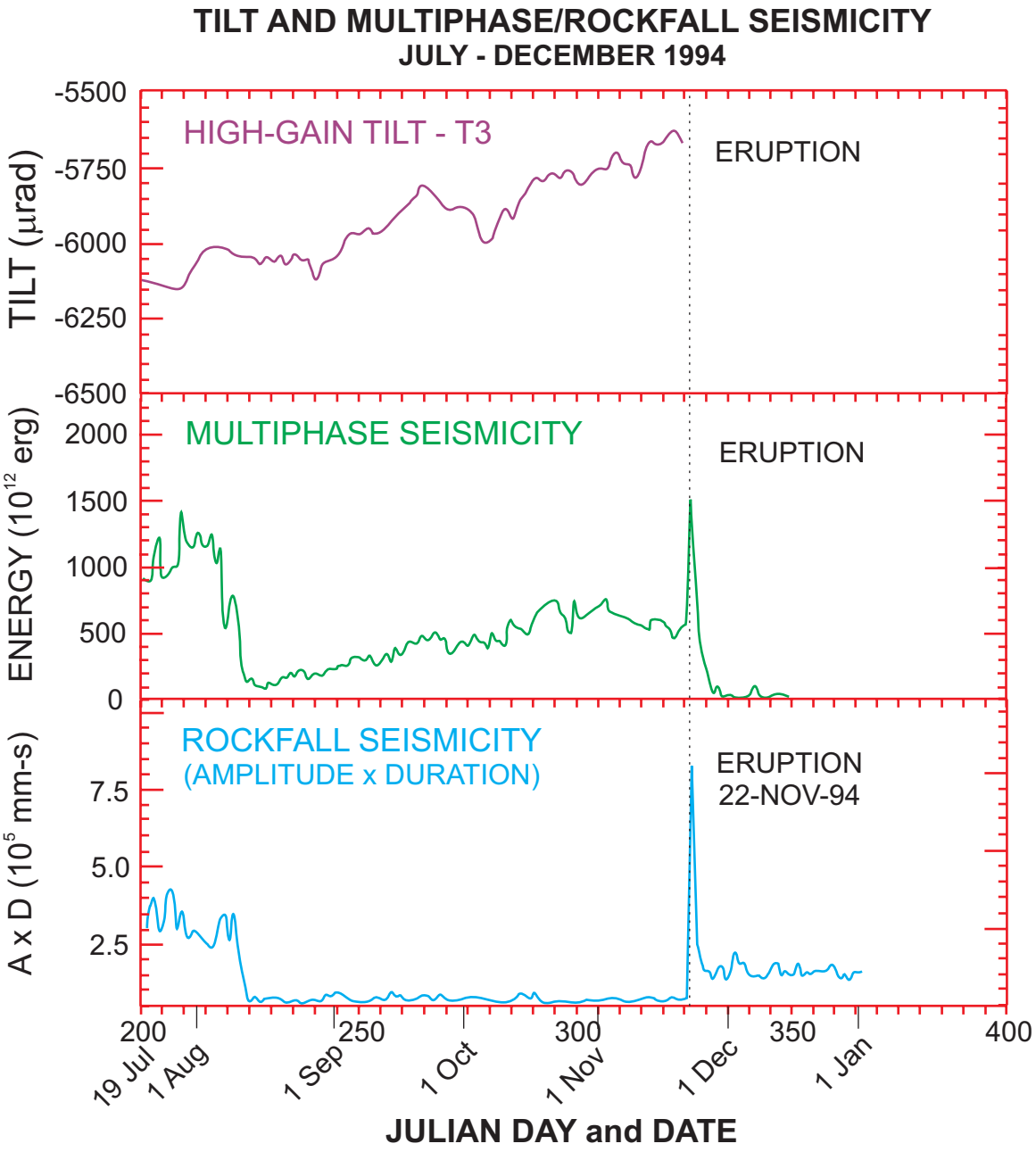

Figure **3-14**. Monitored data in relation to the lava dome collapse of 22 November 1994. Data shown are high-gain tilt at summit station T3, MP earthquake energy, and rockfall

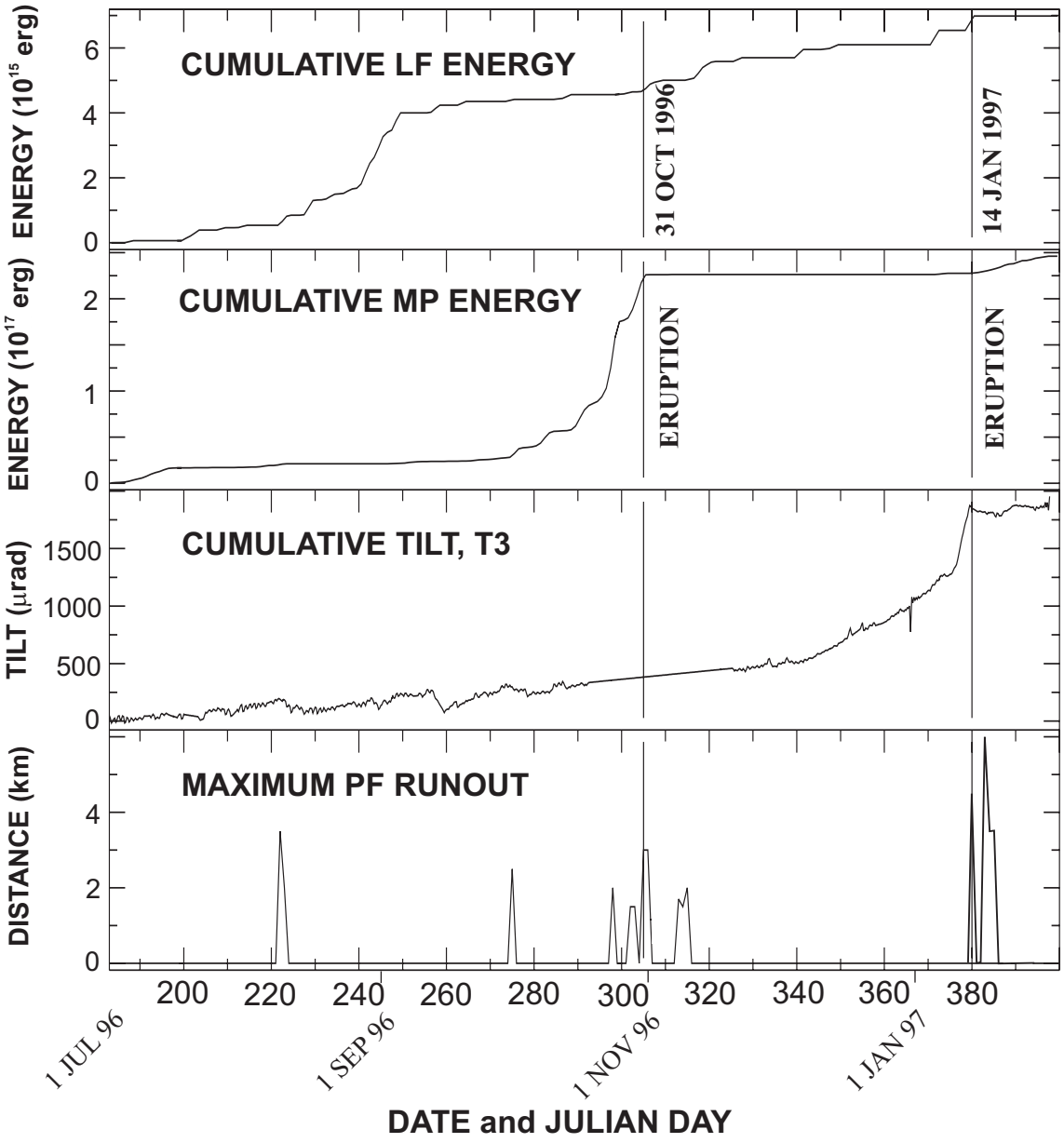

Figure **3-15**. Monitored data in relation to the crisis of 31 October 1996 and the eruption of 14 and 17 January 1997. Data shown are cumulative LF energy, cumulative MP energy, T3 cumulative tilt, and maximum pyroclastic flow runout distance. Note that for the 14 January eruption, tilt is the most diagnostic precursor.

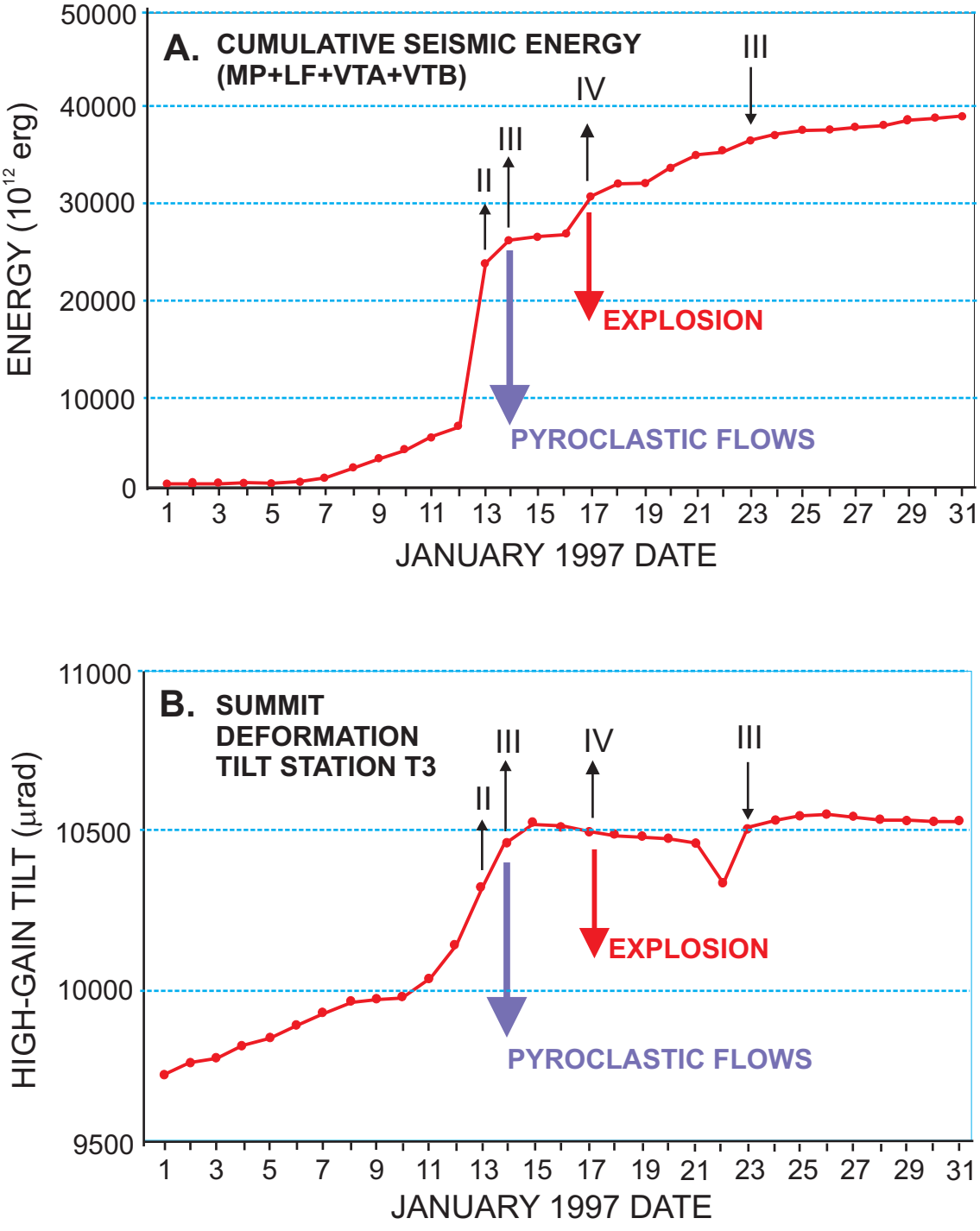

Figure **3-16**. Monitored data in relation to the eruption of 14 and 17 January 1997, and changes in alert level status. (A). Total cumulative seismic energy (sum for MP, LF, VTA, VTB events) versus January 1997 date. The plot mainly reflects energy of MP events, except for the jump on 14 January, due to a VTB swarm. (B). High-gain tilt at T3 versus date.

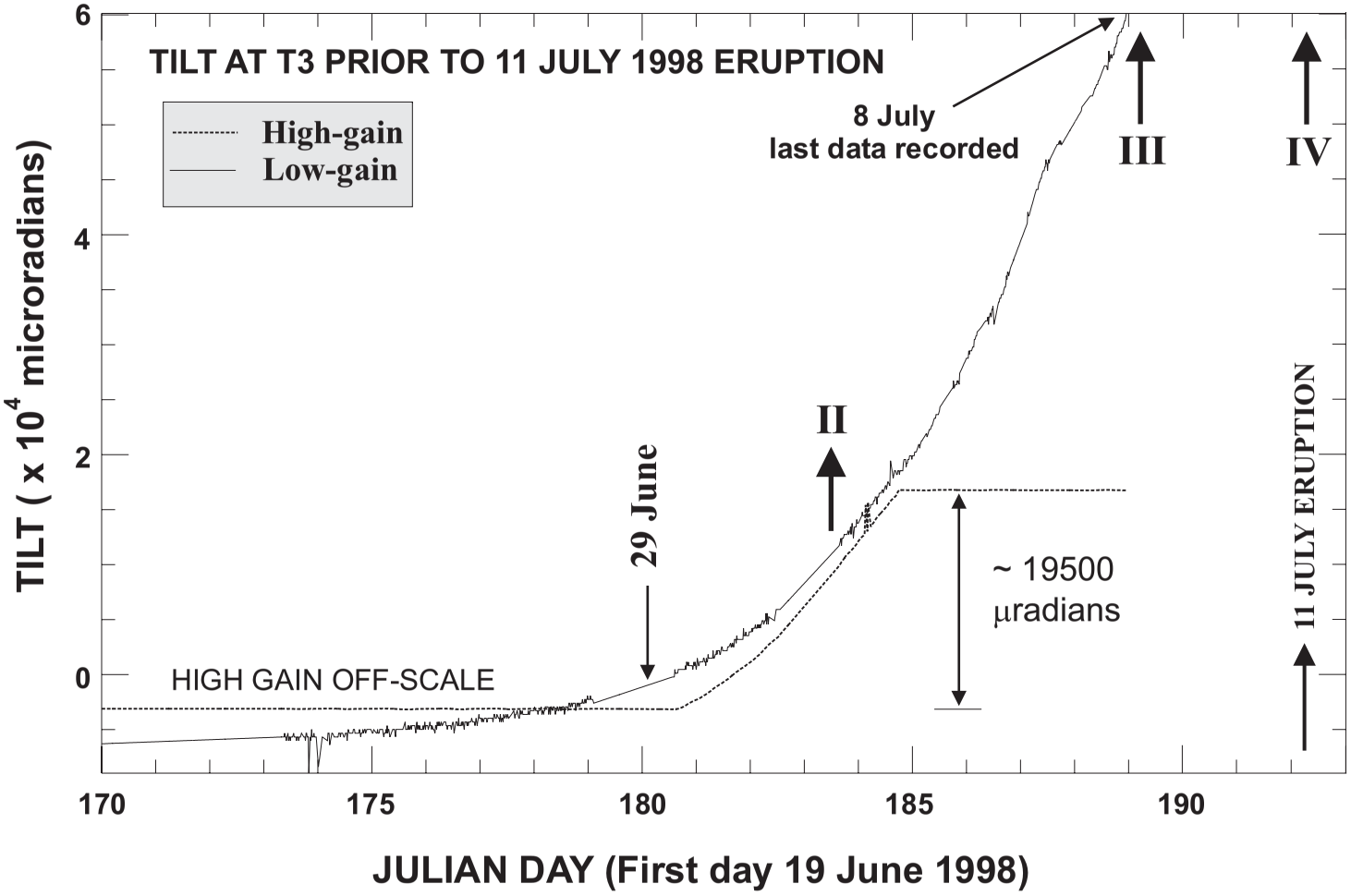

Figure **3-17**. Tilt versus time in Julian days, beginning 19 June 1998, and alert level changes instituted by VSI in response to the increasing activity (see Voight et al., 2000b). The high-gain sensor went off-scale after 19,500 μrad. The low-gain sensor continued to deform at a high rate until the tilt system was destroyed in a partial collapse of the crater rim. The eruption occurred 3 days later on 11 July.

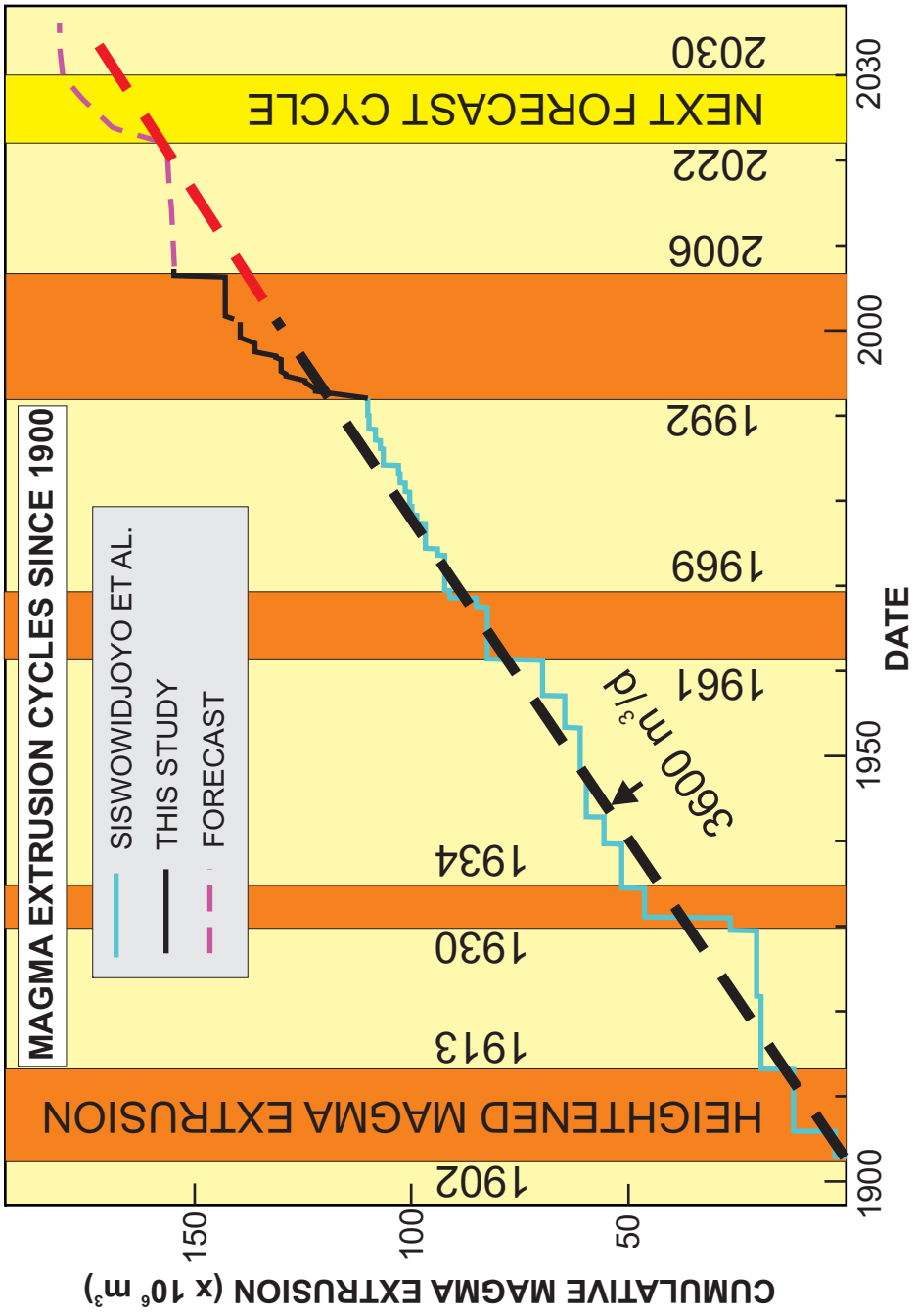

Figure **3-18**. Lava extrusion cyclicity since 1900. Shaded time periods mark heightened lava extrusion rates. Data of 1900-1992 is from Siswowidjoyo et al. (1995), with data of 1992-2000 from this study, 2000-2006 from MVO and GVN reports, and in 2006, C. Newhall (unpub.). Possible forecasts for the next 30-year cycle are empirically derived from 1913-1934, 1934-1969.

dome collapse PF events	Generating mechanism for PF	No. PFs	Max. runout (km)	Dome collapse volume x10^6 m^3	Active lobe volume x10^6 m^3	Lava Extrusion Rate m^3 /day	Glowing Rockfall	PRECURSORS and CORRELATIONS Tilt	seismically recorded Rockfalls	seismicity MP	seismicity LF	seismicity VT-A	seismicity VT-B	SO2	Other
2-Feb-92	very high Q new lobe	52	4	1.9	2.6	220,000	begins on 20-Jan	no tiltmeters installed	Accelerating #'s and E	irregular increase in #'s and E. Spike during	irregular #'s 5 and 4 weeks before.	numerous in years before	a few, but not precursory	20-30t/d 2wks prior 30-50t/d 1wk prior 92 t/d day prior	
3-Feb-93	mod Q (short-tm high Q???)	36	5	????	????	19,000(?)	????	T3: abrupt 530urad increase preceding 12 days, but peaks 2-5 days after event, then deflation. T2: no notable changes	unremarkable weekly AxD max; #'s increase by 2x in week before, but this also unremarkable.	Declining prior, w/ very small spike in E during	none	none	none	decline from 130t/d to 100t/d 2 wks prior.	
14-Mar to 2-Apr-94	high Q new lobe	73	1.75	0.2(?)	0.16	15,000	begins on 14-Feb	T3: 240urad increase 13Feb-7Mar, then deflation 170urad to 14Mar. 80urad inflation coincides w/ PF lull 15-19Mar. Deflation follows, 140urad to 2Apr. T5: irreg. inflation 130urad 5Feb-17Mar. T2: 50urad inflation 15Feb-8Mar. T7: 80urad/day deflation begins 7Dec, ends 4Mar, 200urad inflation to 8Mar accel deflation to 18Mar, slowing to zero tilt change on 2Apr. Total 18Mar-2Apr deflation=1400urad.	Irregular accelerating in #'s and AxD before and during this period, culminates 3 days after end of the period in both AxD and E	no events prior/during. MP suddenly begin on 26Apr	none	none	none	Increase from 60t/d to 110t/d Dec-Mar, but few measurements.	
22-Nov-94	low Q w/ oversteepened endogeneous growth	60	6.5	2.5	2.6	620	none	No short-term precursors. T3: long-term inflation 3.5urad/day w/ 3-7day spikes; slightly accelerating. T2, T5: similar but order of mag less. T6: installed 11-nov, no change. T7: online 11-Nov, 32urad/day inflation prior, 1000urad deflation during 20-24 Nov, 36urad/day deflation after.	no precursor. A spike in # and E this day	declining E prior, spike during.	small swarm late Oct. Zero to 3 events/day begins 11Nov.	none	none prior. 24 events during.	120t/d in May declines to 60t/d in Oct. 70t/d in Nov prior to collapse.	
23-Nov to 27-Nov-95	low Q ? endogeneous growth? rain event?	28	2	0.18	????	1,200	????	T3: Period within an accel inflation ca. 500urad over 2 months begins mid-Sep. T2: lesser mag begins early Sep. T5: lesser mag begins Jun.	AxD and #'s show irregular low increase beginning 27Oct, with short-term peak 5-8Nov. Spikes 23-27Nov	increase from zero events begins 19Sep. #'s and E max 3-9Nov then decline.	Begins 15Aug, spike early Sep, late Sep, mid-Oct. Increase begins 11Nov, peaks 25Nov. Post-event major cluster 11-24Jan	3 events prior 3 months. 1 event during	2 events 25 Oct. 1 event day prior. 1 event during.	120t/d Jan-Jun declines to 60t/d in Oct. 96t/d during Nov prior to collapse.	
9-Aug-96	high Q	25	3.5	0.8	????	24,000	????	T3: notably inflationary w/ spikes, arguably moderately accelerating, begins early May, reaches max 8urad/day	Accelerating #'s and AxD.	Strongly accelerating #'s and E begin 28Jul, but preceded by more pronounced max in early July	Few events Post-event swarm 15Aug-5Sep.	3 events Apr-May	3 large E events 19Apr. 3 small E events May-Jul	100t/d Mar-Apr declines to 49t/d by early Aug.	
31-Oct to 1-Nov-96	short-term (?) high Q endogeneous?	38	3	0.32(?)	1.1	20,000	????	T3: long-term 3urad/day inflation, but goes offline 1 week prior. No obvious change in long-term trend w/ onset of data in late Nov.	Irregular strong accel in #'s and AxD beginning 4-Sep.	Huge increase in #'s overlap into harmonic "batik" quakes.	2 events week prior. 3 events of higher E during.	none	none	70t/d 1-29Oct. 242t/d 30Oct.	heavy rain. 6 small PF's in prior week.
14-Jan-97	very high Q new lobe	81	4.5	0.8	????	170,000	begins late Dec	T3: large, irreg accelerating inflation, ca. 600urad 1 week prior	Irregular moderate increase 1.5-2x begins 24Dec, peaks 5-7Jan.	Appear and strongly accelerate in #'s one week prior, but low E.	Few events, long-term decline. Small spikes mid-Nov. 3 LF 6Jan.	none	3 events week prior. 35 high-E events during	100t/d No precursory changes.	
(17-Jan-97)	fountain collapse	17	6												Vulcanian exp.
11-Jul-98	very high Q new lobe new direction destabilize sector	37	7	3.4 includes old lava	????	46,000	begins on 30-Jun	T3: huge accelerating inflation of 60,000urad in 10 days leading to last data on 8-July.	dramatic increase in #'s and AxD.	Acceleration in #'s	Cluster 4-16Jun. 1 low-E LF 1Jul.	7 events Feb-May, 8 events early June	0 to 5/wk from 11Jan. From 3Jun, # & E go up until 5Jul. Spike during. Spike 19Jul.	no data	small explosion on 30Jun. BAB EDM 1m shortening
(19-Jul-98)	very high Q?	25	5.5	????	????			no summit tilt stations survived	increasing	Declining, but spike during.					

Table **3-1**: Precursors to major dome collapses at Merapi volcano, 1992-1999.

Date	AxD DELZ	AxD PUSZ	2.9-9.9 Hz SSAM DELZ
11/22/94	816,000		
5/22/06	137,000	1,073,000	
5/11/06		79,000	0
5/12/06		265,000	1
5/13/06		506,000	9
5/14/06		1,163,000	100
5/15/06		957,000	118
5/16/06		560,000	26
5/17/06		494,000	35
5/18/06		640,000	26
5/19/06		707,000	10
Subtotal for eruption as of 2400 h, 5/19		5,317,000	325
5/20/06		747,000	88
5/21/06		953,000	153
5/22/06		1,073,000	101
5/23/06		1,518,000	114
5/24/06			78
5/25/06			40
Subtotal for eruption as of 2400 h, 5/25			899

Notes: DELZ and PUSZ refer to vertical-component seismicity recorded at stations Deles and Pusunglondon, respectively. AxD value is a daily summation of amplitude x duration for that station, in mm-s. SSAM refers to seismic spectral amplitude monitoring of the vertical component results from station Deles, and is a daily summation of cumulative amplitudes recorded every 10 minutes as a dimensionless "SSAM" value for various frequency bands.

TABLE **3-2**: Selected Seismic Amplitude Proxies for Dome Collapse Volume, as Calculated by MVO Staff, During the 2006 Eruption (C. Newhall, written commun., 2006).

Cycle No. (Start Date – End Date)	Elevated Flux Phase Time Span	Low Flux Phase Time Span	Elevated Flux Cumulative Lava Extrusion	Low Flux Cumulative Lava Extrusion	Elevated Flux (max rate)	Low Flux
1 (20Jan92 – 13Feb94)	10 months	15 months	11.3×10^6 m^3	1.8×10^6 m^3	0.43 m^3/s (2.5 m^3/s)	0.045 m^3/s
2 (13Feb94 – 6Jul96)	10.5 months	18 months	5.0×10^6 m^3	0.65×10^6 m^3	0.18 m^3/s (0.56 m^3/s)	0.014 m^3/s
3 (6Jul96 – 2Jul98)	11 months	13 months	6.0×10^6 m^3	0.28×10^6 m^3	0.21 m^3/s (2.3 m^3/s)	0.0083 m^3/s
4 (2Jul98 – 31Oct00[1])	5 months	11-13 months[1]	3.5×10^6 m^3	0.26×10^6 m^3	0.26 m^3/s (0.50 m^3/s)	0.0043 m^3/s

Note: Volumes and rates assume DRE=0.8. Latest phases to 2006 are not included.
[1]Time span for low flux phase uncertain due to equivocal description for time of appearance of 2001 dome in GVN Bulletins.

Table **3-3**: Short-Term (2-year) magma flux cycles within the latest period of elevated extrusion rate (Cycle 4 of Table 3-4).

Cycle No. (Start Date – End Date)	Elevated Flux Time Span	Following Low Flux Interlude	Elevated Phase Cumulative Lava Extrusion	Low Flux Phase Cumulative Lava Extrusion	Elevated Flux	Low Flux
1 (1902-1930)	10 years	16 years	19.8×10^6 m^3	1.04×10^6 m^3	0.060 m^3/s	0.0018 m^3/s
2 (1930-1961)	5 years	27 years	30.9×10^6 m^3	18.1×10^6 m^3	0.19 m^3/s	0.022 m^3/s
3 (1961-1992)	8 years	22 years	22.4×10^6 m^3	17.7×10^6 m^3	0.087 m^3/s	0.025 m^3/s
4 (1992-2006)	+15 years	?	44.7×10^6 m^3	?	0.10 m^3/s	?

Note: Volumes and rates in Cycle 4 assume DRE=0.8. As the Cycle 4 low-flux phase is proposed here to have only just begun with the cessation of major activity in July 2006, time spans and rates are not given.

Table **3-4**: Long-term (30-year) magma flux cycles

Chapter 4

Conclusions of the Dissertation Research

4.1 Introduction

The preceding stand-alone chapters have presented results of field campaigns spanning seven years of hiatus and eruptive activity at Merapi volcano (1988-1995). Continued acquisition of tilt records extends the field data to July 1998. Analysis of data includes some results from published works and the unpublished MVO database. Over the longer term, magma flux calculated by others for the first nine decades of the 20th century (Siswowidjoyo et al., 1995) are expanded upon and added to here. In total, a better understanding has been gained of the deformation patterns and magma flux exhibited by Merapi precursory to and during major eruption cycles on several time scales.

4.2 Distance changes

The distance changes that took place at Merapi beginning in 1988 (Chapter 2) occurred during a time concluded to be a phase of low magma flux (Chapter 3). This significant four-year period of accelerating crater-rim deformation took place precursory to the eruption of January/February 1992 and the onset of a multi-year cycle of elevated magma flux, the fourth since 1900, a phase that would last nearly to the end of the decade. The remarkable accelerating dilatation coincided in time with irregularly increasing long-period (LP) seismicity, significant numbers of deep and shallow volcano-tectonic (VT-A and VT-B) earthquakes, increasing total seismic energy, and included a

gas outburst crisis in August 1990, all prior to the eruption outbreak in 1992. Displacements that were observed near the summit of the south flank attained a horizontal rate of at least 1.1 m/year in 1990 and 1991. Lesser though still large rates of 0.3-0.7 m/year were observed over the same period for prisms set on the lava dome. Cross-crater rates of strain accelerated from less than 3×10^{-6} /day (1988-90) to more than 11×10^{-6} /day in the period just prior to the 1992 eruption. The movements reflected a general, though not symmetric, radial and circumferential extension (areal dilatation) over the center of the crater. Large extensions were oriented approximately north-south in the crater area, and were linked to nearly uniaxial stretching of the adjacent summit buttress on the north and east.

The deformation field is interpreted to be the result of slow, upward migration of a pressure source beneath the summit crater. A shallow magma pocket has been inferred to lie centered at roughly 2-km depth (Ratdomopurbo and Poupinet, 2000), and pressurized flow above this level – beginning at least as early as 1988 – is proposed as the cause of the surface deformations. This rising basaltic andesite magma, with phenocryst content greater than 50% by volume and with a strongly silicic interstitial liquid (Hammer et al., 2000), became highly viscous due to degassing and resulting microlite (groundmass) crystallization (Hess and Dingwell, 1996; Hammer et al., 2000). The overall pressure gradient was controlled by magma chamber pressure, shallow-level pressurization due to degassing, and the resistance offered by the upper edifice to conduit propagation.

The large differences in the magnitude of these displacements suggest an inhomogeneous medium in at least the upper edifice. In addition, some movements were probably non-elastic, influenced by joint slip and crack widening in response to the conduit pressurization. The displacements of 1988-1992 were not recovered after the 1992 eruption relieved much of the pressure.

Two deformation models are considered in general terms in Chapter 2. The first model consists of a dike- or elliptical-shaped pressure source. There are problems with this simple model, however, including: (1) The limited lateral extent available for the dike-shaped conduit; (2) the negligible uplifts experienced at crater-rim stations DOZ and ALB while these stations at the same time were experiencing marked outward horizontal displacement; and (3) the high, non-Newtonian viscosity and apparent yield strength of the magma resisting dike propagation.

In a second, alternative general model, focus is placed on the asymmetry and heterogeneity of the edifice using two-dimensional finite difference modeling of a plane strain deformation. This analysis necessarily simplifies the three-dimensional geometry and material property distributions present in the upper edifice of Merapi. The models assume a pressurized dislocation high in the edifice, an assumption consistent with lateral forcing induced by magma-flow pressure gradients augmented by melt degassing and microlite crystallization.

Two situations are compared. In one, the volcano is assumed homogeneous, resulting in displacement fields of similar magnitude on both the north and south flanks. This prediction is contrary to our field observations, which indicate the clear dominance

of south-flank deformation, and relative stability of the central part of the summit area. In addition, modeled displacement vectors high on the flanks displayed large vertical components, also contrary to observations.

A second situation is therefore examined, in which the south flank and summit areas are assumed to have bulk and shear moduli reduced by a factor of 5. This local reduction of modulus is reasonably justified by the numerous fumaroles in the southern sector, and the highly altered lavas locally observed. The result of this model adjustment is enhancement of the deformations experienced by the south flank, in comparison to those on the summit and north flank. Likewise, the displacement vectors on the south flank flatten out, and become at least qualitatively similar to those observed in the field measurements.

In this favored interpretation, the unequal deformations experienced by the edifice reflect mainly the compliance and steep slopes of the south flank and the thin northwest rim, in contrast to the stiff, massive buttress of the summit edifice to the north and east. The deformations observed were then produced by non-symmetric yielding, in response to relatively uniform and possibly symmetric pressures exerted about the conduit. The displacement discontinuity observed at the Gendol breach is interpreted to represent a major rock mass defect that penetrates into the interior of the edifice.

Movements were much smaller after 1992 and continued in this manner for the remainder of the decade, except at stations very local to new dome lobe breakouts. VT-A and VT-B seismic events were also very much reduced in number. This suggests that the onset of the January 1992 eruption relieved much of the pressure. With the lava breakout

and a high rate of effusion, the associated edifice strains occurred at a much reduced rate of 1 to 2 x 10^{-6} /day for cross-crater measurements. For the most part, surveys from 1992 through 1995 suggested that horizontal displacements measured by the summit network did not exceed their 95% error bounds. During this period, the upward flux of magma through the conduit was cyclic but sufficiently active to maintain an effectively open vent system with respect to the conduit wall rocks. Thus, following the outbreak of lava in 1992, high-level conduit pressurization was much reduced, and the edifice suffered little upper-flank deformation.

With the cessation of magma extrusion by early 1999, a roughly 15 month hiatus ensued before activity commenced again by May 2000 with 1998 dome deformation, incandescence, crater rim crack widening, and increasing numbers of VT-A and VT-B events (Smithsonian Institution, 2000a). Field observations finally confirmed new lava having shoved aside portions of the 1998 lobe by 31 October 2000, with a culmination of activity in the relatively rapid extrusion of lava in January and February 2001 (Smithsonian Institution, 2000b).

While detailed surveys of distance changes were not made by VSI personnel in the time leading up to the 2001 eruption, their geological observations of crack widening and the numerous VT events suggest deformation of the summit in a manner similar in style, if not magnitude, to the changes that took place prior to the 1992 eruption. With cessation of extrusion by 1999 and the subsequent hiatus, it is suggested that residence of magma within the conduit and uppermost magma pocket was sufficient in time to again generate significant overpressures due to degassing and microlite crystallization.

Mobility of the south flank prior to 1992 (and somewhat speculatively, in 2000) likely results from the interaction of magmatic pressures, altered zones, and structural discontinuities developed in the upper edifice over the past 200 years or more (Voight et al., 2000). In our conceptual model, the rising magma provides lateral overpressure to force deformation of the south flank, via a pathway affected by earlier history.

The Gendol breach possibly coincides with a flow contact boundary between the steep flanks of abutting viscous lavas erupted out of vents within the now-buried Mesjidanlama crater of 1872 (Neumann van Padang, 1931; Hartmann, 1935). These lavas formed East Dome on the east flank between 1888 and 1909, and West Dome on the south flank during 1911-13 (Neumann van Padang, 1931; Holcomb et al., 1982). The location of their mutual contact was itself perhaps controlled by a moderate breach of 20 meters or more in the 1872 crater rim near the current Gendol breach (Neumann van Padang, 1936). Explanation for the breach simply as a contact between lavas of different ages may be insufficient to explain its structural function as a displacement discontinuity for edifice deformation. Probably the breach contains a radial crack, possibly generated by dome lavas squeezing against the wall of the 1872, 1930, or other craters, or by high-level conduit pressurization. Whatever the origin of this gap, significant fumarolic exhalations at this location during the late 19th century indicate that the old breach lay at the top of a structure that penetrated the edifice (Neumann van Padang, 1936).

The structural discontinuities of buried crater walls and breaches, radial cracks, and the steep lateral contacts of older viscous domes and lava coulées on Merapi thus favor significant non-elastic deformation of the upper edifice during subsequent volcanic

activity. This research demonstrates that moderate-size flank failure from the continuation of such deformation on the steep 40^{o}-60^{o} slopes of the south flank seems entirely feasible, and worthy of a systematic, sustained monitoring program. Some monitoring of this type has been carried out by VSI and collaborators. A moderate-sized upper flank failure would be highly hazardous due to the long-runout capability of an avalanche toward the south, and also because of the possibility of such a failure being accompanied by a violent explosive pyroclastic flow. The latter scenario recalls the catastrophic eruption of 1930, which represented the combination of a flank failure of an old dome complex undermined by freshly extruded lava, and consequent explosive volcanism (Neumann van Padang, 1933).

4.3 The 2006 Eruption

While the 2006 eruption with its timing put it beyond the scope of the present study in any substantive way, several aspects are at least of note here. The eruption was preceded by a hiatus of four years, the longest period of quiet since at least the meager activity of 1988-92 or, more rigorously, the inactivity of 1961-67 (Siswowidjoyo et al., 1995). From the standpoint of precursors it resembles the eruptions that followed the quiet of 1988-92 (Chapter 2) and 1998-2000 (Beauducel et al., 2006) in displaying numerous volcano-tectonic earthquakes and substantial non-elastic inhomogeneous deformation at the summit (C. Newhall, written commun., 2006). During the eruption, unusually high rates up to 2×10^5 m^3/day were recorded, also seen in the early stages of the 1992 eruption over a time span of perhaps ¼ to ½ that of 2006.

Of final note with respect to the conclusions of Chapter 2 is that during impingement and overlap of the growing 2006 dome onto the very upper south flank, a modest collapse of this sector occurred on 4 June, removing some 4 x 10^5 m^3 of old material along the Gendol Breach. Thus a slope failure with some aspects like that of concern in Chapter 2 has now happened. In this instance, and as revealed in the non-explosive collapse of 2 x 10^6 m^3 of the lava dome on 14 June 2006, the conduit and dome were sufficiently degassed to the level excavated by collapse to prevent major explosions from occurring following the sudden exposure of dome and edifice interiors. This in spite of the unusually high rate of extrusion (for Merapi), that indicates faster ascent for magma and thus less time for degassing. As C. Newhall stated in the near aftermath of the crisis (written commun., 2006), we do not know how close Merapi came to its threshold for explosive activity during this crisis, as we do not yet know what the threshold is for Merapi.

4.4 Lava Extrusion Rates and Eruption Cyclicity

Based on the study of lava production rates in the first nine decades of the 20th century, Siswowidjoyo et al. (1995) suggested three periods of elevated extrusion took place at Merapi during the 20th century, namely 1902-1913, 1930-1934, and 1961-1969. Adding to their dataset to 2007 suggests a long-lasting fourth cycle of elevated magma flux covering the period 1992 to at least 2006.

In Chapter 3 new data and resulting estimates of cumulative lava extrusion for the period 1992 to 2006 are combined with the long-term results of Siswowidjoyo et al.

(1995). It is suggested here that the period 1992-2006 represents another period of elevated magma flux that continues the pattern of approximate 30-year cyclicity. While a prolonged +3-year hiatus in activity took place beginning by 2003, the eruption of 2006 was sufficiently vigorous in its lava production to suggest that Merapi overall remains in the "fourth" elevated phase of activity that began in 1992. As such, these last 15 years mark the longest such stretch of elevated lava extrusion in the past 100 years. It remains to be seen if the longer hiatuses preceding the two most recent eruptions (2.5 years, and ~3 years, respectively) are indeed suggesting a shift to lower extrusion rates of a subsequent ~15 to 20 year interlude.

Integrating the new data since 1992 to the long term lava production rates of Siswowidjoyo et al. (1995) yields an adjusted 20th century mean lava extrusion rate of 4.2 x 10^6 m^3 s^{-1} for the last 100 years. It should be noted that in this integration of our results to Siswowidjoyo et al. (1995) no allowance has yet been made for the fact that we have incorporated estimates of rockfall volumes based on seismic *AxD* data into the calculations of cumulative lava erupted. For the decade of the 1990's such an allowance for missing dome volume increases estimates of cumulative lava production by ~25%, and is ultimately dependent upon the reliability of the seismic proxy for volume loss, as well as estimates of DRE adjustment and ash cloud volume loss.

Each 30-year cycle consists of a 5- to 15-year phase of elevated magma flux followed by an interlude of lower (but not zero) flux over a period of 16-27 years. Magma flux during the elevated phases is generally about an order of magnitude higher

(0.9×10^{-1} $m^3 s^{-1}$ to 1.9×10^{-1} $m^3 s^{-1}$) than during interludes of low magma production (0.18×10^{-2} $m^3 s^{-1}$ to 2.5×10^{-2} $m^3 s^{-1}$).

Cycles in the past suggest the possibility for forecasting future cycles. While mean lava extrusion rates remain elevated during 1992-2006, the length of hiatuses have increased since 1998, and suggest a gradual transitioning to a lower extrusion rate period. If so, and the 30-year cyclicity continues at Merapi, lava production will be diminished over the next 15 years compared to the activity between 1992 and 2006.

4.5 Final Remarks

We have investigated correlations of various measurable and observable geophysical parameters at Merapi volcano in order to ascertain potential precursory behavior, as seen in hindsight, and how such behavior reflects instability of the lava dome and dome collapse events.

1. Accelerating crater-rim deformation and pronounced VT seismicity were observed at the summit of Merapi in the years preceding the onset of a new cycle of elevated magma flux at Merapi, the fourth such cycle since 1900.
2. During approximately the first half of the elevated magma flux phase of cycle 4 (1992-1999), crater-rim deformation was in general much reduced, indicating a relative lack of overpressure in the conduit compared to the less open vent conditions in the years leading up to the start of this phase of activity.
3. Pronounced permanent deformation measured at Merapi prior to 1992, and also occurring prior to the 2001 and 2006 eruptions, results from interaction of magmatic

pressures, altered zones, and structural discontinuities developed in the upper edifice over the past several hundred years.

4. Moderate-size flank failure from the continuation of such deformation on the steep south flank slopes of Merapi seems possible and in fact occurred with modest size in 2006. Major hazards are posed by this scenario if it takes place on a scale significantly greater than of 2006, for example, debris avalanche runouts and vertical and directed explosions that could occur during the unroofing of an overpressured magma conduit and/or magma pocket.
5. Rockfalls or pyroclastic flow generation by collapse of unstable portions of the growing lava dome occurred on an often daily basis from January 1992 to at least early 2002.
6. Large ($> 0.2 \times 10^6$ m^3) dome collapses and their accompanying pyroclastic flows were typically generated during periods of elevated extrusion rate of at least 0.17 m^3 s^{-1}. They also correlated somewhat with heightened MP seismicity, and followed upon inflationary crater-rim ground deformation as measured by proximal tiltmeter stations.
7. The characteristics of lava extrusion were affected by extrusion rate. Lava domes and tongues have grown via the extrusion of shear lobes, which then played an important structural role in the generation of rockfalls and pyroclastic flows. The direction of the extruding lobe and the location of the active headwall controlled the locations and directions of subsequent collapses.

8. Smaller collapses may not have necessarily correlated to elevated extrusion rate or to discrete shear-lobe formation, and even the large collapse of November 1994 did not manifest precursory seismic activity and measurable tilt deformation. In some of these cases, environmental factors such as rainfall may have played a roll in the relatively lesser November 1995 collapse, and slow continuing growth into a gravitationally unstable state may have been the lead-in to the large collapse of November 1994.
9. Recent activity between January 1992 and 2006 comprises an elevated average flux phase (0.13 m^3s^{-1}) recognized here as the fourth cycle in magma flux since 1900. Within this elevated flux were shorter-term cycles of magma flux ranging between 1.5 to 2.5 years in length. Four of these shorter-term cycles are recognized within the elevated phase between 1992 and 1999, characterized by magma flux ranging from 0.18 m^3s^{-1} to 0.43 m^3s^{-1} over 5-11 months, and hiatuses of negligible lava production lasting 13-18 months.
10. In the shortest term, crater-rim tilt suggests roughly 5- to 20-day cyclic pressurization during at least some of the elevated phases of magma flux in the yearly cycles of the 1990's.
11. Cumulative lava extrusion for a given cycle does not appear particularly volume dependent, either in absolute terms or in terms of the preceding repose interval.
12. Activity at Merapi in 2006, though vigorous, is interpreted to be near the end of the higher lava eruption phase of cycle 4. In this interpretation, successively longer

hiatuses preceding the eruptions in 2001 and 2006 are signs of a coming shift in lava eruption rate to an eventual lower long-term flux comprising the latter part of cycle 4.

13. If the 30-year cycles continue well into the 21st century, Merapi will soon exhibit low flux compared to the elevated-flux phase of the last 15 years, followed by heightened flux beginning the next cycle, forecast here to begin about the year 2022. Preceding this activity, there will perhaps be a heightened possibility for at least moderate sector collapse and unroofing of degassing magma as the upper edifice deforms in response to the impending activity.

4.6 References

Beauducel, F., Nandaka, M. Agung, Cornet, F.H., Diament, M., 2006. Mechanical discontinuities monitoring at Merapi volcano using kinematic GPS. J. Volcanol. Geotherm. Res. 150, 300-312.

Hammer, J.E., Cashman, K.V., Voight, B., 2000. Magmatic processes revealed by textural and compositional trends in Merapi dome lavas. J. Volcanol. Geotherm. Res. 100, 165-192.

Hartmann, M., 1935. Die Ausbrüche des Gunung Merapi (Mittel-Java) bis zum Jahre 1883. N. Jahrb. Min. Geol. U. Palaont. 75, 127-162 (in German).

Hess, K.-U., Dingwell, D., 1996. Viscosities of hydrous leucogranitic melts: A non-Arrhenian model. Am. Min. 79, 113-119.

Holcomb, R., Djumarma, A., Suparban, F.X., 1982. Geology of the summit region, New Merapi. VSI-Merapi Volcano Observatory, unpub. report, 5 pp.

Neumann van Padang, M., 1931. Der Ausbruch des Merapi (Mittel Java) im Jahre 1930. Zeitsch. f. Vulkanologie 14, 135-148 (in German).

Neumann van Padang, M., 1933. De uitbarsting van den Merapi (Midden Java) in de jaren 1930-1931. Vulkanol. En Seism. Meded. 12, 1-116 (in Dutch).

Neumann van Padang, M., 1936. Die Tätigkeit des Merapi-Vulkans (Mittel-Java) in den Jahren 1883-1888. Zeitsch. f. Vulkanologie 17, 93-113 (in German).

Ratdomopurbo, A., Poupinet, G., 2000. An overview of the seismicity of Merapi volcano (Java, Indonesia), 1983-1994. J. Volcanol. Geotherm. Res. 100, 193-214.

Siswowidjoyo, S., Suryo, I., Yokohama, I., 1995. Magma eruption rates of Merapi volcano, central Java, Indonesia during one century (1890-1992). Bull. Volcanol. 57, 111-116.

Smithsonian Institution, 2000a. Merapi. Bulletin of the Global Volcanism Network 25(11).

Smithsonian Institution, 2000b. Merapi. Bulletin of the Global Volcanism Network 25(12).

Voight, B., Constantine, E.K., Siswowidjoyo, S., Torley, R., 2000a. Historical eruptions of Merapi Volcano, Central Java, Indonesia, 1768-1998. J. Volcanol. Geotherm. Res. 100, 69-138.

Kirby D. Young - Vita

Education

2007 Ph.D. in Geosciences, The Pennsylvania State University, University Park, PA.
1983 M.S. in Geology, The Pennsylvania State University, University Park, PA.
1980 B.S. in Geology, Oregon State University, Corvallis, OR.

Professional Experience

2007 Intern, Montserrat Volcano Observatory, Fleming, Montserrat, BWI.
2006 Field Geologist, Institute of Earth Sciences, University of Iceland, Reykjavik.
2003-2006 Mountaineering instructor, Portland, OR.
2000 IAVCEI-NSF Scholarship, Bali, Indonesia.
1995 Intern, USGS Volcano Disaster Assistance Program, Yogyakarta, Indonesia.
1992-1995 Research Assistant, Penn State University, University Park, PA.
1994 Lecturer, International Training Course for Volcano Observers, UNESCO/Volcanological Survey of Indonesia, Yogyakarta.
1994 Co-Leader, NAGT/GSA Geological Excursion to Iceland.
1988-1991 Geologist, Nittany Geoscience, Inc., State College, PA.
1990 Research Assistant, Penn State University volcano deformation monitoring, Yogyakarta, Indonesia.
1987 Geologist, Ebasco Services, Inc., New York, NY.
1986 Research Assistant, Penn State University, University Park, PA.
1985 Instructor, University of Arizona, Tuscon, AZ.
1980-1984 Teaching Assistant, Penn State University, University Park, PA.
1980-1983 Graduate Fellow, Penn State University, University Park, PA.
1979 Exploration Geologist, Anaconda Copper Co., Denver, CO.
1978-1979 Field Geologist, Forestry Sciences Laboratory, Corvallis, OR.

Professional Activities

American Geophysical Union – Member, Session Chair
International Association of Volcanology and Chemistry of the Earth's Interior, Member
Reviewer - Bull. Geol. Soc. America, J. Volc. & Geotherm. Res., J. Geophys. Res., J. Eng. Geol.

Selected Publications

Young, K. D., Voight, B., Subandrio, Sajiman, Miswanto, and Casadevall, T. J., 2000. Ground deformation at Merapi volcano, Java: Distance changes, June 1988-October 1995, *J. Volcanol. Geoth. Res*, v. 100 (1-4), p. 233-259.

Young, K. D., Voight, B., and Orkan, N. I., 1987. The Iceland perspective: Its role in the development of plate tectonic theory: **in** Hilde, T. W. C., and Carlson, R. L., (conveners), *1987 Geodynamics Symposium: Silver Anniversary Celebration of Plate Tectonics*, pp. 96-98, Geodynamics Research Institute, Texas A & M University, College Station, Texas.

Young, K. D., Jancin, M., Voight, B., and Orkan, N., 1985. Transform deformation of Tertiary rocks along the Tjornes Fracture Zone, north central Iceland: *Journal of Geophysical Research*, v. 90, p. 9986-10010.